



University of Tennessee, Knoxville  
**TRACE: Tennessee Research and Creative  
Exchange**

---

Doctoral Dissertations

Graduate School


---

8-2011

## Strong Spin Orbital Coupling Effect on Magnetic Field Response Generated by Intermolecular Excited States in Organic Semiconductors

Liang Yan  
[lyan4@utk.edu](mailto:lyan4@utk.edu)

Follow this and additional works at: [https://trace.tennessee.edu/utk\\_graddiss](https://trace.tennessee.edu/utk_graddiss)

 Part of the [Polymer and Organic Materials Commons](#), and the [Semiconductor and Optical Materials Commons](#)

---

### Recommended Citation

Yan, Liang, "Strong Spin Orbital Coupling Effect on Magnetic Field Response Generated by Intermolecular Excited States in Organic Semiconductors. " PhD diss., University of Tennessee, 2011.  
[https://trace.tennessee.edu/utk\\_graddiss/1144](https://trace.tennessee.edu/utk_graddiss/1144)

This Dissertation is brought to you for free and open access by the Graduate School at TRACE: Tennessee Research and Creative Exchange. It has been accepted for inclusion in Doctoral Dissertations by an authorized administrator of TRACE: Tennessee Research and Creative Exchange. For more information, please contact [trace@utk.edu](mailto:trace@utk.edu).

To the Graduate Council:

I am submitting herewith a dissertation written by Liang Yan entitled "Strong Spin Orbital Coupling Effect on Magnetic Field Response Generated by Intermolecular Excited States in Organic Semiconductors." I have examined the final electronic copy of this dissertation for form and content and recommend that it be accepted in partial fulfillment of the requirements for the degree of Doctor of Philosophy, with a major in Materials Science and Engineering.

Bin Hu, Major Professor

We have read this dissertation and recommend its acceptance:

Roberto S. Benson, Jayne Wu, Shanfeng Wang

Accepted for the Council:

Carolyn R. Hodges

Vice Provost and Dean of the Graduate School

(Original signatures are on file with official student records.)

**Strong Spin Orbital Coupling Effect on Magnetic Field Response  
Generated by Intermolecular Excited States in Organic Semiconductors**

**A Dissertation Presented for the  
Doctor of Philosophy  
Degree  
The University of Tennessee, Knoxville**

**Liang Yan  
August 2011**

Copyright © 2011 by Liang Yan

All rights reserved.

## **DEDICATION**

I dedicate my work to my parents.

## ACKNOWLEDGEMENTS

I feel deeply indebted to my advisor, Prof. Bin Hu, for his irreplaceable guidance and valuable suggestions about my research work and dissertation. He provided a comfortable and flexible research environment throughout my years in graduate school. I acquired lots of practical and theoretical knowledge from him. Without his guidance and support, I could not have completed this dissertation. I would also like to sincerely thank my committee members for their kind help, including Dr. Roberto Benson, Dr. Jayne Wu, and Dr. Shanfeng Wang.

I owe a large debt of gratitude to Dr. Shin Wang in Oak Ridge National Laboratory, who provided the thermoelectric facility and gave cheerfully of his time and expertise.

Another big thank-you goes to Prof. Carlos F. O. Graeff in Departamento de Física-FC, Universidade Estadual Paulista – UNESP, Bauru, Brazil, who helped me for the EPR measurement and my life when I went to Brazil.

I need to thank Yue Wu, Zhihua Xu, Ming Shao, and Huidong Zang for their kind help in both my study and my personal life.

I would like to thank all other people who worked with me, such as Guoliang Li, Lili Wu, Dr. Lianbin Niu, Michael Garrison Stanford, Jaime Sullivan, Dr. Youzhi Wu, Dr. Tho

Nguyen, Dr. Xinjun Xu, and so on, for their help in my work and the convenience they gave to me.

Finally I need to express my appreciations to my parents.

## ABSTRACT

It has been found that non-magnetic organic semiconductors can show some magnetic responses in low magnetic field ( $<100$  mT). When applying magnetic field, the electroluminescence, electrical current, photocurrent, and photoluminescence could change with magnetic field, which are called magnetic field effects.

Magnetic field effects are generated through spin-dependent process affected by the internal magnetic interaction. In nonmagnetic materials, hyperfine interaction has been supposed to dominantly affect the spin-dependent process recently. But the conclusion was made in weak spin-orbital coupling organic semiconductor. The hyperfine interaction might not be the main reason responsible for magnetic field effects in strong spin-orbital coupling materials. Therefore, the study of magnetic field effects in strong spin-orbital coupling organic semiconductor is important to get a whole view of the origin of the magnetic field effects in nonmagnetic organic semiconductors.

This dissertation will clarify the generation mechanism of magnetic field effect in nonmagnetic organic semiconductors and further explore how the strong spin-orbital coupling affecting the magnetic field effect.

It has been found the intermolecular excited states are important inter-median for magnetic field effects. The change of intersystem crossing at intermolecular excited states



will change the singlet/triplet ratio and further generate magnetic field effects through different recombination and dissociation properties of singlet and triplet intermolecular excited states.

Both the energy transfer effect coupled spin orbital coupling and energy transfer effect free spin orbital-coupling are discussed in the dissertation. The tuning of the magnetic field effect by adjusting the spin-orbital coupling is also established through distance effect and interface effect. It has been found that changing inter-molecular spin-orbital coupling is a critical factor to generate magnetic field effects in organic semiconductors. And the sensitivity of different magnetic field effects to strong spin-orbital coupling strength is depending on the final product.

The internal magnetic interaction can be hyperfine interaction, spin orbital coupling and spin-spin interaction between electrons. The hyperfine interaction and spin orbital coupling are important in nonmagnetic organic semiconductors. But the electron spin-spin interaction is important in magnetic organic semiconductors. The magnetocurrent for magnetic and nonmagnetic organic semiconductors at different temperature has been compared.

# TABLE OF CONTENTS

CHAPTER 1 INTRODUCTION .....	1
1.1 Organic semiconductors.....	1
1.1.1 OLED .....	1
1.1.2 OPV .....	2
1.2 Excited states .....	4
1.2.1 Intramolecular excited state .....	5
1.2.2 Intermolecular excited state .....	6
1.3 Internal magnetic interaction .....	7
1.3.1 Hyperfine interaction .....	7
1.3.2 Spin-orbital coupling .....	8
1.4 Energy transfer.....	9
1.4.1 Förster energy transfer .....	10
1.4.2 Dexter energy transfer.....	11
1.5 Magnetic field effect.....	12
1.6 Mechanism of Magnetic Field Effect .....	15
1.6.1 Intersystem crossing model (polaron pair model) .....	16
1.6.2 Bipolaron model.....	18
1.6.3 Exciton quenching model .....	19
1.6.4 Our model .....	20
1.7 Summary and outline for the dissertation .....	22

CHAPTER 2 DEVICE FABRICATION AND MEASUREMENT .....	25
2.1 Device fabrication .....	25
2.2 Magnetic field effect measurement.....	28
2.2.1 Magnetic field effect on photoluminescence (MFE <sub>PL</sub> ) measurement.....	28
2.2.2 Magnetic field effect on electroluminescence (MFE <sub>EL</sub> ) measurement.....	29
2.2.3 Magnetic field effect on photocurrent (MFP) measurement.....	29
2.2.4 Magnetocurrent (MC) or organic magnetoresistance (OMR) measurement ...	30
2.2.5 Magneto-capacitance (MCP) measurement.....	31
2.3 Other measurement .....	32
CHAPTER 3 INTERMOLECULAR EXCITED STATE RESPONSIBLE FOR MAGNETIC FIELD EFFECT .....	33
3.1 Introduction.....	34
3.2 Experiment.....	35
3.3 Intermolecular excited states responsible for MFEs.....	35
3.4 Separation distance study of singlet exciplex in liquid state .....	39
3.5 SOC effect on MFE from intermolecular excited state .....	43
3.6 Conclusion .....	50
CHAPTER 4 POLYMER BLENDS FROM OPTOELECTRONICS TO SPINTRONICS .....	51
4.1 Abstract .....	52
4.2 Introduction.....	52
4.3 Experiment.....	54

4.4 Result and discussion .....	54
4.4.1 Magnetic field effect on electroluminescence of pure Ir(ppy) <sub>3</sub> and PVK .....	54
4.4.2 MFE from the composite of PVK and Ir(ppy) <sub>3</sub> .....	59
4.4.3 Energy transfer mechanism of MFE <sub>EL</sub> in the composite of PVK and Ir(ppy) <sub>3</sub> .....	59
4.4.4 MFE from the composite of PFO and Ir(ppy) <sub>3</sub> .....	64
4.4.5 Mechanism of MFE <sub>EL</sub> in composite of PFO and Ir(ppy) <sub>3</sub> .....	66
4.5 Conclusion .....	68
CHAPTER 5 THE ROLE OF INTERMOLECULAR SPIN-ORBITAL COUPLING IN MAGNETIC FIELD EFFECTS IN ORGANIC SEMICONDUCTORS .....	69
5.1 Abstract .....	70
5.2 Introduction .....	70
5.3 Experiment .....	73
5.4 Results and Discussion .....	74
5.5 Conclusion .....	88
CHAPTER 6 INTERFACE INDUCED NEGATIVE PHOSPHORESCENCE MAGNETIC FIELD EFFECT IN ORGANIC DOUBLE LAYER LIGHT EMITTING DEVICES .....	90
6.1 Abstract .....	91
6.2 Introduction .....	92
6.3 Experiment .....	93
6.4 Result and Discussion .....	95
6.5 Conclusion .....	104

CHAPTER 7 MAGNETO-CAPACITANCE EFFECT IN ORGANIC RADICAL-	
BASED MATERIALS.....	105
7.1 Abstract.....	106
7.2 Introduction.....	106
7.3 Experiment.....	108
7.4 Results and Discussion .....	108
7.5 Conclusion .....	118
CHAPTER 8 THE COMPARATION OF MAGNETOCURRENT BETWEEN	
MAGNETIC AND NONMAGNETIC MODIFIED C <sub>60</sub> .....	119
8.1 Abstract.....	120
8.2 Introduction.....	120
8.3 Experiment.....	122
8.4 Result and Discussion .....	122
8.5 Conclusion .....	129
CHAPTER 9 CONCLUSION.....	131
References.....	135
VITA .....	136

## LIST OF FIGURES

Figure 1.1 A simple structure of OLED.....	2
Figure 1.2 Typical device structures of organic solar cells. ....	4
Figure 1.3 Singlet and triplet spin configuration in excited states.....	5
Figure 1.4 Exchange energy between singlet and triplet in intramolecular excited state... 5	
Figure 1.5 Exchange energy between singlet and triplet in intermolecular excited state... 6	
Figure 1.6 Hyperfine interaction between electron and nucleus.....	8
Figure 1.7 Electron-hole separation distance effect on exchange energy and internal magnetic interaction in excited states in organic semiconductor.....	9
Figure 1.8 Spectrum overlap requirement for Förster energy transfer process. ....	10
Figure 1.9 Scheme for Dexter energy transfer process, a) from donor singlet to acceptor singlet, b) from donor triplet to acceptor triplet.....	12
Figure 1.10 Zeeman splitting effect on energy level in intermolecular excited states. ....	14
Figure 1.11 Zeeman Effect on intersystem crossing in intermolecular excited states.....	16
Figure 1.12 The relationship between intermolecular excited states (PPs) and emission or current. ....	17
Figure 1.13 Two polarons and one bipolaron in polythiophene. ....	18
Figure 1.14 The spin blocking effect in triplet bipolarons.....	19
Figure 1.15 The combination of positive and negative MFE on EL and MR. ....	22
Figure 2.1 The ITO glass with four electrode fingers.....	26

Figure 2.2 The picture of device, the left is the ITO glass with electrode fingers, the middle is the device after spin coating of polymer solution, and the right is the final device after thermal evaporation of aluminum. ....	27
Figure 2.3 The experiment setup for MFP measurement. ....	30
Figure 3.1 The chemical structure of PVK and TCNB.....	35
Figure 3.2 a) The PL spectrum of PVK and TCNB doped PVK b) MFE of PL for pure PVK and 1wt% TCNB doped PVK. ....	36
Figure 3.3 The MFP, MFE <sub>EL</sub> and MC of 1wt% TCNB doped PVK. ....	38
Figure 3.4 Chemical structures for Py and DMA. ....	39
Figure 3.5 a) PL spectrum of single component and exciplex of Py+DMA system, b) MFE on PL of single component and exciplex of Py+DMA system in solution, the solvent is the mixture of THF and DMF, THF:DMF=3:7 (volume ratio). ....	40
Figure 3.6 a) PL spectrum of Py+DMA in DMF with different concentration, b) Concentration dependent MFE on PL of Py+DMA. ....	42
Figure 3.7 Heavy metal complex concentration effect on MFE on PL of Py+DMA in mixture solvent of THF:DMF=3:7 system and the chemical structure of Ir77. ....	44
Figure 3.8 Chemical structure of Ir65 and TCNB. ....	45
Figure 3.9 a) PL spectrum of composite Ir65:TCNB:PMMA=2:2:5 and Ir65:PMMA=2:5 , b) EPR spectrum of Ir65:TCNB: PMMA composite.....	45
Figure 3.10 Concentration dependent of PL spectrum from triplet exciplex Ir65+TCNB. ....	46

Figure 3.11 Polymer matrix dielectric constant dependent PL spectrum of triplet exciplex from Ir65+TCNB. ....	47
Figure 3.12 EL spectrum of ITO/Ir65:TCNB:PMMA/Al.....	48
Figure 3.13 OMR of device ITO/Ir65:TCNB:PMMA/Al.....	49
Figure 4.1 Chemical structure of Ir(ppy) <sub>3</sub> and PVK. ....	55
Figure 4.2 a) Normalized electroluminescence spectrum for pure PVK and pure Ir(ppy) <sub>3</sub> b) MFE <sub>EL</sub> of pure PVK and Ir(ppy) <sub>3</sub> .....	57
Figure 4.3 The energy level of both singlet and triplet exciton state of PVK and Ir(ppy) <sub>3</sub> S and T refer to singlet and triplet state. ....	58
Figure 4.4 a) Normalized electroluminescence spectrum for composite of PVK+0.1% Ir(ppy) <sub>3</sub> , the electroluminescence spectrum of pure PVK and pure Ir(ppy) <sub>3</sub> are also shown as reference, b) MFE <sub>EL</sub> of 0.1% Ir(ppy) <sub>3</sub> +PVK and pure PVK at 405nm, c) MFE <sub>EL</sub> of 0.1% Ir(ppy) <sub>3</sub> +PVK and pure Ir(ppy) <sub>3</sub> at 505nm.....	60
Figure 4.5 a) Absorption of Ir(ppy) <sub>3</sub> and photoluminescence of PVK, b) Photoluminescence and electroluminescence of PVK with 0.1% Ir(ppy) <sub>3</sub> .....	62
Figure 4.6 Energy transfer process in electroluminescence of composite of PVK doped with 0.1wt% Ir(ppy) <sub>3</sub> . S and T refer to singlet and triplet state. ....	63
Figure 4.7 Chemical structure of PFO. ....	64
Figure 4.8 a) Electroluminescence spectrum of ITO/PFO+3%Ir(ppy) <sub>3</sub> /Al and ITO/PFO/Al, b) MFE on electrofluorescence and electrophosphorescence in ITO/PFO+3%Ir(ppy) <sub>3</sub> /Al, FEL refer to the electrofluorescence, PEL refer to the electrophosphorescence. ....	65



Figure 4.9 Overlap of absorption of Ir(ppy) <sub>3</sub> and the photoluminescence of PFO.....	66
Figure 4.10 Energy transfer process in electroluminescence of composite of PFO doped with 3wt% Ir(ppy) <sub>3</sub> . S and T refer to singlet and triplet state. ....	67
Figure 5.1 Chemical structures for Ir65, Ir77 and Ir(ppy) <sub>3</sub> .....	74
Figure 5.2 Magnetocurrent is shown for Ir(ppy) <sub>3</sub> :PMMA and Ir(ppy) <sub>3</sub> :PS composites as compared to pure Ir(ppy) <sub>3</sub> molecules. The weight ratio of Ir(ppy) <sub>3</sub> : polymer is 1:2. ....	75
Figure 5.3 The intra- and inter- molecular SOC for Ir(ppy) <sub>3</sub> in solid state, electron spin $\mu_s$ and orbital magnetic field $B_{orb}$ occurring within a single molecule and between adjacent molecules. M1 and M2 are two adjacent Ir(ppy) <sub>3</sub> molecules. ....	78
Figure 5.4 EPR spectra for Ir(ppy) <sub>3</sub> :PS composite with weight ratio of 1:2 and pure Ir(ppy) <sub>3</sub> .....	80
Figure 5.5 Electroluminescence spectrum of Ir65, Ir77 and Ir(ppy) <sub>3</sub> and their composite in PMMA matrix. ....	81
Figure 5.6 MC from dispersion of Iridium complex in PMMA devices, a) Ir77:PMMA=1:2.5 b) Ir65:PMMA=1.5:2.5. ....	82
Figure 5.7 a) MC of ITO/ Ir77+PMMA/Al, Ir77:PMMA=x:2.5, b) MC of ITO/Ir77+PMMA/Al at different Ir77 concentration. ....	86
Figure 5.8 The spin orbital coupling effect on intersystem in intermolecular and intramolecular excited state. ....	88
Figure 6.1 Chemical structures of Ir67, Ir77 and P2.....	94
Figure 6.2 MFE of ITO/ Ir77+PMMA/PVA (5nm)/Al, Ir77:PMMA=4:2.5 and ITO/Ir67+PMMA/PVA (5nm)/Al, Ir67:PMMA=4:2.5. ....	96

Figure 6.3 a) MFE of ITO/Ir77+PMMA/Al, ITO/PVA/Ir77+PMMA/Al and ITO/Ir77+PMMA/PVA/Al, Ir77:PMMA=4:2.5, b) C-V measurement for ITO/Ir77+PMMA/PVA/Al and ITO/Ir77+PMMA/Al, Ir77:PMMA=4:2.5. ....	97
Figure 6.4 a) MFE of ITO/PVA (5nm)/Ir77+PMMA/Al, Ir77:PMMA=x:2.5, b) MFE of ITO/Ir77+PMMA/PVA(5nm)/Al with different Ir77 concentration. ....	99
Figure 6.5 MFE of ITO/P2/PVA (5nm)/Al and ITO/P2/Al.....	100
Figure 7.1 Normalized absorption spectrum of PANiCNQ in NMP and the chemical structure of PANiCNQ.....	109
Figure 7.2 Magneto-capacitance on ITO/PANiCNQ/Al at different frequency.....	110
Figure 7.3 Energy levels of singlet and triplet radical ion pair under magnetic field. a) for intramolecular radical ion pair, b) for intermolecular radical ion pair. ....	112
Figure 7.4 Chemical structures of BBOT and TPD.....	113
Figure 7.5 a) Magneto-capacitance of ITO/TPD:BBOT:PMMA=4:4:10/Al, b) Photo-induce capacitance change at different frequency of ITO/TPD:BBOT: PMMA=4:4:10/Al. ....	114
Figure 7.6 Chemical structure of Ir65 and TCNB. ....	116
Figure 7.7 a) Magneto-capacitance of ITO/TPD:BBOT:PMMA=4:4:10/Al, b) Photo-induce capacitance change at different frequency of ITO/TPD:BBOT:PMMA= 4:4:10/Al. ....	117
Figure 8.1 Chemical structure of magnetic and nonmagnetic modified C <sub>60</sub> .....	124
Figure 8.2 a) M vs H hysteresis loop recorded at 90K and 300K, b) Enlarged M vs H hysteresis loop recorded at 90K and 300K. ....	125

Figure 8.3 Magnetocurrent of Fe-free and Fe-containing modified C <sub>60</sub> device at 77K..	126
Figure 8.4 Magnetocurrent of device ITO/C <sub>60</sub> (>DPAF-C <sub>9</sub> )-FeO <sub>x</sub> (1/1,w/w):PMMA (2:4) /Al at different temperature.....	127
Figure 8.5 Variation of zero field cooled (ZFC) and field cooled (FC) magnetization with temperature measured at an applied magnetic field of 100 Oe.....	128
Figure 8.6 Normalized curve for both hysteresis and magnetocurrent. ....	129

# **CHAPTER 1**

## **INTRODUCTION**

### **1.1 Organic semiconductors**

Organic semiconductors include two types: small molecules and polymers. Both of them are constructed by pi-bond based conjugated structures, which allow the delocalized pi-electrons move through the entire conjugated structures. And people use Su-Schrieffer-Heeger (SSH) theory model<sup>1</sup> to treat the organic semiconductor as the band structure in inorganic semiconductors. The highest occupied molecular orbital (HOMO) is like the valance band in inorganic semiconductor and the lowest unoccupied molecular orbital (LUMO) is like the conduction band in inorganic semiconductor. The organic semiconductors are widely used in organic light emitting diodes (OLEDs), and they can potentially be used in organic photovoltaic (OPV) devices, organic transistors, and organic spintronics devices. The magnetic field effect we studied is mainly in OLED and OPV devices.

#### **1.1.1 OLED**

OLEDs have been developed since 1980s,<sup>2-5</sup> now OLEDs are used in television screens, computer monitors, and small, portable system screens such as mobile phones. The OLEDs convert the input electric energy in the electric circuit into light. The OLEDs

usually contain the cathode, organic emitting layer, and the anode three layer components, as shown in Figure 1.1 (Here is the simplest case; the real OLED may contain other layer components). The electrons and holes are injected from the cathode and anode, correspondingly. The electron and hole will form a negative polaron or positive polaron with the distortion of the charge's surroundings. And they will transport in the organic semiconductors under the drift of the electrical field. After they meet with each other, they could form weakly bonded electron-hole pair with relative long separation distance (intermolecular electron-hole pair). And the intermolecular electron-hole pair will further get closer and form the exciton, which is highly bonded electron-hole pair with small separation distance. The exciton will recombine to emit a photon, generating the electroluminescence (EL).

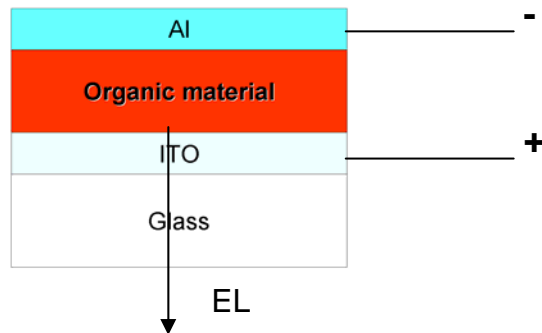


**Figure 1.1 A simple structure of OLED.**

### **1.1.2 OPV**

The organic photovoltaic device also starts from 1980s, <sup>6,7</sup> but now it has not got commercialized. The best power conversion efficiency is 8.3% from Konarka company

(by March, 2011),<sup>8</sup> which is much lower than over 40 percent efficiency in inorganic photovoltaic devices. But it is also fast developing and has a good future in energy conversion technology. It converts the incident light into electric energy. Usually the light source is the sun light, then it is called organic solar cell. The typical structure of OPVs is a sandwich structure containing: cathode, active layer, and anode, as shown in Figure 1.2. The active layer usually is a bulk heterojunction containing both donor and acceptor. The cathode and anode are two materials with different work function, which will generate build-in electric field in the device. When the incident photon energy fits the absorption of the active layer, it will be absorbed by the active layer and generating excitons, which are the highly bonded electron-hole pairs. When the excitons diffuse to the donor-acceptor interface, the electron transfer will occur between the donor and acceptor, separating the electron and hole in exciton and generating the contact charge transfer complex. The contact charge transfer complex would further dissociated under build-in electric field, forming polaron pair (intermolecular electron-hole pair). Then dissociated electron and hole would transport towards respective electrodes under the drift of build-in electric field and collected by the electrodes generating photocurrent. It should be noted that the photo-generated electron-hole pair also can recombine and emit a photon generating the PL or undergo the non-radiative emission. Therefore, the dissociation and recombination always compete with each other. For good OPV performance, the recombination should be minimized.

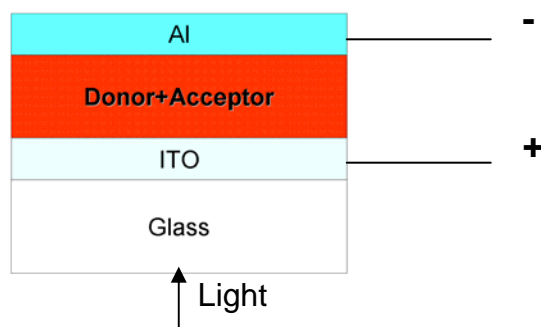


**Figure 1.2 Typical device structures of organic solar cells.**

## **1.2 Excited states**

Excited states in organic semiconductors are electron-hole pairs. According to the electron-hole separation distance, there are intramolecular excited states and intermolecular excited states. Because both of the electron and hole has a spin  $1/2$ , the excited states have four spin configuration, one singlet state and three triplet states, as shown in Figure 1.3. The singlet and triplet states have different energy levels, the energy difference between singlet and triplet is the exchange energy. The different electron-hole separation distance will lead large difference in exchange energy and internal magnetic interaction strength.<sup>9</sup> These two factors would largely affect the magnetic field effects.

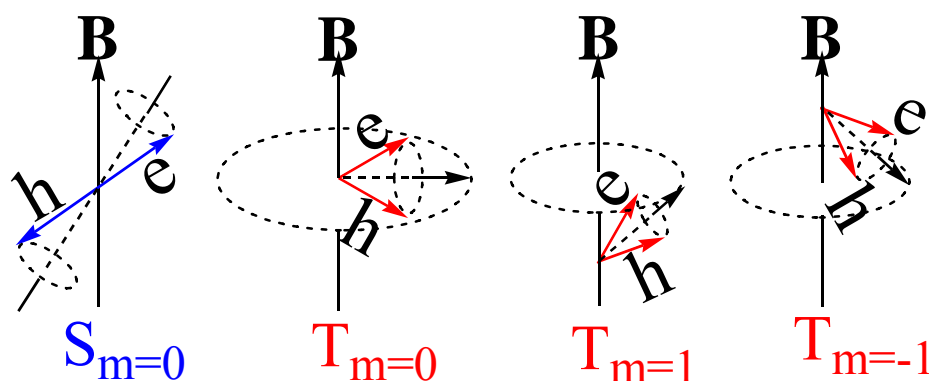


**Figure 1.3 Singlet and triplet spin configuration in excited states.**

### 1.2.1 Intramolecular excited state

Intramolecular excited state is also called exciton in organic semiconductors. The intramolecular excited state is the electron-hole located in one molecule. The electron-hole separation distance usually is in  $10^{-10}$  m order. The singlet level is higher than the triplet level, as shown in Figure 1.4. In the intramolecular excited state the exchange energy is relative large, about 0.7eV in lots of conjugated polymers.<sup>10</sup>

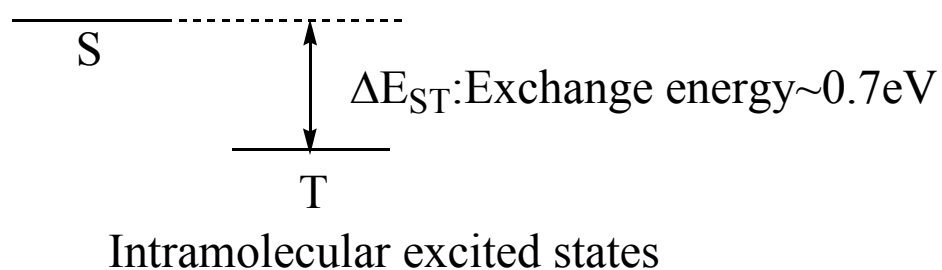


**Figure 1.4 Exchange energy between singlet and triplet in intramolecular excited state.**



### 1.2.2 Intermolecular excited state

The intermolecular excited states are the loosely bounded electron-hole pair located in two molecules with relative long separation distance. In conjugated structure, the electron or hole in single molecule usually is a radical ion in chemistry or a polaron in physics.<sup>11</sup> Therefore, the intermolecular excited states are also called radical ion pairs or polaron pairs. Because of the relative long separation distance, the exchange energy in intermolecular excited state is very small. And the triplet level might be a little bit higher than singlet level, as shown in Figure 1.5. Usually the system exhibiting the emission from charge transfer complex or exciplex under photo excitation could be thought as the system containing intermolecular excited states. Under electrical excitation, the injected electrons and holes can also form the loosely bonded electron-hole pairs (intermolecular excited states).



## Intermolecular excited states

**Figure 1.5 Exchange energy between singlet and triplet in intermolecular excited state.**

## 1.3 Internal magnetic interaction

In general, there are two types of internal magnetic interaction in nonmagnetic organic materials. One is the hyperfine interaction; the other is the spin-orbital coupling. The internal magnetic interaction is responsible for the spin-moment conservation in magnetic field effects. And the internal magnetic interaction can also cause the splitting of the triplet energy levels, which is called internal Zeeman splitting.

### 1.3.1 Hyperfine interaction

Hyperfine interaction is the magnetic dipole interaction between the nucleus spin and the electron spin<sup>12</sup>, as shown in Figure 1.6. The hyperfine interaction widely exists in organic semiconductors. But the hyperfine interaction strength is not strong in organic materials, usually several mT external magnetic field could overcome the hyperfine interaction. It should be noted that the hyperfine interaction is from the spin-spin interaction from nucleus and electron. The spin from nucleus is necessary for hyperfine interaction. For hydrogen atom  $^1\text{H}$ , the nucleus spin is  $1/2$ , it with a hyperfine interaction constant of 507 gauss.<sup>13</sup> But for the  $^2\text{H}$  atom, the hyperfine interaction is much weaker. Therefore, the isotope substitution is an important method to study hyperfine interaction.

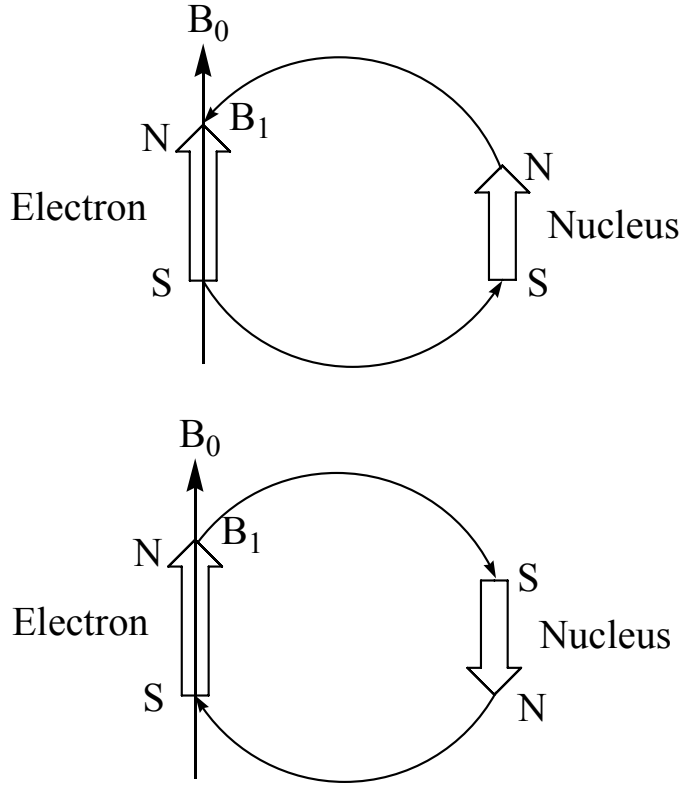


**Figure 1.6 Hyperfine interaction between electron and nucleus.**

### 1.3.2 Spin-orbital coupling

The spin-orbital coupling is the coupling between the electron spin momentum and its orbital angle momentum. From the electron view of point, the nuclear is rotating surround the electron. And the nuclear charge or the atomic number will affect the orbital current. Therefore, the spin-orbital coupling strength will be largely dependent on the atomic number. In hydrogen like atom, the spin orbital coupling strength is proportional to the power 4 of atomic number<sup>14</sup>, as shown in Equation (1.1).

$$SOC \propto Z^4 \quad (1.1)$$

In organic semiconductor the spin-orbital coupling usually is weak due to the light atoms. But if the heavy atoms were introduced into the structure, the spin orbital coupling can be enhanced. It is noted that organic semiconductors can be divided into singlet and triplet semiconducting materials with weak and strong internal magnetic interaction, respectively.

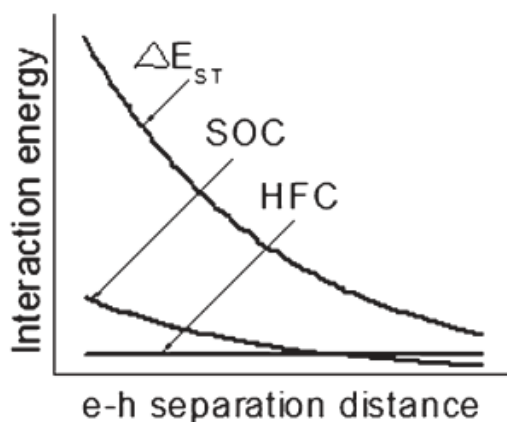


**Figure 1.7 Electron-hole separation distance effect on exchange energy and internal magnetic interaction in excited states in organic semiconductor.**

The internal magnetic field would also be affected by the separation distance. The hyperfine interaction do not change much by the distance while spin orbital coupling strength would change a lot with separation distance<sup>9</sup>, as shown in Figure 1.7.

## 1.4 Energy transfer

Energy transfer is a process commonly existing in organic light emitting devices. It transfers the energy of excited state from one molecule (donor) to another molecule

(acceptor). There are two types of energy transfer, the Förster energy transfer and the Dexter energy transfer.

#### 1.4.1 Förster energy transfer

The mechanism for Förster energy transfer is resonance mechanism associated with the Coulombic interaction between electrons. Förster energy transfer is the long range electric dipole-dipole interaction.<sup>15</sup> Usually it requires the overlap of the photoluminescence spectrum of the donor and the absorption spectrum of the acceptor, as shown in Figure 1.8. The distance between donor and acceptor can be much larger than the molecular diameter; usually it can be 5-10 nm.

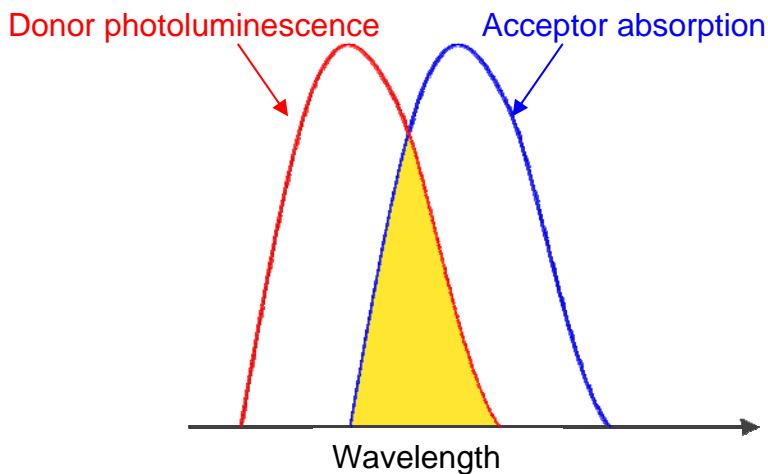


**Figure 1.8 Spectrum overlap requirement for Förster energy transfer process.**

In principle, the Förster energy transfer is allowed from donor singlet to acceptor singlet but not from donor triplet to acceptor singlet; because the latter is spin forbidden. However, because the triplet radiation decay is also spin forbidden, the triplet states will

have very long lifetime. Then the energy transfer will also occur by the resonance mechanism because the small transfer rate will be compensated by the long lifetime of donor triplet.

#### **1.4.2 Dexter energy transfer**

Dexter energy transfer is based on the exchange interaction between electrons. Therefore, it requires the overlap of electron clouds between the donor and acceptor. At the overlap region of electron clouds of donor and acceptor, the excited electron of donor may also appear on acceptor. The Dexter energy transfer happens at short range, usually 0.5-1 nm<sup>16</sup>. The donor and acceptor should be much closer than the resonance mechanism energy transfer (Förster energy transfer). The Dexter energy transfer follows the spin conservation. Only singlet to singlet and triplet to triplet transfers are allowed, as shown in Figure 1.9.

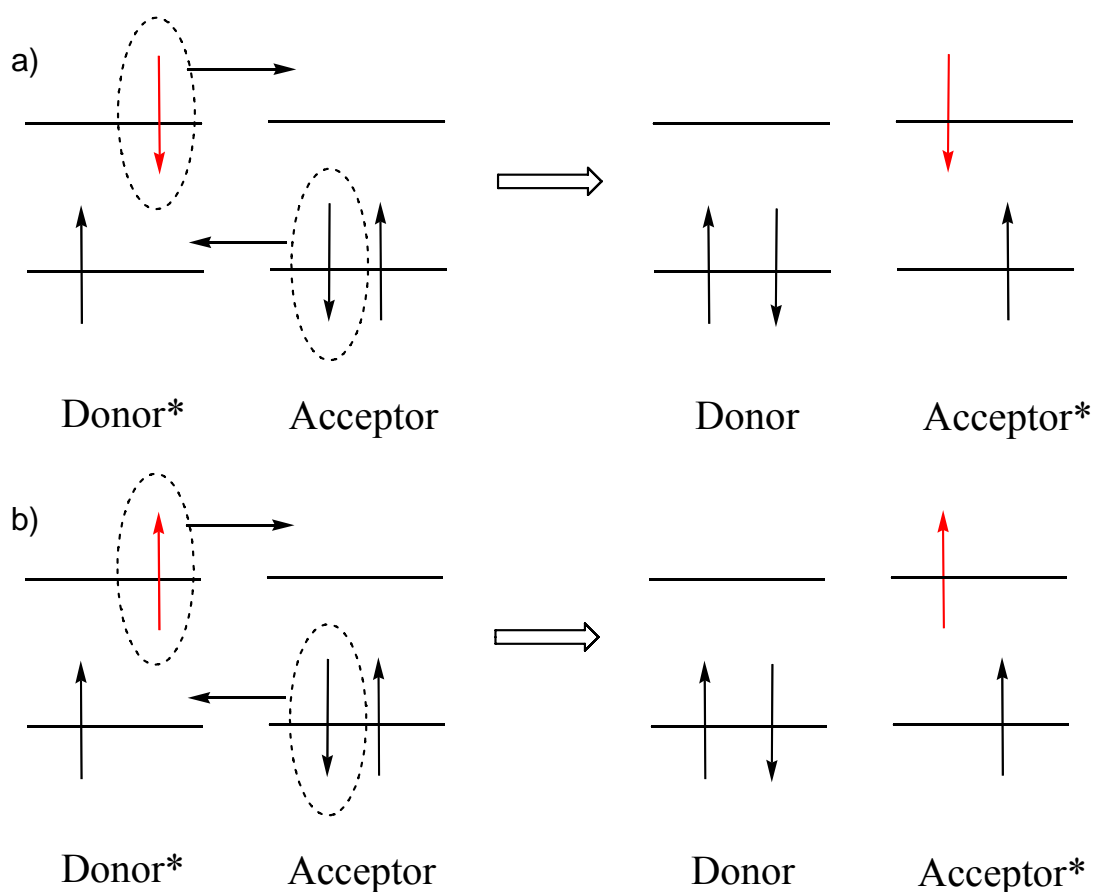


**Figure 1.9 Scheme for Dexter energy transfer process, a) from donor singlet to acceptor singlet, b) from donor triplet to acceptor triplet.**

## 1.5 Magnetic field effect

It has been found that non-magnetic organic semiconductors can show some magnetic responses in low magnetic field (several hundred mT). When applying magnetic field, the electroluminescence (EL),<sup>17- 23</sup> electric current (EC),<sup>18,24- 43</sup> photocurrent (PC)<sup>44- 50</sup> and even photoluminescence (PL)<sup>46,51- 56</sup> could change with magnetic field. In general, these responses were called magnetic field effects (MFEs), and these magnetic responses were

called MFE on electroluminescence ( $\text{MFE}_{\text{EL}}$ ), organic magnetoresistance or magnetocurrent (OMR or MC), MFE on photocurrent (MFP) and MFE on photoluminescence ( $\text{MFE}_{\text{PL}}$ ), correspondingly. People have found the magnetic field effect is generated through spin-dependent process. But the detailed mechanism for magnetic field effect is still unclear. Several models have been proposed and the problem which spin dependent process is the direct responsible for the magnetic field effect are under studying. And the one of the internal magnetic interaction hyperfine interaction has been supposed to dominantly affect the spin-dependent process.<sup>57,58</sup> While in another singlet semiconducting material  $\text{Alq}_3$ , whose spin orbital coupling strength is relative stronger,<sup>59</sup> no clear hyperfine effect was observed.<sup>60</sup> But the conclusion was made in weak spin-orbital coupling organic semiconductor. The other type of organic semiconductor, the strong spin-orbital coupling organic semiconductor, has got less attention. Only little work has been done in the strong spin-orbital coupling organic semiconductor.<sup>26, 61-63</sup> On the other hand, in the strong spin-orbital coupling organic semiconductor, spin-orbital coupling is much stronger than the hyperfine interaction. The hyperfine interaction might not be the main reason responsible for magnetic field effects. Therefore, the study of magnetic field effects in strong spin-orbital coupling organic semiconductor is important to get a whole view of the origin of the magnetic field effects in nonmagnetic organic semiconductors. This dissertation will clarify the generation mechanism of magnetic field effect in nonmagnetic organic semiconductors and further explore how the strong internal magnetic interaction-spin-orbital coupling affecting the magnetic field effect.



In general, magnetic field has two effects: Zeeman Effect and momentum effect.

The Zeeman Effect is the splitting of the three triplet levels under external magnetic field, as shown in Figure 1.10. The splitting energy for an electron is proportional to the external magnetic field strength, as expressed in Equation (1.2).

$$\Delta E_{split} = g\mu_B B \quad (1.2)$$

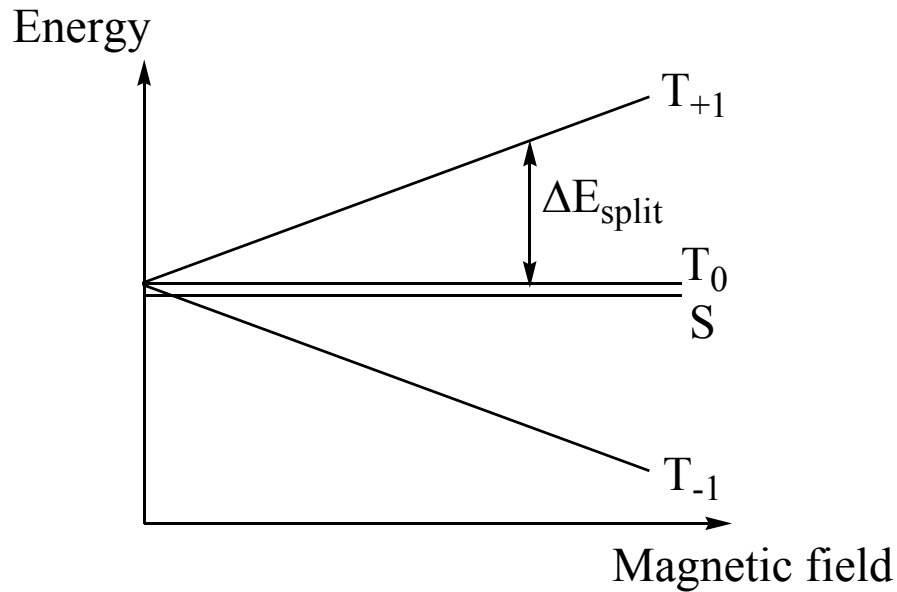


**Figure 1.10 Zeeman splitting effect on energy level in intermolecular excited states.**

Here,  $g$  is the  $g$ -factor, (usually around 2, 2.0023192 for a free electron)<sup>64</sup>, the  $B$  the magnetic field strength, and  $\mu_B$  is the Bohr magneton,  $9.27400915(23) \times 10^{-24}$  J/T. From here we can get the splitting energy is about in the order of  $10^{-5}$  eV, with the magnetic field we are using, about 300mT. It is much smaller than the exchange energy of

intramolecular exchange energy. Therefore, the magnetic field effect usually is not from the intramolecular excited states.

It is noted that spin-dependent processes must require spin momentum conservation to occur. The spin-momentum conservation can be satisfied by internal magnetic interaction. When an external magnetic field is comparable to internal magnetic interaction, the spin-momentum conservation can be partially affected. The influenced spin-momentum conservation can essentially affect the spin-dependent processes, consequently generating MFEs in electroluminescence, photoluminescence, photocurrent, electrical current.

## **1.6 Mechanism of Magnetic Field Effect**

The mechanism for magnetic field is not very clear yet. There are several mechanisms based on different spin dependent processes. And for different magnetic field effect channel, the mechanisms are slightly different. In general according to the spin dependent processes, there are three types of mechanism for magnetic field effects: bipolaron mechanism, intersystem crossing mechanism and exciton quenching mechanism. The bipolaron mechanism is focus on the mobility related process. The intersystem crossing mechanism focus on the dissociation or recombination related process. The exciton quenching mechanism is focus on the spin dependent exciton quenching process especially for the triplet exciton quenching process due to the long lifetime of triplet exciton.

### 1.6.1 Intersystem crossing model (polaron pair model)

The intersystem crossing (ISC) model is based on the magnetic field change the spin dependent intersystem crossing in intermolecular excited states (polaron pairs). Therefore, the intersystem crossing model also is called polaron pair model. This model has been widely used in  $\text{MFE}_{\text{PL}}$ ,<sup>46,51-55</sup>  $\text{MFE}_{\text{EL}}$ ,<sup>18,19</sup>  $\text{MFP}$ <sup>44-48</sup> and MC (or OMR)<sup>18,26,31,38,39</sup>. The intersystem crossing is the transition between the singlet and triplet levels. In the intramolecular excited state under photo excitation, most of the excitons are in singlet configuration. But in the intermolecular excited state under electrical excitation, the singlet/triplet ratio has the limit of 25%, if the spin orbital coupling effect is not considered. The main idea of ISC model is the singlet/triplet ratio changed by magnetic field through the spin-dependent ISC process, as shown in Figure 1.11.

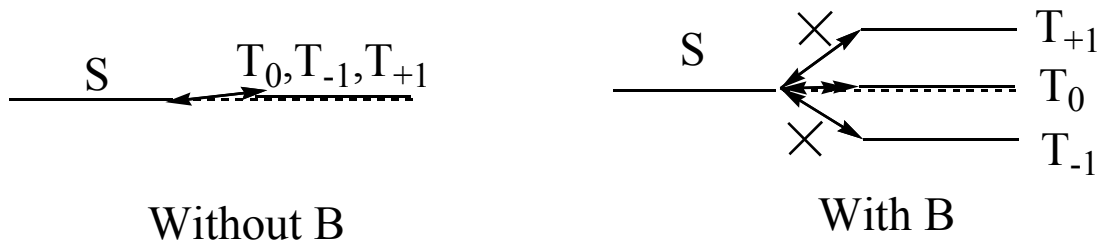


**Figure 1.11 Zeeman Effect on intersystem crossing in intermolecular excited states.**

At zero magnetic field, in intermolecular excited state, the three triplet level is degenerated and the singlet state is with similar energy due to the small exchange energy. Therefore, the intersystem crossing from singlet states to the three triplet states is all efficient. When applying external magnetic field, the degenerate triplet excited state energy level could be split into three non-degenerate triplet energy levels due to external

Zeeman Effect. Thus the intersystem crossing between the singlet excited state and triplet excited states ( $T_{-1}$  and  $T_{+1}$ ) would be partially blocked due to splitting energy larger than exchange energy. But people hold different opinion on the intersystem crossing result, whether the singlet states increase or the triplet states increase. Because of the large different exchange energy, this effect is significant for intermolecular excited states, polaron pair (PP) states, but can be ignored for relative intramolecular excited states, excitons. Therefore, the singlet/triplet ratio in PP state could be obviously changed by external magnetic field. The singlet and triplet polaron pairs could further dissociate into free electrons and holes to generate current or become closer to form excitons and finally give out emission, as shown in Figure 1.12.

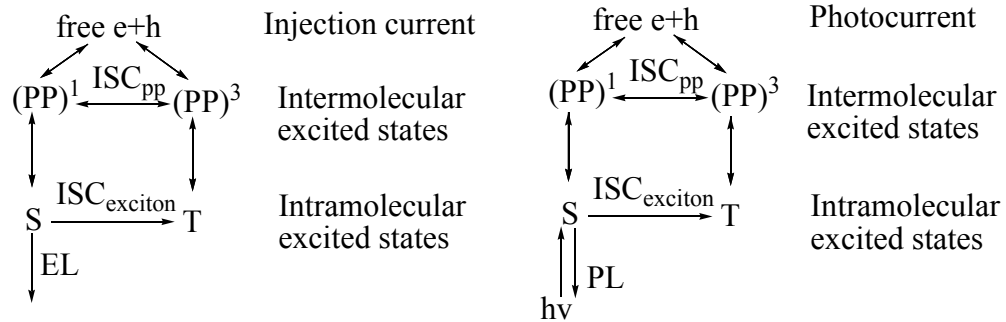


**Figure 1.12 The relationship between intermolecular excited states (PPs) and emission or current.**

And the contribution of singlet and triplet polaron pairs for dissociation<sup>18,44,45,47,48,65</sup> or recombination<sup>26,31,38,39</sup> was different. As a result of the change in singlet/triplet ratio in PP states by external magnetic field, the emission (EL or PL) or the current (photocurrent or dark current) would change with external magnetic field. Thus the external magnetic field

changed the intersystem crossing in order to change singlet/triplet polaron pair ratio and further give the magnetic responses.

### 1.6.2 Bipolaron model

The bipolaron model<sup>26,66</sup> is based on the spin dependent bipolaron formation mechanism. It is used in OMR (MC) and  $\text{MFE}_{\text{EL}}$ . Two polarons with the same polarity in the organic semiconductors can form a bipolaron with two charges when the bipolaron is energy favorable.<sup>67</sup> Figure 1.13 shows the polaron and bipolaron in polythiophene.

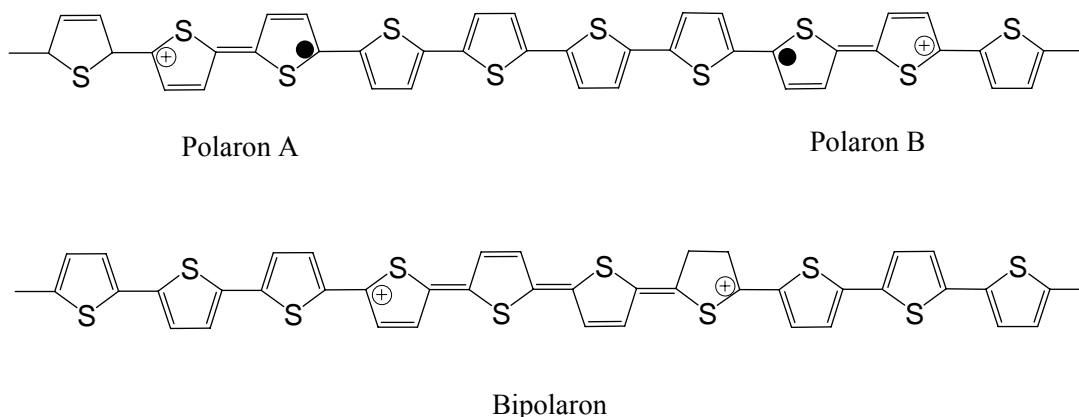


**Figure 1.13 Two polarons and one bipolaron in polythiophene.**

The bipolarons also have singlet and triplet spin configuration. And the mobility of singlet bipolaron is larger than the triplet bipolaron because the triplet bipolaron has the spin block effect, as shown in Figure 1.14. At zero magnetic field, the singlet configuration in bipolaron is the dominate component in organic semiconductors because the spin-spin interaction between the two polarons will low the energy of singlet

bipolaron. After applied the magnetic field the triplet bipolaron formation would increase due the interruption to the spin-spin interaction from external magnetic field. As a result, the triplet configuration in bipolaron gets increased. Due to its low mobility compared to the singlet bipolaron, the average mobility would be reduced. It would lead to the decrease of current, which means positive magnetoresistance.

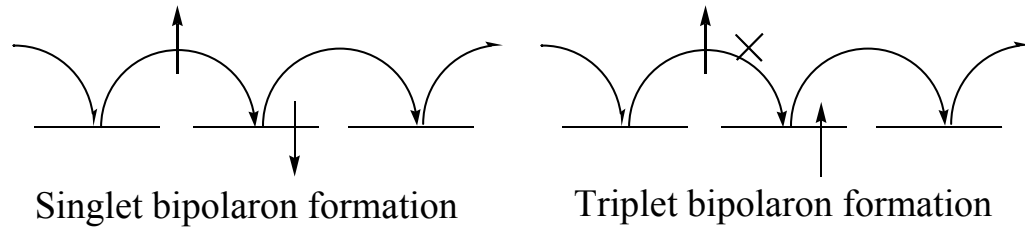


**Figure 1.14 The spin blocking effect in triplet bipolarons.**

The bipolaron mode also has been used to explain the negative magnetoresistance through the theoretical calculation.<sup>24</sup> A negative sign can be obtained when also including long range Coulomb repulsion. The long range Coulomb repulsion is believed to enhance bipolaron formation. When more bipolarons are formed, there are less free carriers to carry a current. By applying a magnetic field, the number of bipolarons is decreased but the number of free charge carriers is increased, which gives a negative OMR.

### 1.6.3 Exciton quenching model

Exciton quenching model is based the spin dependent exciton quenching process, which includes: exciton-charge reaction and exciton-exciton annihilation. In the past, TCR model and TTA model were used in MFE<sub>PL</sub>. But recently people also used in MC and MFE. Both of them are focus on the triplet exciton quenching process because of the long

lifetime of triplet exciton. Therefore, they can be called triplet-charge reaction (TCR) model<sup>31,34,35,40</sup> and triplet-triplet annihilation (TTA) model.<sup>68,69</sup>

The TCR model is based on the triplet exciton react with free or trapped charge carrier, as shown in Equation (1.3)<sup>70,71,72</sup> and Equation (1.4)<sup>73,74</sup>. The reaction can generate extra charge carrier in the organic semiconductor. It has been found that the rate constant of TCR process can be reduced by the external magnetic field.<sup>75,76</sup> As a result, the generated free carriers were reduced by magnetic field.



The TTA process is two triplet excitons collide with each other and eventually annihilate into a singlet exciton, generating a delayed fluorescence, as shown in Equation (1.5).<sup>77</sup> It has been observed that the negative MFE for the delayed fluorescence in organic molecular crystals and proposed that magnetic field can modulate the triplet-triplet annihilation (TTA) reaction rate constant.<sup>78,79</sup>



#### 1.6.4 Our model

Our model combined the intersystem crossing and triplet charge reaction mechanism.<sup>28,65</sup>

The intersystem crossing was changed by magnetic field. Then the singlet ratio in polaron pair state was increased while the triplet polaron pair ratio was reduced. This would lead to the increase in singlet exciton and consequently get the increasing in

electrofluorescence (EL), which means positive MFE on EL. The singlet polaron pairs were easier dissociated to free charge carriers than triplet polaron pairs.<sup>80,81</sup> This caused the current increasing; it meant resistance decreasing or negative OMR. Therefore, singlet related MFE is always positive to emission and current. The triplet excited states could react with free or trapped charges to generate free charges. But this reaction rate would be suspended by increasing external magnetic field. Either the density of triplet polaron pairs or triplet excitons reducing or the triplet charge reaction rate reducing could deduce the density of free charges, which produced by triplet charge reaction. This meant the current density decreasing, the resistance increasing or positive MR. And the reduced charge carrier will further cause the decrease in secondary polaron pairs, which were generated by the charge carrier produced by triplet-charge reaction. It might lead to the decrease in EL, which is the negative MFE on EL. Therefore, triplet related MFE are always negative for fluorescence emission and current. In this way, we can get both positive and negative MFE on EL and current. In the device, the MFE on EL and current should be the sum of these two components. Then it can generate the transition of MFE on EL or OMR from positive to negative or from negative to positive, as shown in Figure 1.15.



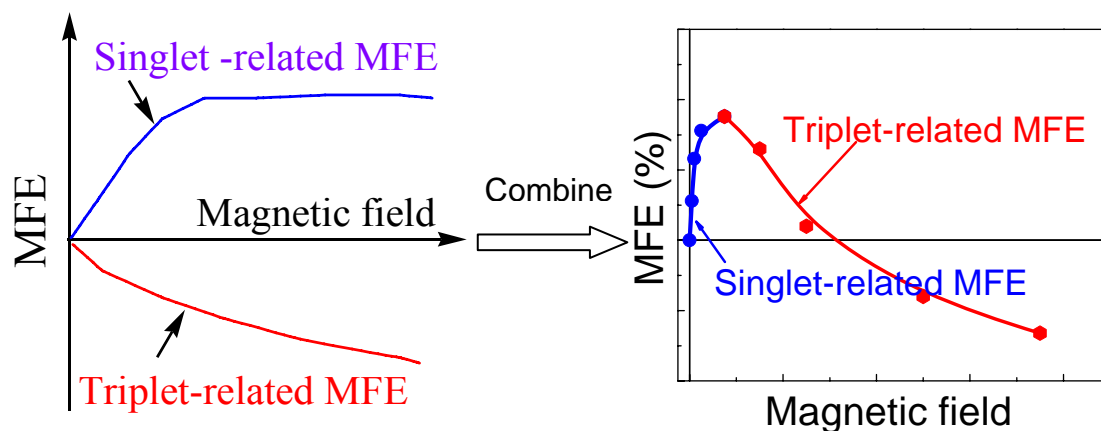


**Figure 1.15** The combination of positive and negative MFE on EL and MR.

## 1.7 Summary and outline for the dissertation

This dissertation topic is to clarify the generation mechanism of magnetic field effect in nonmagnetic organic semiconductors and further explore how the strong internal magnetic interaction-spin-orbital coupling affecting the magnetic field effect. The magnetic field effect in non-magnetic organic semiconductor has been found in PL, EL, PC and EC. People have found the magnetic field effect is generated through spin-dependent process. But the detailed mechanism for magnetic field effect is still unclear. Several models have been proposed and the problem which spin dependent process is directly responsible for the magnetic field effect is still under studying. And the one of the internal magnetic interaction, hyperfine interaction, has been supposed to dominantly affect the spin-dependent process. But the conclusion was made in singlet dominate

organic semiconductor, such as DOO-PPV and PFO. The other type of organic semiconductor, the triplet dominate organic semiconductor such as Ir(ppy)<sub>3</sub>, has got less attention. Only little work has been done in the triplet organic semiconductor. On the other hand, in the triplet dominated organic semiconductor, another magnetic interaction, spin-orbital coupling is much stronger than the hyperfine interaction. The hyperfine interaction might not be the main reason responsible for magnetic field effects. Therefore, the study of magnetic field effects in strong spin-orbital coupling organic semiconductor is important to get a whole view of the origin of the magnetic field effects in nonmagnetic organic semiconductors. In this dissertation, the following concepts will be discussed.

- 1) Energy transfer effect on MFE in polymer blend with different spin orbital coupling strength.
- 2) The role of intermolecular excited state in MFE and the two important factors: separation distance and spin orbital coupling.
- 3) The role of intermolecular spin-orbital coupling plays in magnetic field effects in the system only exist spin orbital coupling strength.
- 4) Interface induced negative phosphorescence magnetic field effect in strong spin orbital coupling system.
- 5) A new type of magnetic field effect: Magneto-capacitance effect in organic radical-based materials.
- 6) The comparison of magnetocurrent between magnetic and nonmagnetic organic semiconductors.

This dissertation contains 9 chapters. Chapter 1 will give the introduction to related information about the magnetic field effect in organic semiconductors. Chapter 2 will present the device fabrication condition and experiment method for studying magnetic field effect. Chapter 3 will discuss the important role of intermolecular excited states in magnetic field effect and will present the factors, the separation distance and spin orbital coupling, which can affect magnetic field effect in intermolecular excited states. Chapter 4 will discuss the magnetic field effect in the system energy transfer effect combined with spin orbital coupling effect. Chapter 5 will discuss the magnetic field effect in the system only with spin orbital coupling effect and without energy transfer effect. In Chapter 6, the interface induced magnetic field effect in strong spin-orbital coupling system will be discussed. Chapter 7 will introduce a new magnetic field effect in organic semiconductor; the spin orbital coupling effect on this new magnetic field effect is also discussed. Chapter 8 will compare the magnetic field effect in magnetic and nonmagnetic organic semiconductor with median spin-orbital coupling strength. Chapter 9 will give the summary of this dissertation.

## CHAPTER 2

### DEVICE FABRICATION AND MEASUREMENT

#### 2.1 Device fabrication

The magnetic field effect measurements except magnetic field effect on photoluminescence ( $\text{MFE}_{\text{PL}}$ ) almost are based on sandwich structure devices, such as magnetic field effect on electroluminescence ( $\text{MFE}_{\text{EL}}$ ), magnetocurrent (MC), organic magnetoresistance (OMR), magneto-capacitance (MCP) and magnetic field effect on photoluminescence (MFP). The device fabrication is the important first step for magnetic field effect measurements, which require stable, efficient devices. The device fabrication contains following steps:

- 1) Making electrode fingers: Indium tin oxide (ITO) half coated glass is purchased from Shenzhen Nanbo Company in China. The thickness of ITO film is around 200 nm with the average roughness 2 nm. The electrical and optical measurement shows the electrical square resistance is about  $15 \Omega/\square$  and the optical transmission is over 85 %. Four 4cm long copper wires are connected on the ITO glass by Microcircuit Silver - Type L epoxy from Transene Company. The structure of ITO glass is shown in Figure 2.1. The silver epoxy is cured on hotplate at  $175^{\circ}\text{C}$  for 15 minutes.

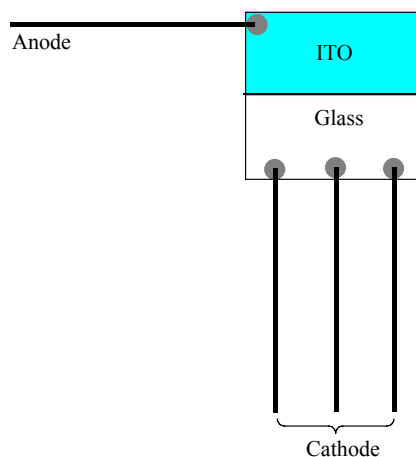


**Figure 2.1 The ITO glass with four electrode fingers.**

- 2) Cleaning: The cooled ITO glass with four fingers was put into a 250ml beaker with a PTFE holder. They are cleaned in ultrasonic bath by deionized water with cleaning agent, deionized water twice, acetone and chloroform in sequence. Each solvent will clean for 15 minutes. After that, the ITO glass was dried in vacuum oven for 30 minutes.
- 3) Solution preparation: certain amount polymer or small molecules were weighted by Ohaus AP2500 balance. The chemicals will be transferred into a glove box with nitrogen gas protection. The polymers will be dissolved by solvents in pre-cleaned sample vials, and placed on the shaker to shake until the polymers are completely dissolved. After that the solution will be filtrated by Millipore 13mm Nonsterile Millex Filter with Hydrophobic PTFE Membrane (Pore Size: 0.2  $\mu\text{m}$  or 0.45  $\mu\text{m}$ ).
- 4) Spin coating: The pre-cleaned ITO glass with electrode fingers was placed on the holder of the EC101D spin coater from Headway Research Inc in the glove box with nitrogen gas protection. The solution after filtration was dripped on the pre-cleaned

ITO glass. The ITO glass will rotate at certain speed controlled by the spin coater. After the spin coater stopped, the polymer film was formed on top of the ITO glass. The typical thickness of the polymer layer is 70-100 nm.

- 5) Metal electrode evaporation: The ITO glass with polymer films was taken out from the glove box and put into the chamber of a Cooke CV301-T-FR2 vacuum thermal evaporator. At the same time, the ITO glass was covered by a shadow mask. The whole system was pumped by a mechanic pump until the vacuum reached  $2 \times 10^{-2}$  Torr. Then the system was continued pumping by a turbo pump until the vacuum reached  $2 \times 10^{-6}$  Torr. The metal used as cathode, such as aluminum, was thermal evaporated. The typical thickness of the metal layer is about 30-50 nm. After cool down, the device was taken out from the evaporator and stored in vacuum. The structure of the device is shown in Figure 2.2. The effective area of the electrode is  $0.05 \text{ cm}^2$ .

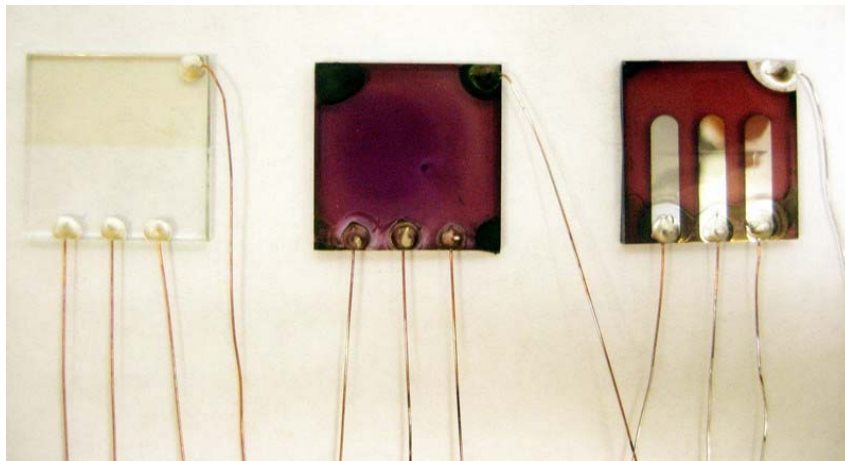


**Figure 2.2 The picture of device, the left is the ITO glass with electrode fingers, the middle is the device after spin coating of polymer solution, and the right is the final device after thermal evaporation of aluminum.**

## 2.2 Magnetic field effect measurement

Magnetic field effect measurement includes the magnetic field effect on photoluminescence ( $\text{MFE}_{\text{PL}}$ ), magnetic field effect on electroluminescence ( $\text{MFE}_{\text{EL}}$ ), magnetocurrent (MC), organic magnetoresistance (OMR), magneto-capacitance (MCP) and magnetic field effect on photoluminescence (MFP). The magnetic field was applied by an electromagnet from Newport Instrument. The power of the electromagnet is supplied by Sorensen DLM 80-7.5 Programmable DC Power Supply controlled by a Labview program. The typical magnetic field scan process is keeping at 0 mT for 50 seconds then increasing from 0 to 320mT in 50 seconds and decreasing back to 0 mT again in another 50 seconds, and keeping at 0 mT for the last 50 seconds. The experiment setup of MFP measurement is shown in Figure 2.3 as an example.

### 2.2.1 Magnetic field effect on photoluminescence ( $\text{MFE}_{\text{PL}}$ ) measurement

The sample for  $\text{MFE}_{\text{PL}}$  measurement, which is the polymer film spin coated on glass substrate or solution in quartz cuvette, is placed in the dark room between the two poles of electromagnet at room temperature under the protection of nitrogen gas. The excitation light source is the Xenon lamp of Fluorolog®-3 spectrofluorometer from Jobin Yvon Inc or Kimmon IK series He-Cd laser (325 nm). A liquid light guide is used to guide the light to the sample. The photoluminescence from the sample is also guided by another liquid light guide to the detector of Fluorolog®-3 spectrofluorometer and recorded in time-based acquisition mode when the typical magnetic scan process is running. The  $\text{MFE}_{\text{PL}}$  is defined as Equation 2.1, where  $I_B$  and  $I_0$  are the photoluminescence intensity with and without magnetic field, correspondingly.

$$MFE_{PL} = \frac{I_B - I_0}{I_0} \times 100\% \quad (2.1)$$

### 2.2.2 Magnetic field effect on electroluminescence (MFE<sub>EL</sub>) measurement

The organic light emitting device is placed in the tube containing liquid nitrogen in the gap of the electromagnet in the dark room. The Keithley 2400 General-Purpose Source Meter is used as the power source to drive the OLED. To avoid the current response effect under magnetic field (MC or OMR effect), the OLED is driven under constant current mode. Usually the MFE<sub>EL</sub> is measured at 1mA current. The electroluminescence signal is guided to the detector of Fluorolog®-3 spectrofluorometer by a liquid light guide and recorded in time-based acquisition mode when the typical magnetic scan process is running. The MFE<sub>EL</sub> is defined as Equation 2.2, where  $I_B$  and  $I_0$  are the electroluminescence intensity with and without magnetic field, correspondingly.

$$MFE_{EL} = \frac{I_B - I_0}{I_0} \times 100\% \quad (2.2)$$

### 2.2.3 Magnetic field effect on photocurrent (MFP) measurement

The device for MFP measurement is placed in the dark room between the two poles of electromagnet at room temperature under the protection of nitrogen gas. The excitation light source is the Xenon lamp of Fluorolog®-3 spectrofluorometer or Kimmon IK series He-Cd laser (325 nm) or 100mW/cm<sup>2</sup> white light with the standard sun light spectrum from 67005 Newport 300W sun simulator. A liquid light guide is used to guide the light to the sample. The photocurrent signal was monitored by Keithley 2400 General-Purpose



Source Meter at constant voltage of 0 V when the typical magnetic scan process is running. The  $MFE_{PL}$  is defined as Equation 2.3, where  $I_B$  and  $I_0$  are the photocurrent with and without magnetic field, correspondingly. The experiment setup of MFP measurement is shown in Figure 2.3 as an example.

$$MFP = \frac{I_B - I_0}{I_0} \times 100\% \quad (2.3)$$

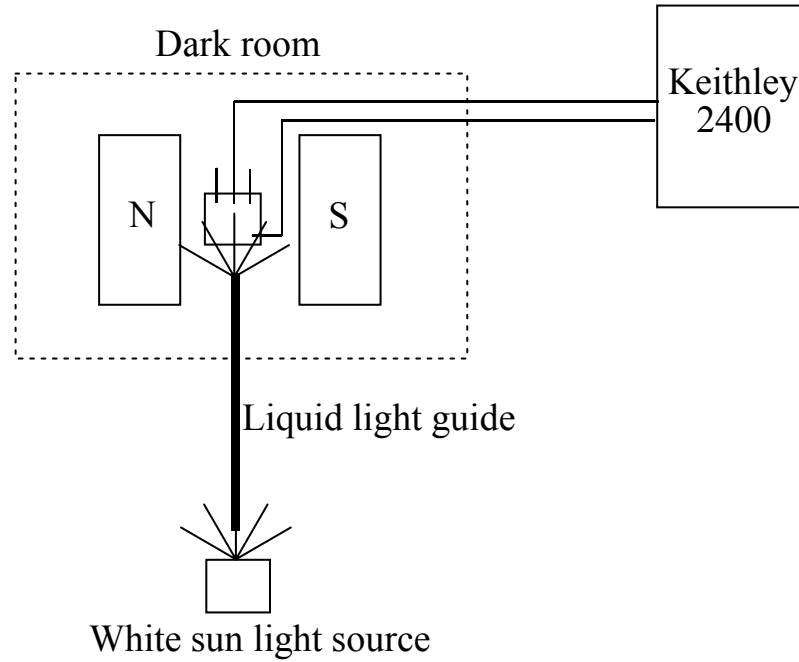


**Figure 2.3 The experiment setup for MFP measurement.**

#### **2.2.4 Magnetocurrent (MC) or organic magnetoresistance (OMR) measurement**

The device is placed in the tube containing liquid nitrogen in the gap of the electromagnet in the dark room. For OMR measurement, the device can be driven in constant current mode or constant voltage mode. Due to the magnitude of the magnetic response is much

smaller in constant current mode, we choose constant voltage mode to measure OMR, which can also be called MC. The MC or OMR are compared at same current density from different devices. The current in the device is monitored by Keithley 2400 General-Purpose Source Meter when the typical magnetic scan process is running. The MC is defined as Equation 2.4, where  $I_B$  and  $I_0$  are the current with and without magnetic field, correspondingly.

$$MC = \frac{I_B - I_0}{I_0} \times 100\% \quad (2.4)$$

The OMR is defined as Equation 2.5, where  $R_B$  and  $R_0$  are the electric resistance with and without magnetic field, correspondingly.

$$OMR = \frac{R_B - R_0}{R_0} \times 100\% \quad (2.5)$$

If consider the constant voltage mode and combine Ohm's law  $R=V/I$ , where  $R$  is the resistance,  $V$  is the voltage and  $I$  is the current, we can get  $OMR = \frac{I_0 - I_B}{I_B} \times 100\%$ , where

$I_B$  and  $I_0$  are the current with and without magnetic field, correspondingly. The relationship between MC and OMR is  $MC = -OMR \times \frac{1}{1 + OMR}$ , if OMR is small, then  $MC \approx -OMR$ .

### 2.2.5 Magneto-capacitance (MCP) measurement

The device for MCP measurement is placed in the dark room between the two poles of electromagnet at room temperature under the protection of nitrogen gas. The capacitance of the device was measured by Agilent E4980A Precision LCR meter at time based

acquisition mode with fixed frequency, 0 V DC bias and 50 mV AC voltage. The MCP can be measured with light illumination or without light illumination. When MCP is measured with light illumination, the light source is 100mW/cm<sup>2</sup> white light with the standard sun light spectrum. The light is guided to device by liquid light guide. The MCP is defined as Equation 2.6, where  $C_B$  and  $C_0$  are the capacitance of the device with and without magnetic field, correspondingly.

$$MCP = \frac{C_B - C_0}{C_0} \times 100\% \quad (2.6)$$

### 2.3 Other measurement

Photoluminescence and electroluminescence spectrum are measured by Fluorolog®-3 spectrofluorometer. The optical absorption spectrum is measured by PerkinElmer Lambda 35 UV/VIS spectrometer. The film thickness is measured by Veeco diCaliber (004-1001-000) Atomic Force Microscope. C-V measurement is taken by Agilent E4980A Precision LCR meter with 50mV AC voltage at 300Hz-500Hz.

**CHAPTER 3**

**INTERMOLECULAR EXCITED STATE RESPONSIBLE FOR**

**MAGNETIC FIELD EFFECT**

### 3.1 Introduction

Magnetic responses have been found in many organic semiconductors, including the magnetic responses in, electroluminescence (EL)<sup>17-23</sup>, photocurrent (PC)<sup>44-50</sup>, current or resistance<sup>18,24-43</sup> and photoluminescence (PL)<sup>46,51-56</sup>. All these responses were called magnetic field effects (MFEs), and named as MFE<sub>PL</sub>, MFE<sub>EL</sub>, MFE<sub>PC</sub> and MFE<sub>C</sub> correspondingly. These magnetic responses were supposed coming from same origin, excited states (electron-hole pairs)<sup>65</sup>. The excited states have both singlet and triplet states with different spin precessions. When applying magnetic field, it can not only disturb the spin precession of the excited states but also split the triplet excited state sublevels. And then the magnetic field would lead to the change of ratio of singlet/triplet states. Because the singlet and triplet states have different contribution to emission and transport properties through excited state dissociation<sup>80,81</sup> and excited state charge reaction processes<sup>70-75</sup>, different magnetic responses could be found. We found the electron-hole separation distance played an important role in determining the magnetic field effects. The electron-hole distance can affect the magnetic field effect on disturbing spin precession and ratio of splitting energy and exchange energy, it leads to the difference in MFEs of intermolecular excited states (relative long distance) and intramolecular excited states (relative short distance). By affecting the exchange energy between singlet and triplet states, strong donor-acceptor interaction could change the magnetic responses. The spin orbital coupling is also important for magnetic response. If the magnetic field could not compete with spin orbital coupling, it could not affect spin precession and generate MFEs.

## 3.2 Experiment

poly(N-vinylcarbazole) (PVK), 1,2,4,5-tetracyanobenzene (TCNB), pyrene (Py), N,N-dimethylaniline (DMA), tetrahydrofuran (THF), dimethylformamide (DMF), polystyrene (PS), poly(methyl methacrylate) (PMMA), poly(acrylonitrile) (PAN), polyethylene glycol (PEG) are purchased from Sigma-Aldrich. Bis(2-(9,9-dibutylfluorenyl)-1-isoquinoline(acetylacetonate) Iridium (III) (Ir77), Iridium (III) bis(2-(4,6-difluorephenyl)pyridinato-N,C2) (Ir65) are purchased from American Dye Source, Inc. The magnetic field effect measurement is as mentioned in Chapter 2.

## 3.3 Intermolecular excited states responsible for MFEs

It has been found that the PVK and TCNB, whose chemical structures are shown in Figure 3.1, can form charge transfer complex in ground state.<sup>46,51</sup> And the charge transfer complex could be excited and give out photoluminescence from the singlet charge transfer complex. The fluorescence from charge transfer complex also shows MFE.<sup>46,51</sup>

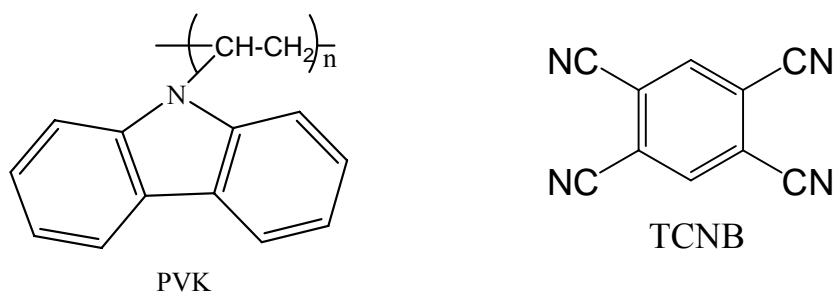


**Figure 3.1** The chemical structure of PVK and TCNB.

We also found magnetic field effect on PL from the charge transfer complex emission but not from the emission of pure component PVK, as shown in Figure 3.2. It is clear that the new peak after mixing the two materials, indicating the formation of charge transfer complex. After introducing these intermolecular excited states, obvious  $\text{MFE}_{\text{PL}}$  could be observed. But for single component, no  $\text{MFE}_{\text{PL}}$  could be observed due to the lack of relative large separation distance electron-hole pairs.

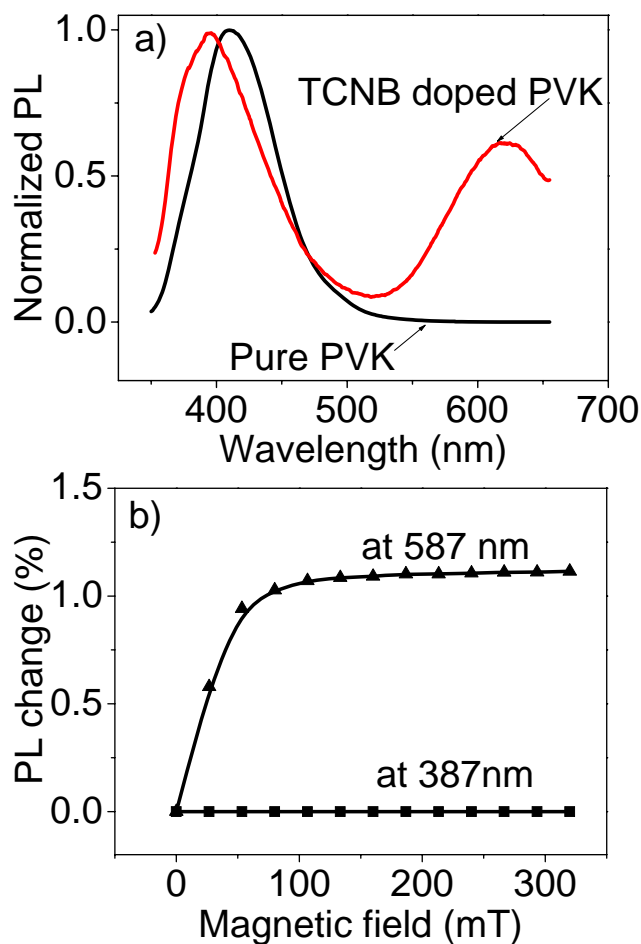


**Figure 3.2 a) The PL spectrum of PVK and TCNB doped PVK b) MFE of PL for pure PVK and 1wt% TCNB doped PVK.**

It should also be noted that in the system of composite of PVK and TCNB, MFP, MFE on EL and MC can be observed, shown in Figure 3.3. The MFE on PL and MFP are both positive, which is well fit our model, singlet states would increase with magnetic field but not the triplet states. The MFE on PL is the direct reflection of the singlet exciton. It indicates the increase of singlet state in polaron pair states. And under electrical excitation, the situation is similar. Both the emission from singlet exciton and the current increase with magnetic field, which also indicates the singlet excited states ratio is increasing under external magnetic field. It should be noted that both of the emission and the current enhanced by the external magnetic field. It suggests the singlet polaron pair can contribute to the recombination and dissociation at the same time.



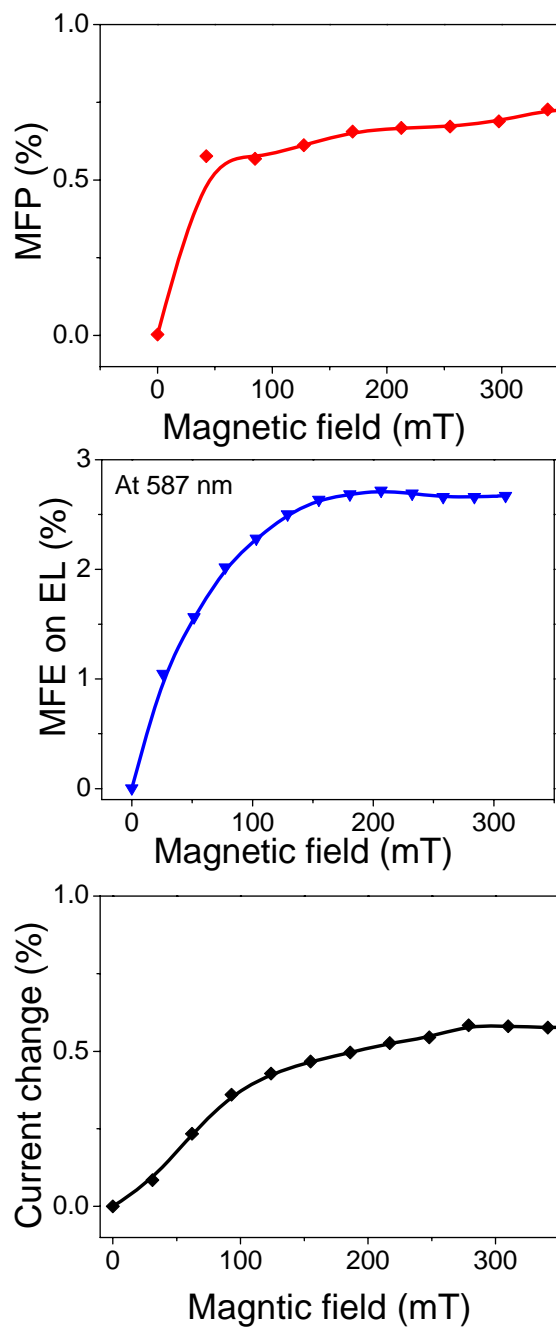


**Figure 3.3 The MFP,  $MFE_{EL}$  and MC of 1wt% TCNB doped PVK.**

### 3.4 Separation distance study of singlet exciplex in liquid state

We studied the well known liquid state exciplex system Py and DMA for magnetic field effect on photoluminescence<sup>52,53</sup> their chemical structure is shown in Figure 3.4.

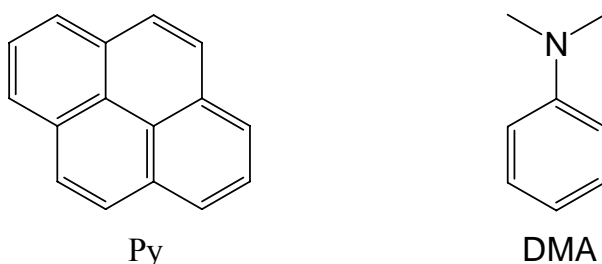


**Figure 3.4 Chemical structures for Py and DMA.**

People have studied the magnetic field effect on the PL of the exciplex formed between Py and DMA.<sup>52,53</sup> Figure 3.5a shows the exciplex PL spectrum with the PL spectrum for each single component. And the MFE on PL were also studied. The exciplex (intermolecular excited state) showed clear MFE on PL, while the single component (intramolecular excited state) did not show MFE on PL. This is consistent with the singlet exciplex in solid state (PVK+TCNB system). It further support that intermolecular excited state is important for magnetic field effect. The external magnetic field can change the singlet/triplet ratio in intermolecular excited state. When there is no external magnetic field, the internal magnetic field such as hyperfine interaction and spin orbital coupling would flip the spin momentum. After apply external magnetic field, if the external magnetic field is comparable to internal magnetic field, it will disturb the

internal magnetic field modulated ISC to get a new ratio between singlet and triplet states.

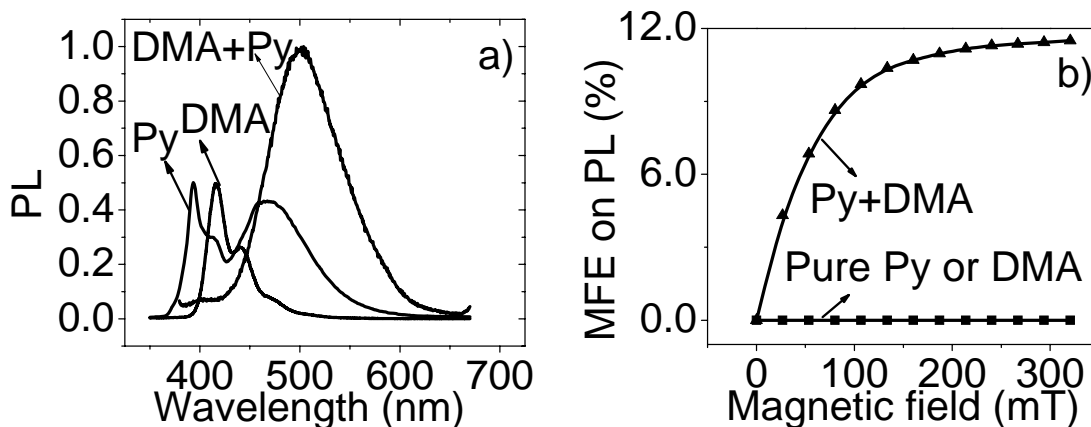


**Figure 3.5 a) PL spectrum of single component and exciplex of Py+DMA system, b) MFE on PL of single component and exciplex of Py+DMA system in solution, the solvent is the mixture of THF and DMF, THF:DMF=3:7 (volume ratio).**

Because the internal magnetic interaction is weak interaction it is very sensitive to the distance between electron and hole. The interaction reduces very fast when increasing the distance. Therefore, the magnetic field effects show strong dependent on the distance, the larger distance lead to weaker internal magnetic interaction causing larger MFE. In Figure 3.6, by changing the concentration of the liquid solution, we changed the distance between electron and hole. The PL spectrums were shifted and the  $MFE_{PL}$  showed clear decreasing trend after increasing the distance. Here are two effects from the mount of solvent DMF. The first one is the dielectric effect, that the DMF have a large dielectric constant<sup>82</sup> of 36.7. If the solution contains more DMF, the average dielectric constant of

the solution will increase. It can be reflected from the red shift of the PL spectrum. And people have found the dielectric constant will affect the  $MFE_{PL}$ . But for the solution without adding any DMF, the solvent is DMA itself, whose dielectric constant<sup>83</sup> is about 4.91. The dielectric constant of DMA is small, which suggest the separation distance of radical ion pair is also small. But in weak polar solvent investigators have found magnetic field effect is very little, because of the limitation of solvent separated radical ion pair, which is the intermolecular excited state in solution.<sup>84</sup> It should be noted that the dielectric constant effect can also help to change the distance because the Coulomb interaction between the Py and DMA radical ion pair will be screened by the dielectric background. With more DMF the dielectric constant is larger; the dielectric screening is also stronger, which will lead to larger separation distance. The second effect of DMF is the dilution effect, that the DMF dilute the concentration of Py and DMA molecules. It means the distance between Py and DMA can be increased. For the situation without adding DMF, the distance between Py and DMA can be consider being the smallest, that the Py are always surrounded by DMA molecules. The Py and DMA are almost contacted with each other. As a result of the two effects, the exchange energy will be very large without DMF. It makes the external magnetic field splitting can be omitted. Consequently, the magnetic field effect on PL could not be detected. After adding DMF, the separation distance between Py and DMA will become larger and the exchange energy will be smaller. Then the magnetic field effect can be observed after adding DMF.

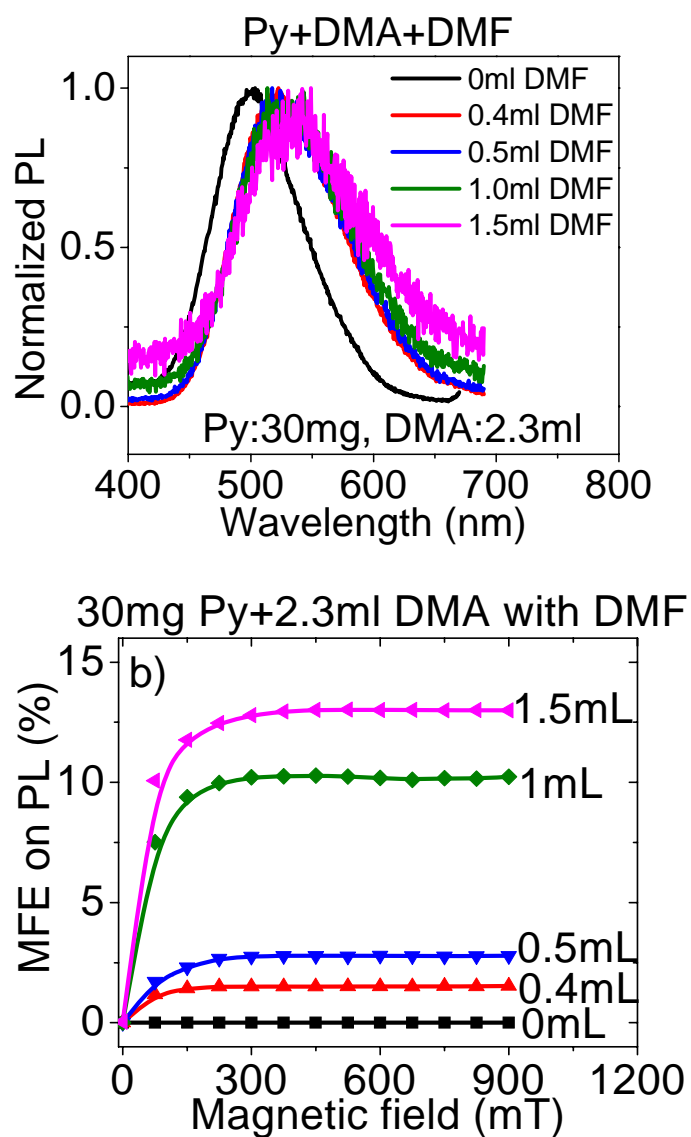


**Figure 3.6 a) PL spectrum of Py+DMA in DMF with different concentration, b) Concentration dependent MFE on PL of Py+DMA.**

### 3.5 SOC effect on MFE from intermolecular excited state

In general, the spin-orbital coupling can exist inside a molecule and between two adjacent molecules, namely intra-molecular and inter-molecular spin-orbital coupling in triplet semiconducting materials. Especially, the intra-molecular spin-orbital coupling and inter-molecular spin-orbital coupling are responsible for the spin-momentum conservation required in intra-molecular and inter-molecular spin-dependent processes, respectively. Therefore, intra-molecular and inter-molecular spin-orbital coupling can be used to generate MFEs by affecting the intra-molecular and inter-molecular spin-dependent processes through spin-momentum conservation. Furthermore, inter-molecular spin-orbital coupling can be conveniently tuned by changing inter-molecular distance. Thus, inter-molecular spin-orbital coupling provides a facile mechanism to tune the MFEs in triplet semiconducting materials.

External magnetic field should be comparable to internal magnetic field. If the internal magnetic field is too strong, the external magnetic field could not interrupt the internal magnetic field. Therefore, we can use internal magnetic field interaction, such as SOC, to change the external magnetic field effect. We use heavy metal complex Ir77, to change the internal magnetic interaction in the liquid state singlet exciplex system Py:DMA. Figure 3.7 shows the heavy metal complex Ir77 concentration dependent MFE on PL and the chemical structure of Ir77. With higher concentration of Ir77 the SOC interaction was

enhanced the MFE get smaller. It points out the stronger internal magnetic field the external magnetic field show less effect.

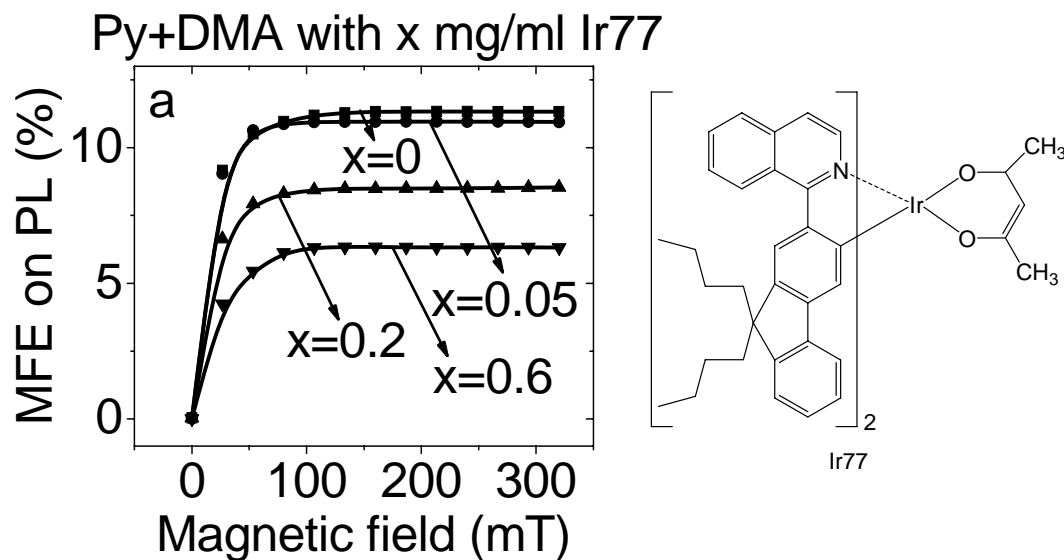


**Figure 3.7 Heavy metal complex concentration effect on MFE on PL of Py+DMA in mixture solvent of THF:DMF=3:7 system and the chemical structure of Ir77.**

Another system of Ir65, whose structure is shown in Figure 3.8, mixed with TCNB can also show the exciplex emission at about 587nm, as shown in Figure 3.9a. (The peak at about 470 nm is from Ir65.) And from the EPR measurement (Figure 3.9b), it clear shows the electron transfer states under light illumination but without the light illumination the EPR spectrum did not show clear charge transfer. The lifetime of the emission at 587nm is about 0.4  $\mu$ s. We consider the exciplex emission is from triplet exciplex based on these two evidences.

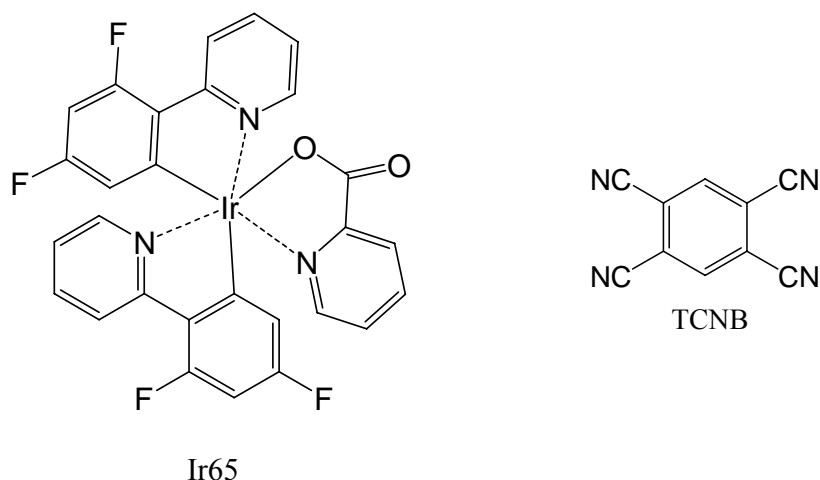


**Figure 3.8 Chemical structure of Ir65 and TCNB.**

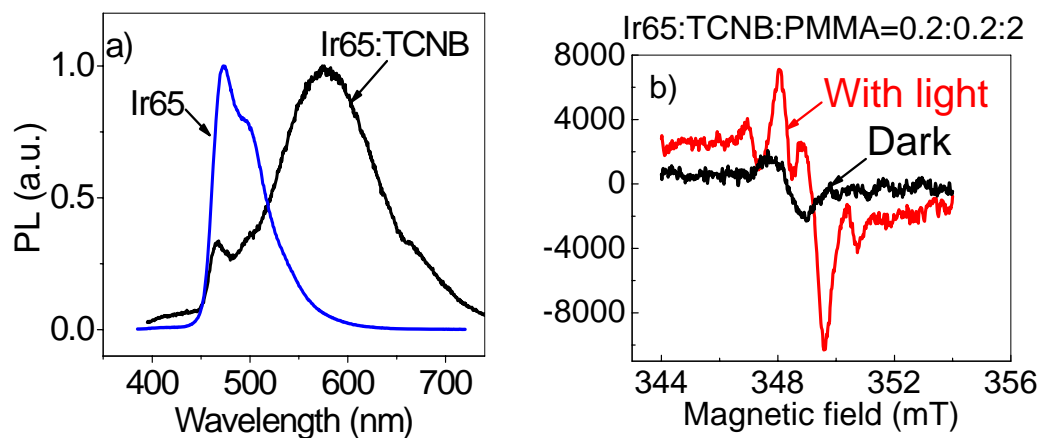


**Figure 3.9 a) PL spectrum of composite Ir65:TCNB:PMMA=2:2:5 and Ir65:PMMA=2:5 , b) EPR spectrum of Ir65:TCNB: PMMA composite.**

We have studied the MFE on PL, EL and MC in this triplet exciplex system. For the MFE on PL, we did not observe clear MFE for the triplet exciplex emission. This is due to the strong SOC effect introduced by the Ir65 molecules. Then we change the ratio



between Ir65:TCNB complex and inert polymer matrix PMMA to change the distance between Ir65 and TCNB. Distance can have two effects. One is to adjust the SOC effect from Ir65, the other is to tune the exchange energy as we did in the singlet exciplex system. The PL spectrum is shown in Figure 3.10. With diluting the concentration of the triplet exciplex, the emission from triplet exciplex gradually decreases. At relative high concentration 1:1:5 and 1:1:10, the triplet exciplex emission can be easily observed. At lower concentration 1:1:20, we can only observe a shoulder from triplet exciplex. At the lowest concentration 1:1:30, the triplet exciplex almost disappeared. But even at this low concentration, the  $\text{MFE}_{\text{PL}}$  is still absent.

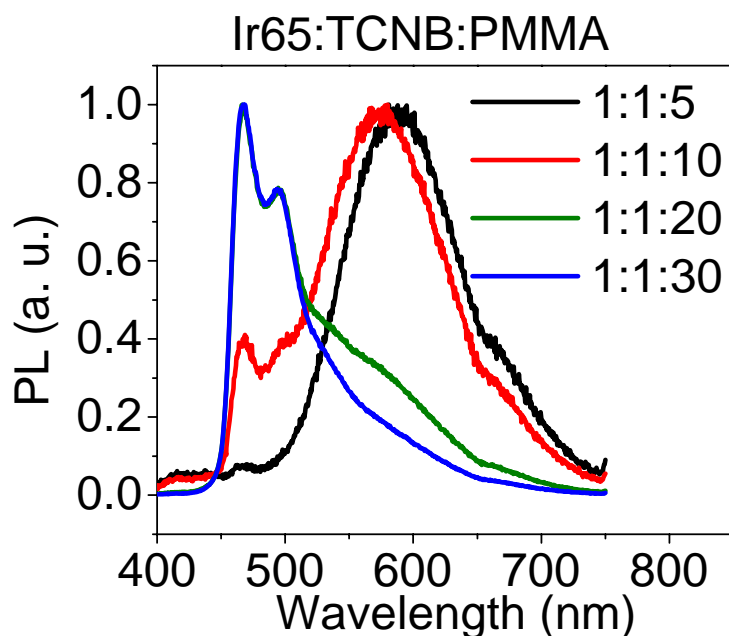


**Figure 3.10** Concentration dependent of PL spectrum from triplet exciplex

**Ir65+TCNB.**

By changing the concentration, the  $\text{MFE}_{\text{PL}}$  did not take place. Then we changed the matrix with different dielectric constant, as shown in Figure 3.11. From PS  $\epsilon=2.5$ ,<sup>85</sup> PMMA  $\epsilon=3.6$ ,<sup>85</sup> PAN  $\epsilon=5.5$ ,<sup>85</sup> to PEG  $\epsilon>10$ ,<sup>86,87</sup> the dielectric constant is increasing. Then the stronger dielectric screening could be expected, which will lead to larger separation distance. But even for very large dielectric constant PEG, there is no  $\text{MFE}_{\text{PL}}$  been observed.

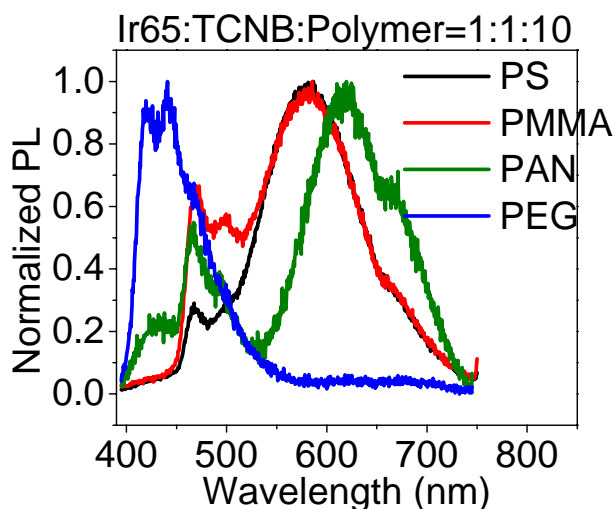


**Figure 3.11 Polymer matrix dielectric constant dependent PL spectrum of triplet exciplex from Ir65+TCNB.**

From the above discussion, no matter how we change the distance between triplet exciplex, no  $\text{MFE}_{\text{PL}}$  could be observed. This is different from the singlet exciplex system, in which we can easily change the magnitude of  $\text{MFE}_{\text{PL}}$  by changing the distance or dielectric constant. This suggests the spin orbital coupling has large influence on magnetic field effect on PL.

In the electroluminescence, the EL spectrum of the exciplex is similar to the photoluminescence as shown in Figure 3.12. But  $MFE_{EL}$  also could not be observed for all the concentration and all polymer matrixes. From these two magnetic measurements, we might expect that the strong spin orbit coupling might destroy all the magnetic responses in the triplet exciplex system.

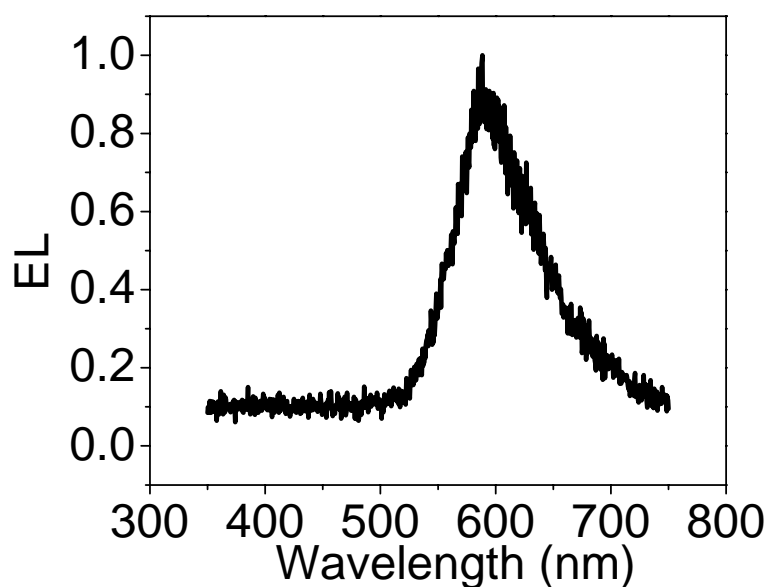


**Figure 3.12 EL spectrum of ITO/Ir65:TCNB:PMMA/Al.**

But the organic magnetoresistance (OMR) measurement gives us different results. Figure 3.13 shows the OMR result from device ITO/Ir65:TCNB:PMMA=2:2:3/Al. We can observe not large but considerable OMR. This result indicates the OMR and  $MFE_{PL}$  or  $MFE_{EL}$  has different sensitivity to spin orbital coupling. OMR is not as sensitive as  $MFE_{PL}$  to strong spin orbital coupling. It might be due to the difference between

recombination and dissociation process. In recombination process the intermolecular excited state will recombine to intramolecular excited state or contacted radical ion pair. Then they will further recombine and emit photon. At intramolecular excited state, they will also be affected by SOC through intersystem crossing. This might readjust the singlet/triplet ratio and the magnetic field effect on EL or PL will disappear. However, in the dissociation process, the intermolecular excited state will dissociate to free ions or free charges. They will not go through intersystem crossing again. There is no second time adjustment. Therefore, the magnetic field effect will remain.

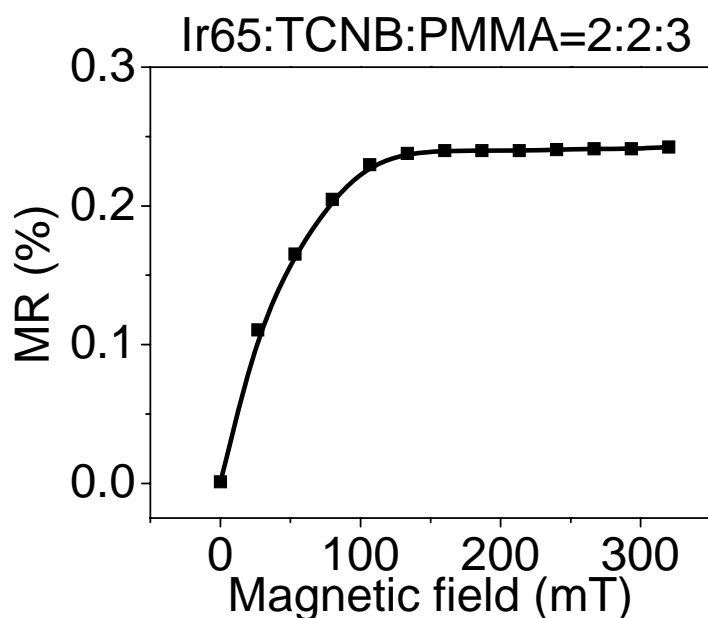


**Figure 3.13 OMR of device ITO/Ir65:TCNB:PMMA/Al.**

### 3.6 Conclusion

We studied the magnetic field effect on PL of intermolecular excited state exciplex in solid and liquid state. The result suggests the external magnetic field not only shows Zeeman splitting effect but also can affect the spin momentum conservation when the external magnetic field is comparable to internal magnetic field. The separation distance effect and SOC effect were found to be important for MFE. The long or short separation distance between donor-acceptor can cause relative small or large exchange energy between singlet and triplet excited states. When the exchange energy is larger, the splitting energy of magnetic field was too small to obtain MFEs. Only when the exchange energy is small, the splitting energy of external magnetic field will lead to the change of the intersystem crossing process. The SOC can quench the magnetic field effects. But the sensitivity of the different magnetic field effect is various according to the different processes to generate final products.

**CHAPTER 4**

**POLYMER BLENDS FROM OPTOELECTRONICS TO**

**SPINTRONICS**

## **4.1 Abstract**

This paper reports the recent experimental studies on electro-optically active polymer blends in organic spintronics. The experimental results indicate that polymer blends offer a convenient methodology to modify the critical parameter: spin-orbital coupling, in spintronics through inter-molecular interaction. Furthermore, the energy transfer in polymer blends can carry magnetic field effects from one component to another component and consequently amplifies the magnetic field effects in polymer blends. As a result, polymer blends are an important class of materials in organic spintronics.

## **4.2 Introduction**

Polymer blends present a fundamental concept to generate nanoscale morphological structures. The nanoscale morphological structures can offer effective control on charge transport and excited processes in optoelectronics where electronic and optic processes can be mutually controlled. Recently, experimental studies have found that polymer blends can have tunable inter-molecular spin-orbital coupling which is a critical parameter in spintronics where magnetic, optic, and electronic processes can be mutually controlled. As a result, polymer blends have become an important class of materials from optoelectronics to spintronics. In optoelectronics organic light emitting diodes (OLEDs) have been widely investigated due to their high potential applications in flexible display and large-area solid-state lighting.<sup>88, 89</sup> Polymer molecular composites<sup>90</sup> or polymer

blends<sup>91</sup> are widely used to control the key processes: balancing degree of bipolar electron and hole injection, electron-hole recombination, energy transfer, and light emission efficiency in the polymer based white OLEDs. Furthermore, people have recently found from magnetic field effect on electroluminescence (MFE<sub>EL</sub>) that the light intensity changed with magnetic field in the OLEDs.<sup>17-23</sup> This experimental finding indicates that organic semiconducting materials including polymers and polymer blends can be used for organic spintronics. There are two possible mechanisms for MFE<sub>EL</sub>. One is that magnetic field changes the formation rate of both the singlet and triplet excited states and further leads their emission changing.<sup>92</sup> The other possible mechanism is that the external magnetic field changed singlet/triplet excited states ratio by affecting intersystem crossing.<sup>18,28,65</sup> In the intersystem crossing mechanism, the competition between internal magnetic interaction, such as spin orbital coupling, and external magnetic field is very important to determine singlet/triplet ratio change caused by the external magnetic field in organic semiconductors. Polymer molecular composites or polymer blends can also show MFE<sub>EL</sub>. In these mixture structures, the energy transfer and spin-orbital coupling are two existing key factors in the determination of magnetic field effects. In our recent work, we studied the MFE<sub>EL</sub> in polymer blend-based devices with energy transfer such as composite of poly(N-vinylcarbazole) (PVK) with tris[2-phenylpyridine] iridium (Ir(ppy)<sub>3</sub>) and poly[9,9-di-(2-ethylhexyl)-fluorenyl-2,7-diyl] (PFO) with Ir(ppy)<sub>3</sub>. We observed by using energy transfer from a strong spin-orbital-coupling material to a weak spin-orbital-coupling material that the MFE<sub>EL</sub> in strong spin-orbital coupling materials could be largely amplified. This experimental finding indicates



that the use of polymer blends presents a new mechanism to amplify magnetic field effects in organic spintronics.

### 4.3 Experiment

The polymer molecular blend was prepared by dispersing the heavy-metal complex Ir(ppy)<sub>3</sub> into a PVK matrix by 0.1wt% and into PFO matrix by 3wt%. The composites were dissolved in chloroform and spun cast on pre-cleaned indium-tin-oxide (ITO) coated glass substrates. The aluminum metal electrode was then thermally evaporated on the polymer blend film under the vacuum of  $2 \times 10^{-6}$  Torr to fabricate light emitting devices with the architecture of ITO/polymer blend/Al. The MFE<sub>EL</sub> was measured at constant current density 20 mA/cm<sup>2</sup> in liquid nitrogen. The MFE<sub>EL</sub> was defined as  $\frac{I_{EL(B)} - I_{EL(0)}}{I_{EL(0)}}$ , where  $I_{EL(B)}$  and  $I_{EL(0)}$  are the electroluminescence intensity at constant current condition with and without magnetic field, respectively.

### 4.4 Result and discussion

#### 4.4.1 Magnetic field effect on electroluminescence of pure Ir(ppy)<sub>3</sub> and PVK

The chemical structures of Ir(ppy)<sub>3</sub> and PVK are shown in Figure 4.1. It is known that the electroluminescence is generated by radiative emission of intra-molecular electron-hole pairs, namely excitons. We know that the excitons have both singlet (S) and triplet (T) states. In general, the singlet/triplet ratio in excitonic states is 1/3 when the electron-hole

pairs are formed. A magnetic field can change electroluminescence by changing the singlet and triplet formation rate or by changing the singlet-triplet intersystem crossing. For the singlet and triplet formation, the experimental result that both of fluorescence and phosphorescence emission in electroluminescence increase with applied magnetic field suggests that both singlet and triplet exciton formation rates increase under the influence of a magnetic field.<sup>92</sup> For the singlet-triplet intersystem crossing, an external magnetic field needs to be strong enough, relative to the internal magnetic field generated by spin orbital coupling, to generate  $\text{MFE}_{\text{EL}}$ . When strong-spin-orbital-coupling  $\text{Ir(ppy)}_3$  molecules are dispersed into weak spin-orbital-coupling PVK matrix, the penetration of delocalized  $\pi$  electrons from the PVK matrix into the magnetic field from orbital current in the  $\text{Ir(ppy)}_3$  molecules can inevitably generate inter-molecular spin-orbital coupling. This inter-molecular spin-orbital coupling can be largely tuned by adjusting the  $\text{Ir(ppy)}_3$  dispersion concentration. In particular, this tunable inter-molecular spin-orbital coupling forms a convenient but effective mechanism to modify the spin-orbital coupling strengths for each component in such polymer blends.

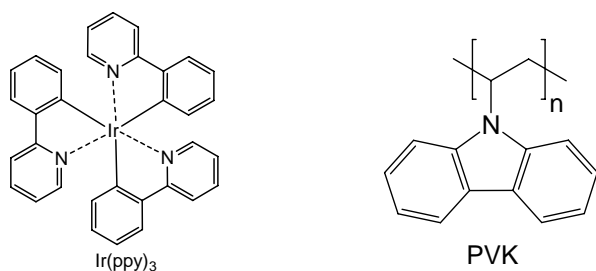


**Figure 4.1 Chemical structure of  $\text{Ir(ppy)}_3$  and PVK.**

The characteristic electroluminescence peaks for individual PVK and Ir(ppy)<sub>3</sub> components are around 405 nm and 505 nm as shown in Figure 4.2a, correspondingly. Figure 4.2b shows the MFE<sub>EL</sub> from individual pure PVK and pure Ir(ppy)<sub>3</sub> components. It should be noted that the pure PVK exhibits a large MFE<sub>EL</sub> with the amplitude of about +10% but the pure Ir(ppy)<sub>3</sub> does not show an appreciable MFE<sub>EL</sub>. This difference could be lead to the spin orbital coupling strength difference in these two materials.

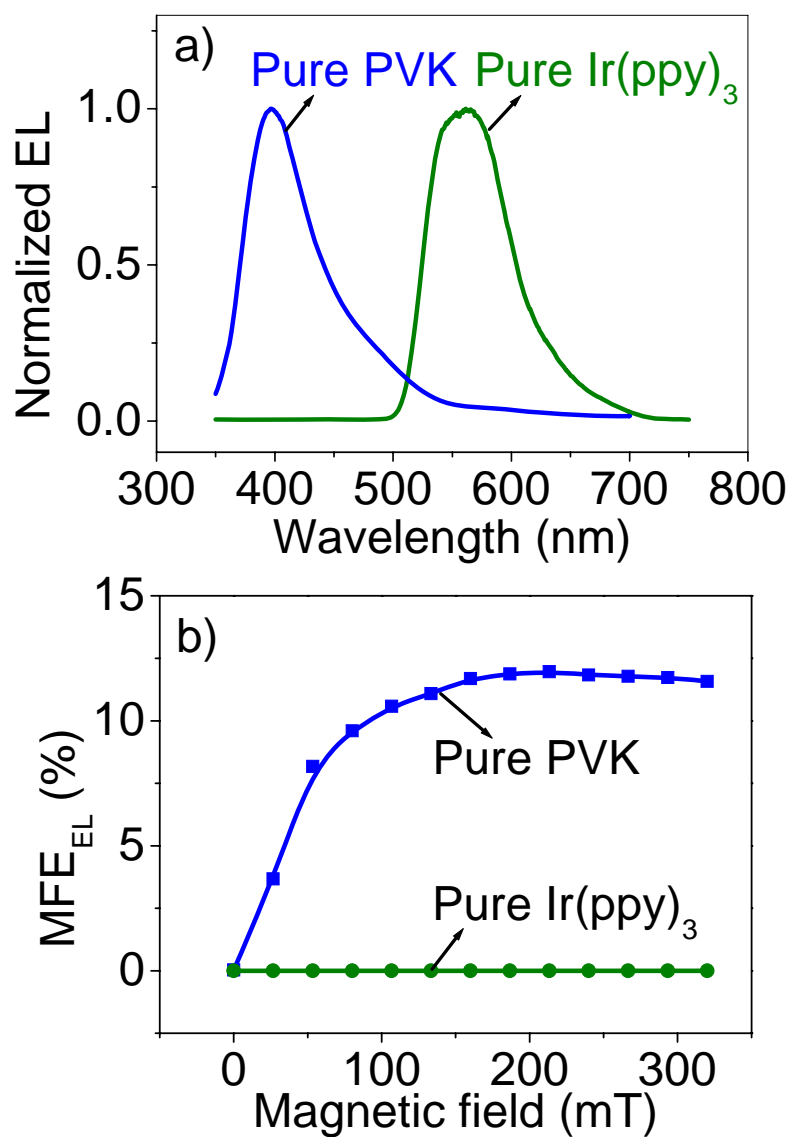


**Figure 4.2 a) Normalized electroluminescence spectrum for pure PVK and pure Ir(ppy)<sub>3</sub> b) MFE<sub>EL</sub> of pure PVK and Ir(ppy)<sub>3</sub>.**

It is obvious that the PVK gives fluorescence from its singlet excitons while the Ir(ppy)<sub>3</sub> generates phosphorescence from its triplet excitons due to the strong spin-orbital coupling caused by the heavy metal Ir complex structure, as shown in Figure 4.3. For weak spin-orbital-coupling materials such as PVK, a low magnetic field of around 10~100 mT is stronger than the internal magnetic field from spin-orbital coupling. As a consequence, significant MFE<sub>EL</sub> can be expected. For the strong-spin-orbital-coupling materials such as Ir(ppy)<sub>3</sub>, a low magnetic field less than 1 T is much weaker than the internal magnetic field generated by spin-orbital coupling.<sup>93</sup> As a result, negligible MFE<sub>EL</sub> can be observed by the first order approximation from the pure Ir(ppy)<sub>3</sub> electroluminescence.

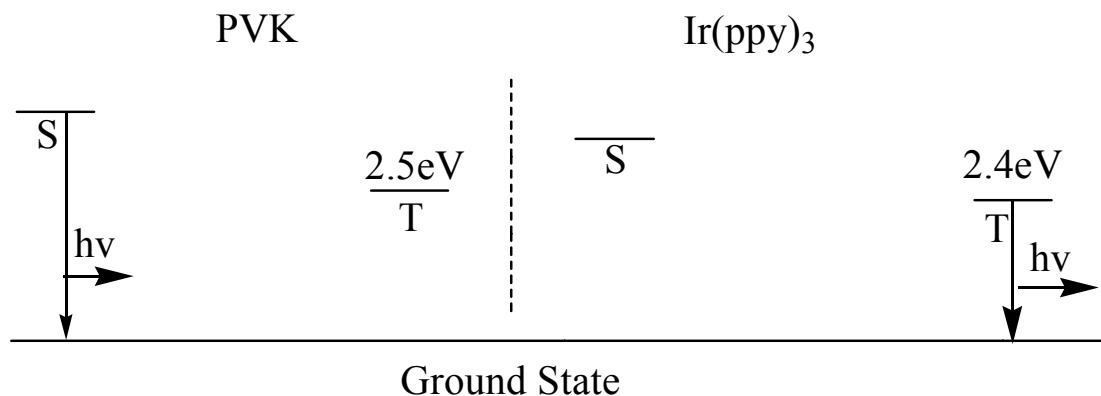


**Figure 4.3 The energy level of both singlet and triplet exciton state of PVK and Ir(ppy)<sub>3</sub> S and T refer to singlet and triplet state.**

#### 4.4.2 MFE from the composite of PVK and Ir(ppy)<sub>3</sub>

After we lightly doped Ir(ppy)<sub>3</sub> into PVK matrix, the PVK + Ir(ppy)<sub>3</sub> blend shows electroluminescence spectrum (Figure 4.4a), which shows both characteristic peaks at 405 nm from the PVK matrix and at 505 nm from the dispersed Ir(ppy)<sub>3</sub> molecules. More importantly, both electroluminescence peaks show clear MFE<sub>EL</sub>. As shown in Figure 4.4b and Figure 4.4c, the PVK matrix shows around +5% MFE<sub>EL</sub> smaller than the pure PVK device. But the dispersed Ir(ppy)<sub>3</sub> surprisingly shows +3% MFE<sub>EL</sub> while the pure Ir(ppy)<sub>3</sub> device gives negligible MFE<sub>EL</sub>. The decrease of MFE<sub>EL</sub> for PVK matrix as compared to pure PVK device is due to the increase in its spin-orbital coupling strength caused by the inter-molecular spin-orbital coupling.<sup>63</sup>

#### 4.4.3 Energy transfer mechanism of MFE<sub>EL</sub> in the composite of PVK and Ir(ppy)<sub>3</sub>

The positive MFE<sub>EL</sub> for the dispersed Ir(ppy)<sub>3</sub> molecules can come from following two possibilities: spin-orbital coupling and energy transfer.

First, the spin-orbital coupling strength of dispersed Ir(ppy)<sub>3</sub> molecules was weakened by the PVK matrix through inter-molecular spin-orbital coupling effects. Then a low magnetic field becomes strong enough to compete with the weakened spin-orbital coupling strength in the dispersed Ir(ppy)<sub>3</sub>. Thus the electroluminescence from the dispersed Ir(ppy)<sub>3</sub> molecules can exhibit significant MFE<sub>EL</sub>.

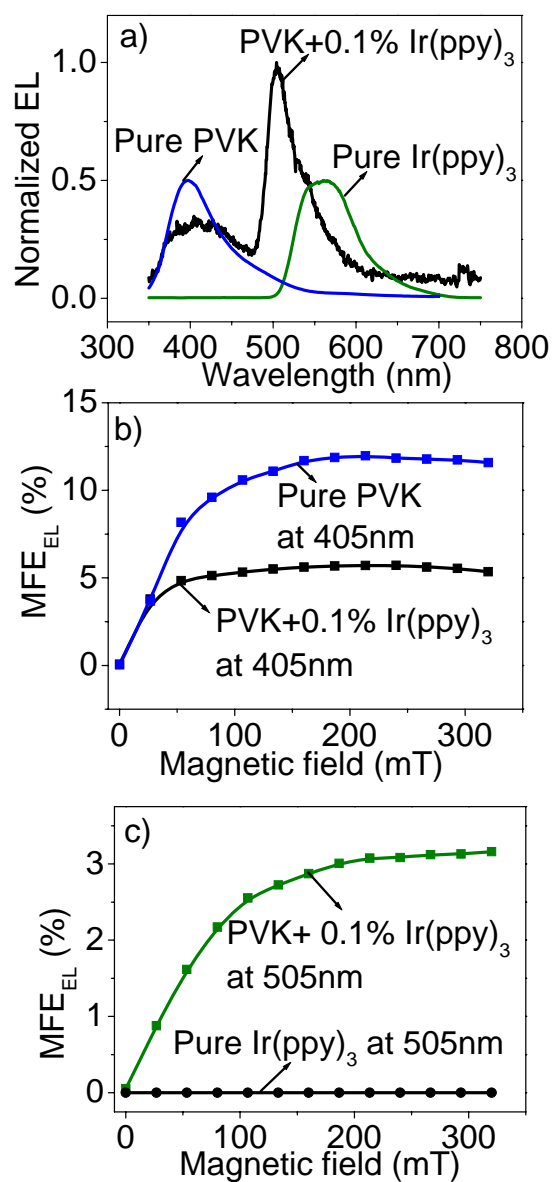


**Figure 4.4 a) Normalized electroluminescence spectrum for composite of PVK+0.1% Ir(ppy)<sub>3</sub>, the electroluminescence spectrum of pure PVK and pure Ir(ppy)<sub>3</sub> are also shown as reference, b) MFE<sub>EL</sub> of 0.1% Ir(ppy)<sub>3</sub>+PVK and pure PVK at 405nm, c) MFE<sub>EL</sub> of 0.1% Ir(ppy)<sub>3</sub>+PVK and pure Ir(ppy)<sub>3</sub> at 505nm.**

Second, the energy transfer from the PVK matrix to dispersed Ir(ppy)<sub>3</sub> molecules can carry the MFE<sub>EL</sub> from the PVK matrix to the dispersed Ir(ppy)<sub>3</sub> molecules, leading to a MFE<sub>EL</sub> in the dispersed Ir(ppy)<sub>3</sub> in the PVK + Ir(ppy)<sub>3</sub> blend. The observed positive MFE<sub>EL</sub> from the dispersed Ir(ppy)<sub>3</sub> molecules can rule out the first possibility: spin-orbital coupling mechanism, because the spin-orbital coupling mechanism should give negative MFE<sub>EL</sub> in triplet electroluminescence through intersystem crossing.<sup>18</sup> Therefore, the energy transfer mechanism is mainly accountable for the positive MFE<sub>EL</sub> observed from the PVK + Ir(ppy)<sub>3</sub> blend.

As shown in Figure 4.5, the UV-vis absorption spectrum of Ir(ppy)<sub>3</sub> and photoluminescence spectrum of PVK have large overlap. Then the sufficient energy transfer from PVK to Ir(ppy)<sub>3</sub> could be expected. And if we compare the photoluminescence and electroluminescence of the composite of PVK and Ir(ppy)<sub>3</sub>, the ratio of the peak height is similar in photoluminescence and electroluminescence, which indicates the energy transfer happens in the electroluminescence. The possibility of charge trapping effect in the electroluminescence could be excluded.



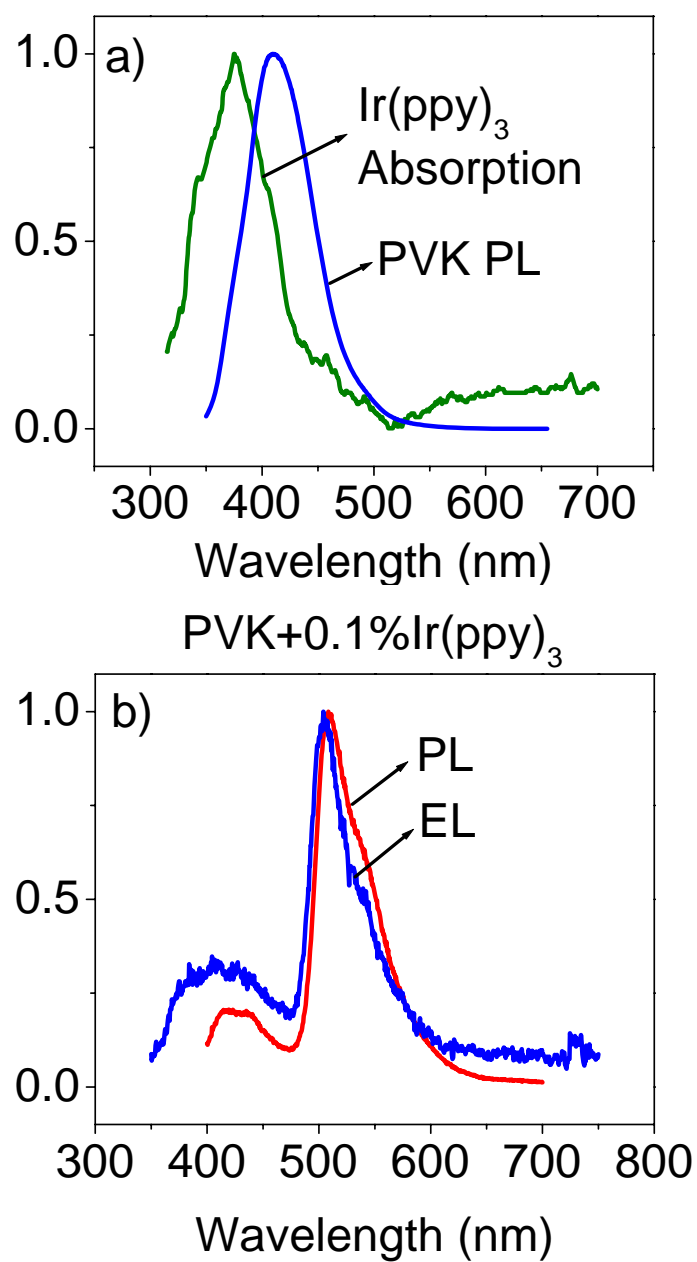


**Figure 4.5 a) Absorption of Ir(ppy)<sub>3</sub> and photoluminescence of PVK, b) Photoluminescence and electroluminescence of PVK with 0.1% Ir(ppy)<sub>3</sub>.**

Figure 4.6 schematically illustrates how energy transfer can amplify the  $\text{MFE}_{\text{EL}}$  for the phosphorescence of heavy-metal complex  $\text{Ir(ppy)}_3$  through polymer blend design. When PVK and  $\text{Ir(ppy)}_3$  were mixed, a low magnetic field would change the intersystem crossing in PVK matrix with the consequence of increasing singlet ratio in the PVK matrix. Then due to the energy transfer, the increased singlets in the PVK matrix are transferred to the singlet states in the dispersed  $\text{Ir(ppy)}_3$  molecules through Förster process. Because of the strong spin-orbital coupling in the dispersed  $\text{Ir(ppy)}_3$  molecules, the intersystem crossing process can be very efficient and especially independent on magnetic field in the  $\text{Ir(ppy)}_3$  component. As a result, almost all singlets are converted into triplets in the dispersed  $\text{Ir(ppy)}_3$  molecules.

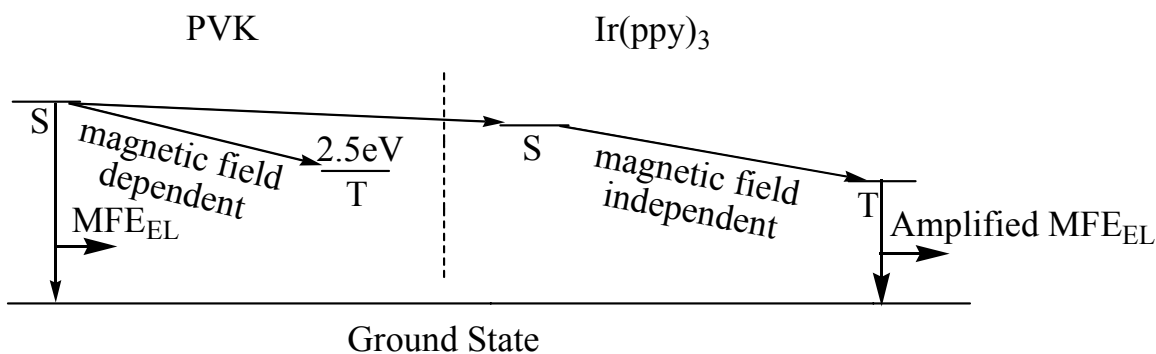


**Figure 4.6 Energy transfer process in electroluminescence of composite of PVK doped with 0.1wt%  $\text{Ir(ppy)}_3$ . S and T refer to singlet and triplet state.**

This means that triplets in the dispersed  $\text{Ir(ppy)}_3$  molecules can essentially increase due to (i) efficient energy transfer from the PVK matrix to the dispersed  $\text{Ir(ppy)}_3$  molecules and (ii) strong intersystem crossing within the dispersed  $\text{Ir(ppy)}_3$  molecules. Therefore, the

MFE<sub>EL</sub> from the dispersed Ir(ppy)<sub>3</sub> molecules can be considerably amplified based on polymer blend design as compared to pure Ir(ppy)<sub>3</sub> molecules.

#### 4.4.4 MFE from the composite of PFO and Ir(ppy)<sub>3</sub>

In the system of PFO doped with Ir(ppy)<sub>3</sub>, the situation is more complicated. PFO is a widely used polymer host with blue emission, whose structure is shown in Figure 4.7. Figure 4.8 showed the EL spectrum and MFE for PFO+3wt% Ir(ppy)<sub>3</sub> system. After dispersing 3wt% Ir(ppy)<sub>3</sub> in PFO, compared the EL spectrum with pure PFO film, there was another peak which was at about 570-580nm, which is also different from Ir(ppy)<sub>3</sub>. This peak from energy is about 2.1-2.2eV, which is very close to PFO triplet energy level (2.3eV)<sup>94</sup>, so we considered it was related to the phosphorescence from PFO. This peak showed the intermolecular SOC in PFO was enhanced by Ir(ppy)<sub>3</sub>. And only the fluorescence peak from PFO could show MFE<sub>EL</sub>, MFE<sub>EL</sub> for the phosphorescence was not observed.

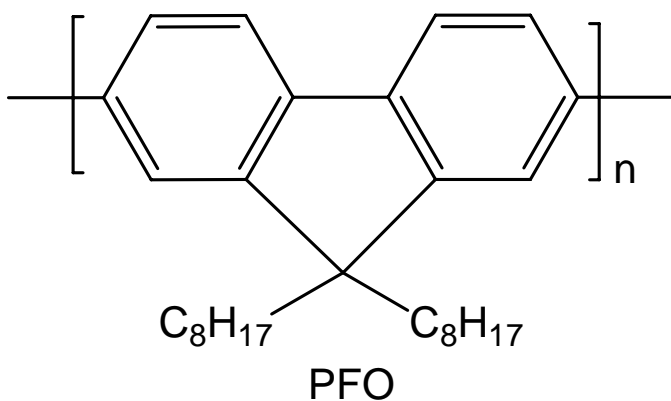


**Figure 4.7 Chemical structure of PFO.**

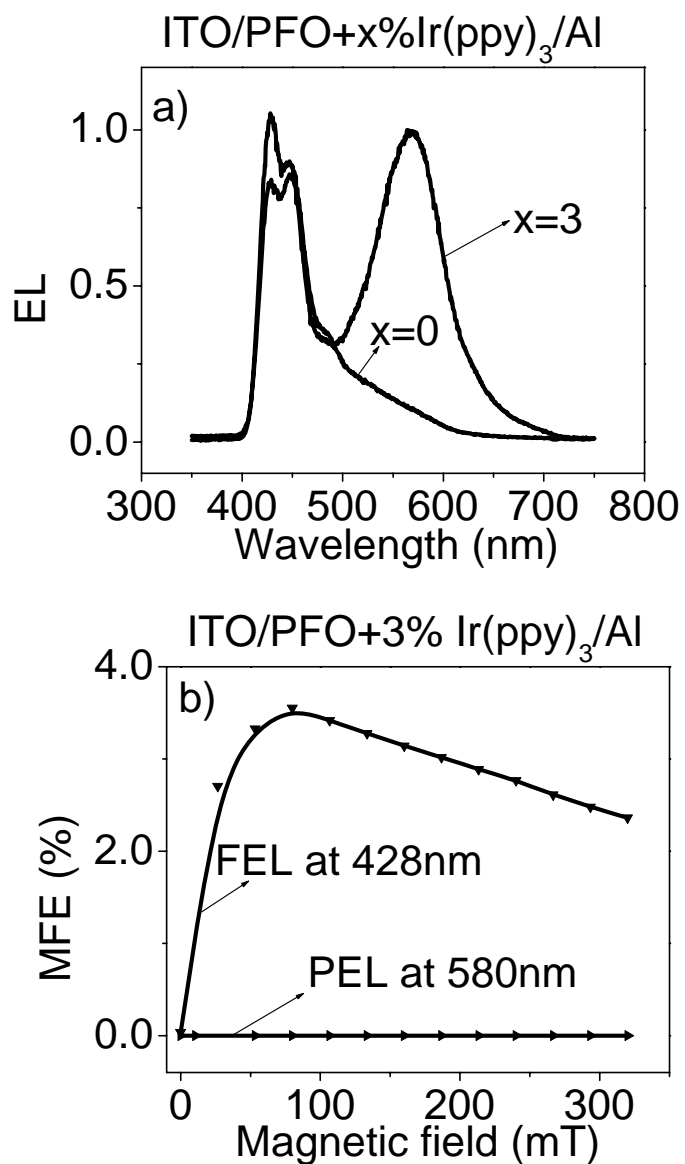


**Figure 4.8 a) Electroluminescence spectrum of ITO/PFO+3%Ir(ppy)<sub>3</sub>/Al and ITO/PFO/Al, b) MFE on electrofluorescence and electrophosphorescence in ITO/PFO+3%Ir(ppy)<sub>3</sub>/Al, FEL refer to the electrofluorescence, PEL refer to the electrophosphorescence.**

#### 4.4.5 Mechanism of $\text{MFE}_{\text{EL}}$ in composite of PFO and $\text{Ir(ppy)}_3$

The possible explanation is still caused by the energy transfer process. But this time it contains both Foster energy transfer and Dexter energy transfer. The Foster energy transfer can be supported by the overlap of absorption of  $\text{Ir(ppy)}_3$  and the PL of PFO, as shown in Figure 4.9. The Dexter energy transfer is well known in OLED fabrication<sup>95</sup>. It has been found that the triplet energy level of the PFO is 2.3 eV, which is lower than the triplet energy level of the  $\text{Ir(ppy)}_3$  around 2.4 eV.<sup>96</sup>

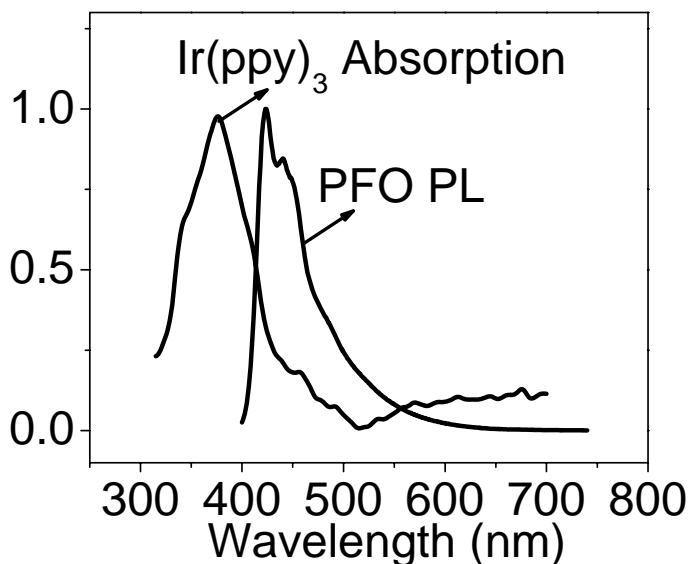


**Figure 4.9** Overlap of absorption of  $\text{Ir(ppy)}_3$  and the photoluminescence of PFO.

This energy transfer mechanism is shown in Figure 4.10. The singlet excitons in PFO molecules went to the  $\text{Ir(ppy)}_3$  singlet level due to the energy transfer process. Then almost 100% the singlet exciton in  $\text{Ir(ppy)}_3$  molecules would change into triplet excitons due to the very strong intramolecular SOC. After that the triplet excitons in  $\text{Ir(ppy)}_3$

would transfer to PFO triplet energy level due to back energy transfer process then the emission from that caused the 570nm phosphorescence peak. When applying magnetic field, the ratio of singlet polaron pairs in PFO would increase but the ratio of triplet polaron pairs would decrease. The increased single polaron pairs would further generate more singlet excitons in PFO. This caused the positive  $MFE_{EL}$  of the fluorescence in PFO. And the decreased triplet polaron pairs would further cause less triplet excitons in PFO in one hand. But in the other hand, through the energy transfer, 100% intersystem crossing and back energy transfer cycle in  $Ir(ppy)_3$ , the increase in singlet exciton in PFO would transfer to  $Ir(ppy)_3$  and then went back through back energy transfer. So it would also enlarge the ratio of triplet exciton in PFO. Thus the decrease in triplet excitons in PFO would be canceled by the cyclic process. So no  $MFE_{EL}$  was observed for the phosphorescence in PFO.

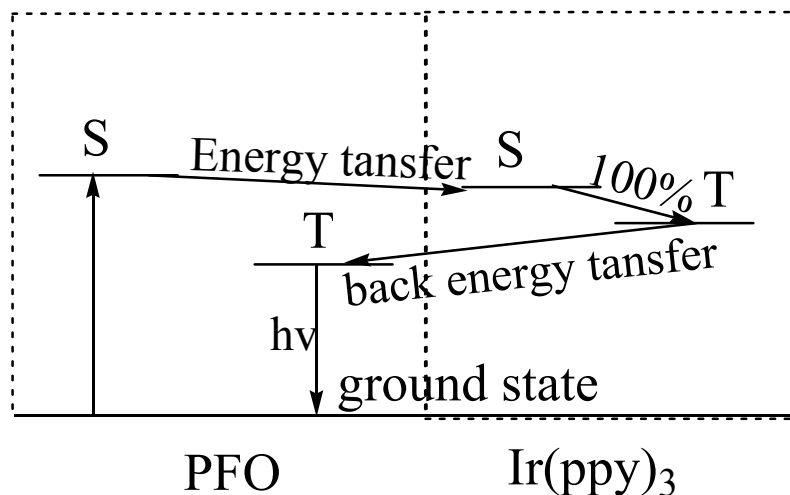


**Figure 4.10 Energy transfer process in electroluminescence of composite of PFO doped with 3wt%  $Ir(ppy)_3$ . S and T refer to singlet and triplet state.**

## 4.5 Conclusion

We have shown that polymer blend design can lead to a substantial tuning on spin-orbital coupling through inter-molecular interaction when a weak-spin-orbital-coupling polymer is mixed with strong-spin-orbital-coupling molecules. The tuning of spin-orbital coupling comes from the penetration of delocalized  $\pi$  electrons from weak-spin-orbital-coupling polymer matrix into the magnetic field of orbital current of the strong-spin-orbital-coupling molecules. On the other hand, the Förster energy transfer can occur from the polymer matrix to dispersed molecules in polymer molecular blends. Especially, this Förster energy transfer can carry the  $\text{MFE}_{\text{EL}}$  from weak-spin-orbital-coupling polymer matrix to strong-spin-orbital-coupling molecules, leading to amplification on the  $\text{MFE}_{\text{EL}}$  in the strong-spin-orbital-coupling molecules. Therefore, polymer blends design presents a new mechanism to amplify magnetic field effects in organic spintronics based on (i) modification of spin-orbital coupling and (ii) Förster energy transfer. However, in the system containing both Förster and Dexter energy transfer effects, the  $\text{MFE}_{\text{EL}}$  from host fluorescence also decreases due to the spin-orbital coupling effect. The EL from phosphorescence of host can be observed instead of the phosphorescence of guest. And the  $\text{MFE}_{\text{EL}}$  on phosphorescence will be limited by the coexistence of the Förster and Dexter energy transfer.

**CHAPTER 5**

**THE ROLE OF INTERMOLECULAR SPIN-ORBITAL COUPLING**

**IN MAGNETIC FIELD EFFECTS IN ORGANIC**

**SEMICONDUCTORS**



## 5.1 Abstract

Organic semiconductors exhibit magnetic responses on electrical current (MC) under low magnetic field. This response is due to the spin dependent intersystem crossing processes of intermolecular electron-hole pairs in organic semiconductors. The external magnetic field always needs to compete with internal magnetic interactions to satisfy the spin momentum conservation to flip the spin for the intersystem crossing process in intermolecular electron-hole pair states. Then MC would be generated from different channels. Therefore, the strength of internal magnetic interaction, such as hyperfine interaction and spin-orbital coupling, would determine if the magnetic field can be observed in a given magnetic field. We found considerable magnetic response can be observed when the intermolecular spin-orbital coupling is reduced. It indicates that changing inter-molecular spin-orbital coupling is a critical factor to generate MC in organic semiconductors.

## 5.2 Introduction

It has been experimentally found that organic semiconductors can show magnetic responses in electrocurrent<sup>18,24-43,65,68,69</sup> to externally applied low magnetic field (< 100mT), which was named as magnetocurrent (MC) or organic magnetoresistance (OMR) with nonmagnetic electrode, which is different the situation with magnetic electrode.<sup>25, 97, 98</sup> However, phosphorescent organic semiconductors always exhibit

negligible MC.<sup>26,62,63</sup> The negligible MC has formed a difficulty for phosphorescent organic semiconductors to be used in magneto-optoelectronic applications. Based on electrical drifting theory, the MC can be generated by magnetically changing charge mobility or density, forming mobility-based MC<sup>26,29,34,37,40,42,43</sup> and density-based MC<sup>18,19,28,38,39,63,65</sup>. In mobility-based MC, organic semiconductors need to have spin-spin interaction between charge carriers. Applying magnetic field can disturb this spin-spin interaction through magnetic scattering and consequently modifies charge motilities, generating mobility-based MC. However, experimental studies have found that organic semiconductors exhibit negligible mobility-based MC.<sup>99-102</sup> These experimental findings imply that bulk organic semiconductors lack appreciable spin-spin interaction. As a result, magnetically changing charge density becomes a practical method to generate MC, giving density-based MC. In density-based MC, there are two channels, namely dissociation and charge-reaction to generate the MC. Specifically, in dissociation channel applied magnetic field can change the singlet and triplet ratios in polaron-pair states through intersystem crossing. This can lead to a positive MC through dissociation channel based on the experimental argument that singlets have larger dissociation rates due to stronger ionic properties in wavefunctions as compared to triplets.<sup>80,81</sup> In dissociation channel magnetic field-dependent intersystem crossing is a key process. We know that the intersystem crossing requires spin-momentum conservation. A magnetic field can affect the spin-momentum conservation through magnetic scattering and consequently changes the intersystem crossing with the consequence of increasing singlets and decreasing triplets in polaron-pair states towards the generation of magnetic

field effects.<sup>18,28,65</sup> In charge-reaction channel, the excitons formed from injected bipolar charge carriers can react with free charges, generating exciton-charge reaction, when they are within close proximity.<sup>70-72</sup> The exciton-charge reaction can break excitons into free charges.<sup>73,74</sup> Although both singlet and triplet excitons can be involved in charge reaction, triplet excitons can dominate charge reaction due to the long lifetimes. An applied magnetic field can perturb the spin interaction between a triplet exciton and a charge in triplet-charge reaction and consequently decreases the triplet-charge reaction rate constant.<sup>75,76</sup> Therefore, charge reaction channel can lead to a negative MC. More importantly, in density-based MC both dissociation and charge reaction channels are dependent of inter-molecular spin-orbital coupling (SOC). Specifically, an applied magnetic field competes with inter-molecular SOC to conserve spin-momentum in both intersystem crossing and charge reaction. As a result, changing inter-molecular SOC can modify the density-based MC through dissociation and charge reaction channels.

The organic semiconductors can be separated into types: singlet organic semiconductor and triplet organic semiconductor, according to the spin orbital coupling strength in the material. Recently, it has been found that the hyperfine interaction is accountable for the MFEs in singlet semiconducting DOOPPV<sup>58</sup>. On the other hand, in another singlet semiconducting material Alq<sub>3</sub>, it does not suggest hyperfine interaction is responsible to MC<sup>60</sup>. In addition, Alq<sub>3</sub> has relative strong spin orbital coupling strength<sup>59</sup>. We believe it is caused by the relative strong spin orbital coupling. It indicates the importance of spin-orbital coupling for MC. In this work we investigate how spin-orbital coupling affects the

MC in triplet semiconducting materials, which is important for organic light emitting diodes<sup>103,104</sup> and organic solar cells<sup>105</sup>. We use Iridium complex molecules to introduce inter-molecular spin-orbital coupling through molecular dispersion in an inert polymer matrix PMMA. It should be noted that strong SOC in Iridium complex molecules almost completely quenches MC in the pure film because strong spin-orbital coupling plays a dominate role in the competition between internal magnetic interaction and external magnetic field. On the other hand, changing the intermolecular distance can lead to large modification to the exchange energy and intermolecular SOC. Therefore, the dispersion of Iridium complex molecules into an inert polymer matrix provides an opportunity for us to investigate the effects of intermolecular SOC on MC in organic semiconductors.

### 5.3 Experiment

The iridium heavy-metal complex molecule, fac-tris(2-phenylpyridine) Iridium ( $\text{Ir(ppy)}_3$ ), Bis(2-(9,9-dibutylfluorenyl)-1-isoquinoline(acetylacetonate) Iridium (III) (Ir77) and Iridium (III) bis(2-(4,6-difluorephenyl)pyridinato-N,C2) (Ir65) were purchased from America Dye Source, Inc. and used as triplet organic semiconducting material. The poly (methyl methacrylate) (PMMA) and polystyrene (PS) were used as polymer matrix. The chemical structures of Ir65, Ir77 and  $\text{Ir(ppy)}_3$  are shown in Figure 5.1. PMMA and PS are insulators and the charge transport below the dielectric rupture occurs through the dispersed Iridium complex molecules. The Iridium complex molecules were used in organic light-emitting diodes with two different forms: bulk and composite films spin

cast from chloroform solutions. The organic light-emitting diodes were fabricated with indium tin oxide (ITO) and aluminum (Al) electrodes. The Al electrode was thermally evaporated under the vacuum of  $2 \times 10^{-6}$  Torr. The MC was measured at constant-voltage mode. The MC amplitude was given by the relative change in electrical current caused by applied magnetic field. MC can be expressed by  $\frac{I_B - I_0}{I_0}$ , where  $I_B$  and  $I_0$  are the electrical current with and without an applied magnetic field. The electron parametric resonance (EPR) was measured by JES-FA200 Electron Spin Resonance Spectrometer from JEOL Inc, working at X-band (9GHz).

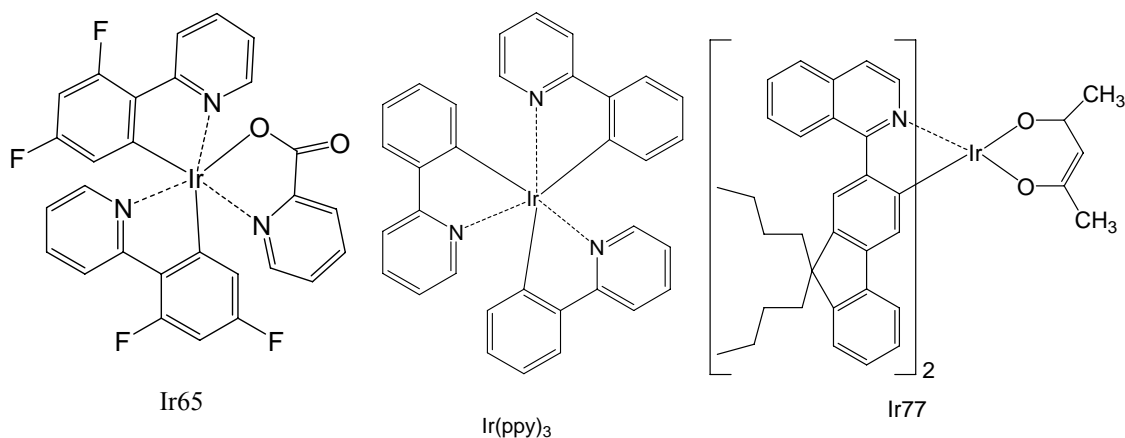


**Figure 5.1 Chemical structures for Ir65, Ir77 and Ir(ppy)<sub>3</sub>.**

## 5.4 Results and Discussion

It can be seen in Figure 5.2 that the heavy-metal complex Ir(ppy)<sub>3</sub> exhibits a negligible effect on MC. However, positive and negative MC can be observed when the Ir(ppy)<sub>3</sub> molecules are dispersed into inert PS and PMMA matrices, respectively. The strong spin-orbital coupling due to the heavy atom effect in Ir(ppy)<sub>3</sub> can have the magnetic energy of

$\sim 100 \mu\text{eV}$ .<sup>93</sup> We know that the electroluminescence and electric current from bulk triplet  $\text{Ir(ppy)}_3$  film shows negligible dependence of magnetic field<sup>63</sup>.

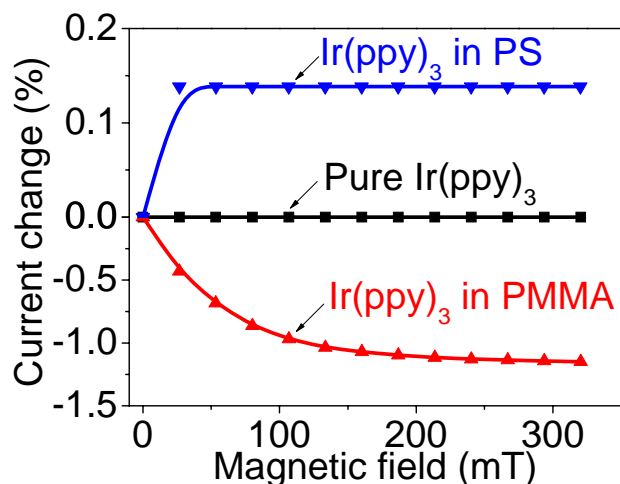


**Figure 5.2 Magnetocurrent is shown for  $\text{Ir(ppy)}_3$ :PMMA and  $\text{Ir(ppy)}_3$ :PS composites as compared to pure  $\text{Ir(ppy)}_3$  molecules. The weight ratio of  $\text{Ir(ppy)}_3$ :polymer is 1:2.**

In general, the spin-orbital coupling is the spin momentum coupled with the orbital momentum inside a molecule and between two molecules, namely intramolecular and intermolecular spin-orbital coupling. We know that the intra-molecular and inter-molecular SOC are determined by molecular structure and packing, respectively. For a given molecular structure, inter-molecular SOC can be largely tuned through molecular packing. But, it should be noted that the inter-molecular SOC, generated by the magnetic interaction between the  $\pi$  electron spins and orbital magnetic field between two adjacent molecules, becomes negligible in non-heavy metal complex molecules where orbital field

is weak. For phosphorescent organic semiconductors, the overall SOC consists of both intra-molecular and inter-molecular components.

It should be noted that the intermolecular excited states are responsible for magnetic field effect. Therefore, intermolecular spin-orbital coupling provides a facile mechanism to tune the MC in triplet semiconducting materials. Molecular dispersion can weaken inter-molecular spin-orbital coupling due to molecular dilution effect, when triplet Ir(ppy)<sub>3</sub> molecules are dispersed in an inert polymer matrix. Therefore, it can be theoretically argued that the inter-molecular spin-orbital coupling is a critical parameter in the determination of magnetic field effects in triplet organic semiconducting materials. Especially, the dispersion can largely change inter-molecular spin-orbital coupling and consequently generate a substantial tuning on magnetic field effects. Nevertheless, external magnetic field needs to compete with internal magnetic interaction contributing to the energy conservation through Zeeman splitting and momentum conservation through magnetic scattering. As a consequence, changing inter-molecular distance can largely tune inter-molecular SOC, leading to a modification on overall SOC for phosphorescent organic semiconductors.

We know that the MC can be generated by three different channels: transport (bipolaron model)<sup>26,29,34,37,40,42,43</sup>, dissociation (polaron pair model)<sup>18,19,28,38,39,63,65</sup> and exciton-charge reaction (triplet charge reaction model)<sup>31,34,35,40</sup>. But there is one common point that the weaken of the intermolecular SOC during the dispersion of Ir(ppy)<sub>3</sub> into PMMA

plays an important role in generating the MC. Figure 5.3 shows the intramolecular SOC and intermolecular SOC. The intramolecular SOC in isolated Ir(ppy)<sub>3</sub> molecule is shown as Equation (5.1), where  $\hat{L}$  and  $\hat{S}$  are orbital field and electron spin,  $\xi$  is the spin-orbit coupling constant, respectively. If there is another Ir(ppy)<sub>3</sub> molecule nearby, there will be an intermolecular SOC contribution add to the total SOC strength, as shown as Equation (5.2). Here  $\hat{H}_{intra}$  is the intramolecular SOC strength,  $\hat{H}_{inter}$  is the intermolecular SOC strength between molecule 1 and 2.

For intramolecular SOC

$$\hat{H}_{SO} = \xi \hat{L} \cdot \hat{S} \quad (5.1)$$

For intermolecular SOC

$$\hat{H}_{SO} = \hat{H}_{intra} + \hat{H}_{inter} = (\xi_{intra} \hat{L}_{intra} + \xi_{inter} \hat{L}_{inter}) \cdot \hat{S} \quad (5.2)$$

In our device of Ir(ppy)<sub>3</sub>:PMMA composite, the electrons and holes were injected by external electrical field. When they were in intermolecular electron-hole pair states, the intermolecular SOC strength ( $\hat{H}_{inter}$ ) was weaker than pure Ir(ppy)<sub>3</sub> film due to the distance separation increases caused by the PMMA between Ir complexes molecules. Therefore, the external magnetic field could compete with the weakened intermolecular SOC to generate MC.



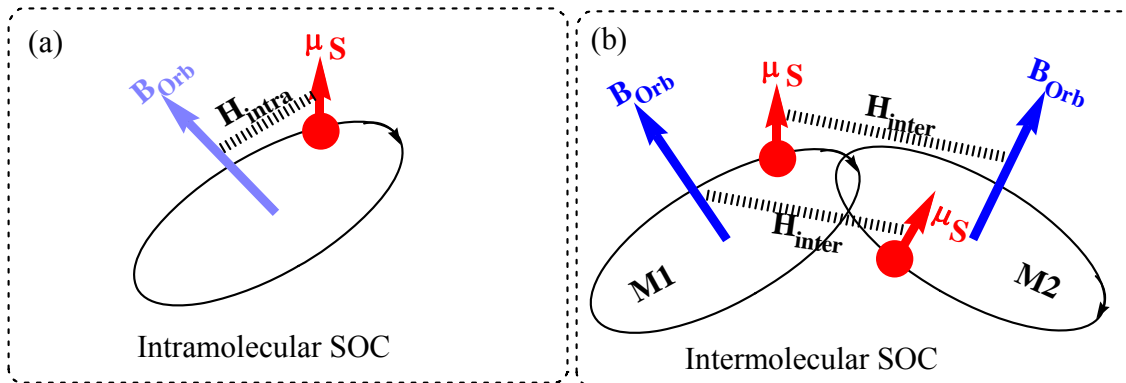


**Figure 5.3 The intra- and inter- molecular SOC for Ir(ppy)<sub>3</sub> in solid state, electron spin  $\mu_s$  and orbital magnetic field  $B_{Orb}$  occurring within a single molecule and between adjacent molecules. M1 and M2 are two adjacent Ir(ppy)<sub>3</sub> molecules.**

Now we further examine the inter-molecular SOC when the phosphorescent Ir(ppy)<sub>3</sub> molecules are dispersed in an inert polymer matrix. We know that dispersing the Ir(ppy)<sub>3</sub> molecules into an inert polymer matrix can, in general, form three phases: separated Ir(ppy)<sub>3</sub> molecules, aggregated Ir(ppy)<sub>3</sub> molecules, and continuous polymer morphologies. For separated Ir(ppy)<sub>3</sub> molecules, changing molecular concentration can directly modify the inter-molecular SOC by varying the inter-molecular distances. The dispersion effect is well common in Ir complex with strong spin orbit coupling strength. After dispersion all the Ir complexes show considerable magnetocurrent effect. For the aggregated Ir(ppy)<sub>3</sub> molecules, changing molecular concentration can change their domain sizes and consequently affects the sum of inter-molecular SOC components associated with each molecule within a given domain. From theoretical estimation<sup>106</sup>, we can suggest that the summation of individual inter-molecular SOC components can gradually increase the entire inter-molecular SOC for a single domain before reaching

saturation with the domain size of  $\sim 5$  nm. Here, we carefully examined intermolecular spin orbital coupling upon  $\text{Ir(ppy)}_3$  dispersion in an inert polymer matrix by using electron parametric resonance (EPR). In EPR spectrum, the EPR peak clearly shifts to a lower magnetic field after the  $\text{Ir(ppy)}_3$  molecules are dispersed in an inert polymer matrix as shown in Figure 5.4. The microwave frequencies for the pure  $\text{Ir(ppy)}_3$  and  $\text{Ir(ppy)}_3$ :PS sample are 9069.301 MHz and 9067.264 MHz, correspondingly. This EPR peak shift indicates that the  $g$  factor decreases from 1.9936 to 1.9895 from the  $\text{Ir(ppy)}_3$ :PS composite to pure  $\text{Ir(ppy)}_3$ . And the linewidth of the EPR spectrum changed from 17.2 Gauss to 21.8 Gauss from the  $\text{Ir(ppy)}_3$ :PS composite to pure  $\text{Ir(ppy)}_3$ . Both the  $g$  factor<sup>107</sup> and the linewidth<sup>108</sup> of the EPR spectrum suggest that inter-molecular SOC strength is reduced after the dispersion. Therefore, the EPR result confirms that dispersing  $\text{Ir(ppy)}_3$  molecules in an inert polymer matrix can lead to a reduction in inter-molecular SOC for phosphorescent organic molecules. In particular, weakening the inter-molecular SOC can increase the role of applied magnetic field on spin-momentum conservation involved in intersystem crossing and exciton-charge reaction. As a result, changing the inter-molecular SOC can essentially tune a density-based MC in phosphorescent organic semiconductors.

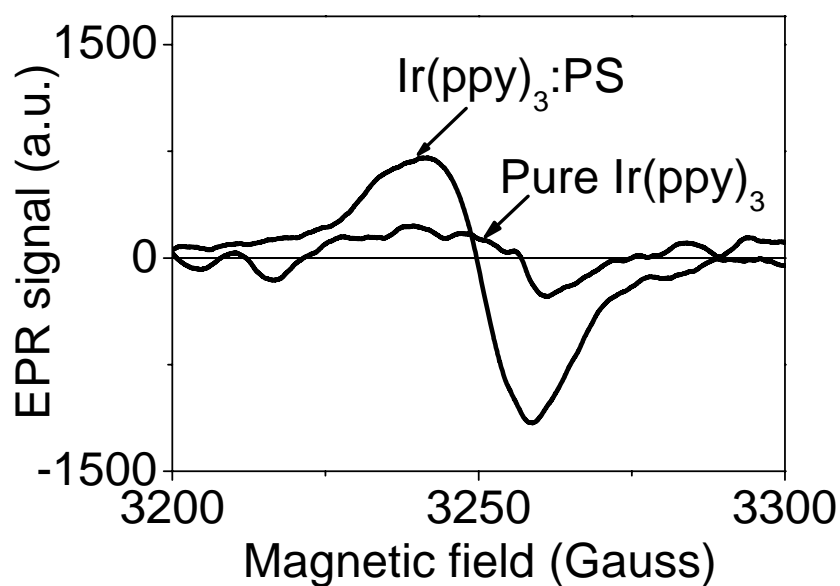


**Figure 5.4 EPR spectra for Ir(ppy)<sub>3</sub>:PS composite with weight ratio of 1:2 and pure Ir(ppy)<sub>3</sub>.**

It should be noted that the spin-orbital coupling in the Ir complex molecules is also related to the ligand group. With different ligand, not only the spin-orbital coupling strength is different but the exciton energy and energy level are also different. By changing the ligand group, people has synthesized Ir complex with different emission color and energy level. We also study the dispersion of different Ir complex with different emission color: blue (Ir65), green (Ir(ppy)<sub>3</sub>) and red (Ir77), whose electroluminescence spectra are shown in Figure 5.5.

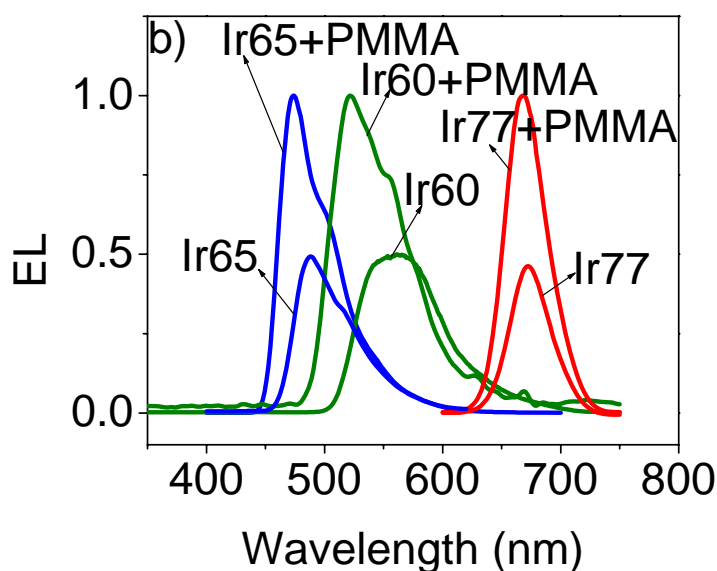


**Figure 5.5 Electroluminescence spectrum of Ir65, Ir77 and Ir(ppy)<sub>3</sub> and their composite in PMMA matrix.**

All the Ir complex have strong spin orbital coupling strength, which can be reflected by the probability of intersystem crossing of the singlet excited state ( $S_1$ ) to the triplet excited state ( $T_1$ ). For Ir77 the value of probability of intersystem crossing is not available, for Ir65 and Ir(ppy)<sub>3</sub> the intersystem crossing probability is 95% and 97%, correspondingly.<sup>109</sup> The magnetoresistance results for Ir65 and Ir77 are shown in Figure 5.6. Both of them show negative MC, which is consistent with the result from Ir(ppy)<sub>3</sub>. It indicates the dispersion effect is not a unique phenomenon only for Ir(ppy)<sub>3</sub>. Therefore, the dispersion effect induced MC should be linked to the common in the three system, the decreasing in intermolecular SOC.

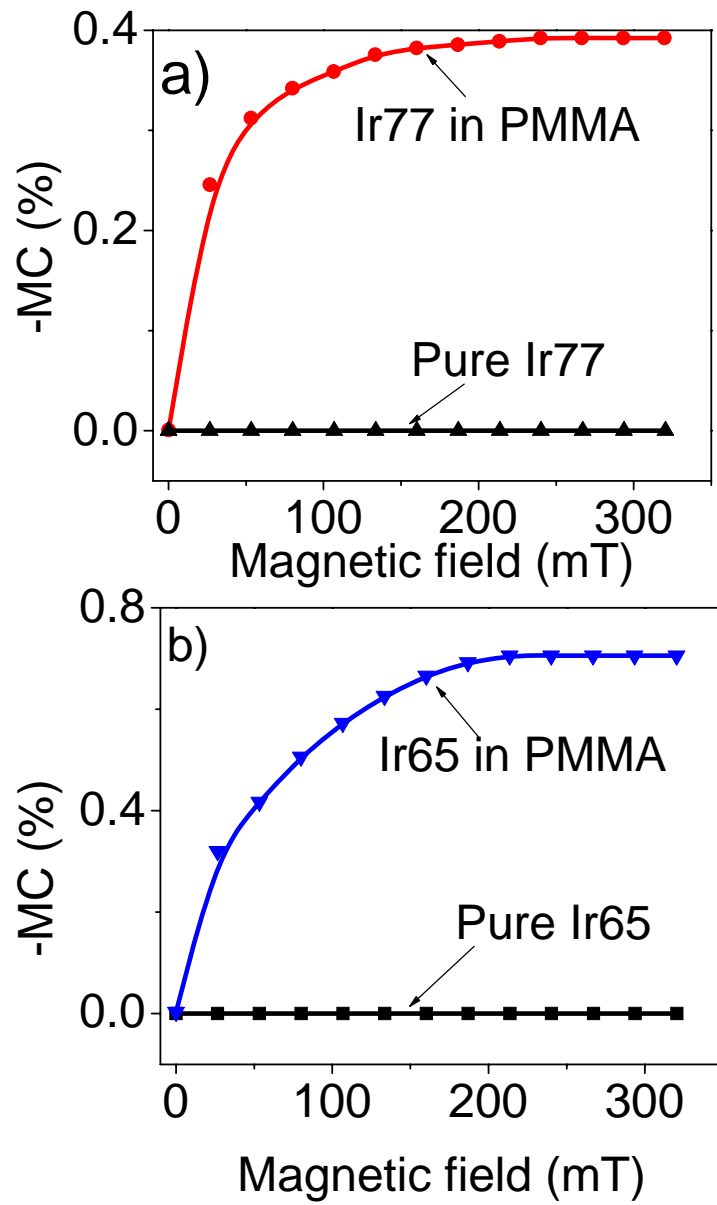


**Figure 5.6 MC from dispersion of Iridium complex in PMMA devices, a) Ir77:PMMA=1:2.5 b) Ir65:PMMA=1.5:2.5.**

We should particularly note from the negative magnetocurrent that the triplet-charge reaction is a dominant channel in the generation of density-based MC in the Ir(ppy)<sub>3</sub>:PMMA system. On contrast, the positive magnetocurrent indicates that the dissociation is a main channel in the generation of density-based MC in the Ir(ppy)<sub>3</sub>:PS system. Clearly, the PMMA and PS matrices lead to negative and positive MC, respectively, for the phosphorescent Ir(ppy)<sub>3</sub> molecules. We know that the PMMA and PS have different dielectric constants<sup>85</sup> ( $\epsilon_{\text{PMMA}} = 3.6$ ,  $\epsilon_{\text{PS}} = 2.5$ ). Dielectric matrix can provide a background of electric field for both the dissociation in polaron-pair states and the charge reaction in excitonic states in the generation of density-based MC. Therefore, both dissociation and charge reaction channels can be affected by matrix dielectric constant. On one hand, increasing matrix dielectric constant can increase the dissociation rates for both singlet and triplet polaron pairs through Onsager process.<sup>110</sup> This minimizes the difference between singlet and triplet dissociation yields in polaron pairs. Therefore, increasing the matrix dielectric constant can then decrease the effects of intersystem crossing on the dissociation in polaron-pair states. As a consequence, the dissociation channel of generating positive MC becomes less important upon increasing matrix dielectric constant. On the other hand, the excitonic states are essentially metal-to-ligand charge-transfer states in the Ir(ppy)<sub>3</sub> molecules<sup>111-114</sup>. The charge-transfer states are more sensitive to surrounding electric field due to their stronger ionic wavefunctions as compared to Frenkel excitons. Therefore, increasing the matrix dielectric constant can enlarge the wavefunction of a charge-transfer state through electrical polarization. This can increase the Coulomb interaction between an excitonic state and a charge in the

generation of triplet-charge reaction. As a result, the triplet-charge reaction channel of generating negative MC becomes more important upon increasing the matrix dielectric constant. It can be clearly seen in Figure 5.2 that the PMMA with higher dielectric constant and the PS with lower dielectric constant can generate negative and positive MC by enhancing the triplet-charge reaction and dissociation, respectively, in phosphorescent Ir(ppy)<sub>3</sub> molecules when the inter-molecular SOC is weakened through molecular dispersion.

We also studied the concentration effect on MC for the system Ir77 dispersed in PMMA. Figure 5.7 showed how the MC changed with Ir77 concentration. The magnitude of MC first showed an increasing trend then went down to zero when the Ir77 concentration was high. This was due to the combination of two effects. One is the concentration effect on polaron pair density; the other was the intermolecular SOC effect. The increasing part was due to the polaron pair state density. At first the Ir77 concentration was low, the density of intermolecular states was also low due to lots of PMMA chain fully separated the Ir77 molecules. When the Ir77 concentration was increasing in the film, the intermolecular states also increased and the MC showed an increasing trend. But when the concentration of Ir77 was high, the intermolecular SOC effect would dominate the process. When more Ir77 was added, the intermolecular SOC was stronger. Then the external magnetic field was difficult to compete with the intermolecular SOC. When the Ir77 concentration was high, a decreasing trend would appear. And at last for pure Ir77 film no MC was observed. This decreasing trend starting from 60% Ir77 is consistent

with the intermolecular SOC mechanism. This result is consistent with the expectation from intermolecular spin-orbital coupling theory. It further supports that intermolecular spin-orbital coupling strength will determine the magnetoresistance in heavy metal complex.



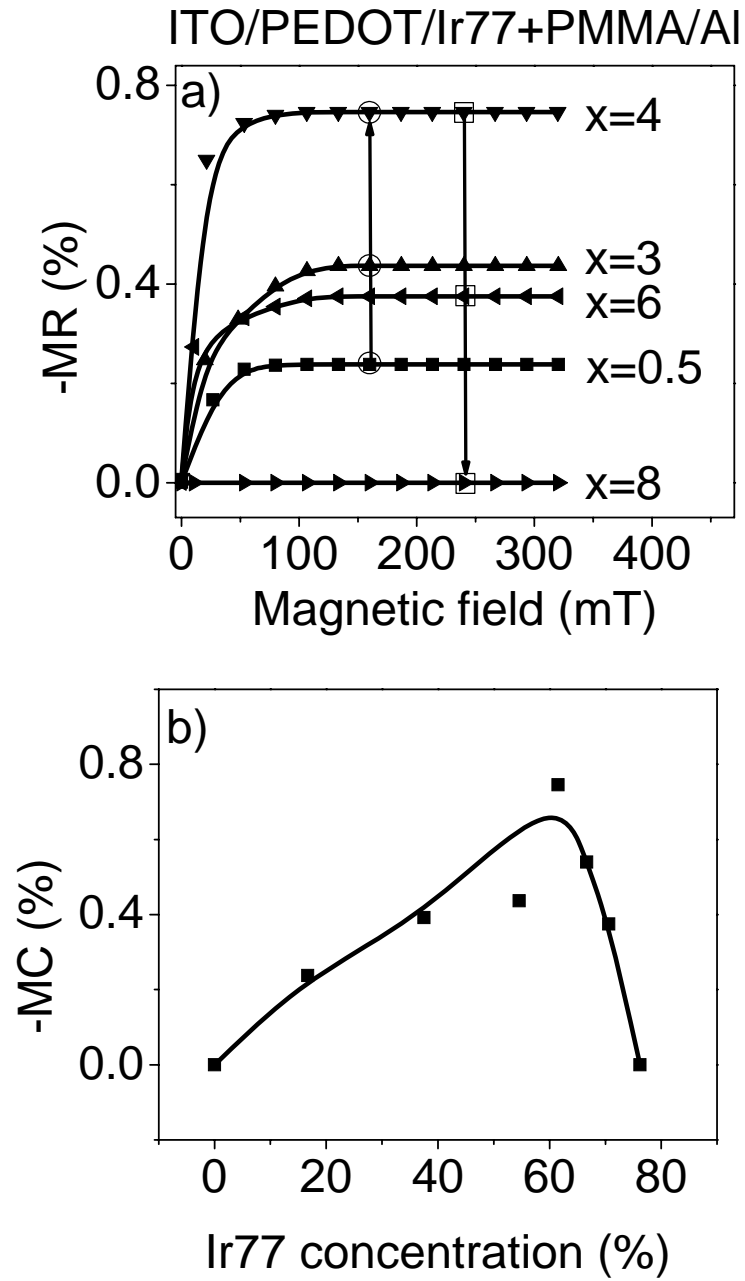


**Figure 5.7 a) MC of ITO/ Ir77+PMMA/Al, Ir77:PMMA=x:2.5, b) MC of ITO/Ir77+PMMA/Al at different Ir77 concentration.**

It should also be noted that in all Iridium complex dispersed system, considerable MC could be observed, and meanwhile, no clear trace of  $\text{MFE}_{\text{EL}}$  could be observed. The possible mechanism is the efficient ISC due to strong SOC readjust the S/T ratio in intramolecular excited state (excitonic state). After forming intermolecular excited state, the electron and hole became closer to be in one molecule, which was in excitonic state, the intramolecular SOC strength ( $\text{SOC}_{\text{intra}}$ ) was strong due to no PMMA chain was in the between to weaken the SOC and the distance between electron and hole was small. As a result, the external magnetic field could not change the intersystem crossing between singlet and triplet excitons. And due to very strong intramolecular SOC in  $\text{Ir}(\text{ppy})_3$  molecules the triplet excitons had almost 100% ratio<sup>115</sup>, which meant there were almost no singlet excitons but only triplet excitons. No matter how the external magnetic field changed the ratio between singlet and triplet polarons, when they got closer to form the excitonic states, we would always have almost 100% triplet excitons. This process looked like a cycle as shown in Figure 5.8. At intermolecular excited states, the intercrossing rate constant  $k_{\text{inter}}$  is not large; the external magnetic field changes the singlet/triplet ratio at intermolecular excited states. But because of the almost 100% intersystem crossing rate constant  $k_{\text{intra}}$  at intramolecular excited state, all excitons change into triplet states. In this way, the density of triplet excitons was locked. It would not change with external magnetic field.

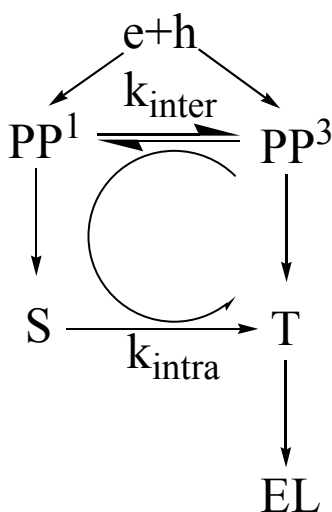


**Figure 5.8 The spin orbital coupling effect on intersystem in intermolecular and intramolecular excited state.**

## 5.5 Conclusion

The strong SOC from heavy-metal complex structures forms a difficulty to generate magnetic field effects in phosphorescent organic semiconductors. We find that dispersing phosphorescent Ir(ppy)<sub>3</sub> molecules into an inert polymer matrix can generate positive and negative MC. This experimental observation suggests that inter-molecular SOC is a key parameter to generate magnetic field effects in phosphorescent organic semiconductors. In essence, the strength of inter-molecular SOC determines the amplitude of magnetic field effects in phosphorescent organic semiconductors. The EPR studies confirm that phosphorescent Ir(ppy)<sub>3</sub> molecules form significant inter-molecular SOC. In particular,

dispersing Ir(ppy)<sub>3</sub> molecules into an inert polymer matrix can largely change strength of inter-molecular SOC. As a consequence, positive and negative MC can be observed for phosphorescent organic semiconductors in lower and higher dielectric matrices, respectively, when inter-molecular SOC is weakened based on molecular dispersion. Clearly, our experimental studies indicate that changing inter-molecular SOC forms an effective mechanism to tune magnetic field effects in heavy-metal complex molecules. Furthermore, changing matrix dielectric constant can switch the density-based MC between dissociation and charge reaction channels, tuning MC between positive and negative values in phosphorescent organic semiconductors. The difference between the MC and  $\text{MFE}_{\text{EL}}$  suggests the spin orbital coupling is important not only in intermolecular excited state but also in intramolecular excited state.

**CHAPTER 6**

**INTERFACE INDUCED NEGATIVE PHOSPHORESCENCE**

**MAGNETIC FIELD EFFECT IN ORGANIC DOUBLE LAYER**

**LIGHT EMITTING DEVICES**

## 6.1 Abstract

Organic semiconductors exhibit magnetic responses on electroluminescence, photocurrent, photoluminescence and electrical current under low magnetic field. These responses are due to the spin dependent processes of intermolecular electron-hole pairs in organic semiconductors, which require spin momentum conservation. Because the intermolecular electron-hole pairs are loosely bonded, with relatively longer separation distance compared to intramolecular electron-hole pairs, the exchange energy between singlet and triplet states is small. The external magnetic field will compete with the internal magnetic interaction, such as hyperfine interaction and spin-orbital coupling, to affect the spin dependent processes in intermolecular electron-hole pairs to generate magnetic responses in organic semiconductors. Investigators have observed considerable magnetic response after adjusting the spin-orbital coupling strength through modifying the intermolecular spin-orbital coupling interaction in strong spin-orbital coupling materials. But the magnetic response on electroluminescence has not been observed. And by using the insulating layer, a positive interface induced magnetic response on electrophosphorescence has been found. In our system, the interfacial induced magnetic response on electrophosphorescence is negative; different from the one has been found. The different sign might suggest the different mechanism behind. And the system containing both electrofluorescence and electrophosphorescence with the insulating layer has also been studied to identify the possible mechanism.

## 6.2 Introduction

It has been experimentally found that organic semiconductors can show magnetic responses in the electroluminescence,<sup>17-23</sup> electric current,<sup>18,24-43,65</sup> photocurrent<sup>44-50</sup> and photoluminescence<sup>46,51-56</sup> to externally applied low magnetic field ( $< 100$  mT). These responses have been called magnetic field effects (MFEs). In general, the MFEs can be attributed to internal spin dependent processes of intermolecular electron-hole pairs in organic semiconductors. The intermolecular electron-hole pairs are loosely bonded, with relatively longer distance compared to intramolecular electron-hole pairs.<sup>80</sup> The relative long separation distance will lead to small exchange energy between singlet and triplet states. This makes the magnetic interaction possible to affect the spin-dependent process in intermolecular electron-hole pairs. When an external magnetic field is comparable to internal magnetic interaction, it can essentially affect the spin-dependent processes of intermolecular electron-hole pairs and change the singlet/triplet ratio of intermolecular electron-hole pairs. Due to the different dissociation and recombination properties of singlet and triplet electron-hole pairs, it consequently generates MFEs in electroluminescence, photoluminescence, photocurrent, electrical current. However, strong internal magnetic interaction can lead to negligible MFEs<sup>26,62,63</sup>. As a result, the internal magnetic interaction plays a critical role in the generation of MFEs in organic semiconductors. It is noted that organic semiconductors can be divided into singlet and triplet semiconducting materials with weak and strong internal magnetic interaction, respectively. It is known that the internal magnetic interaction arises from hyperfine interaction or spin-orbital coupling. In singlet organic semiconducting materials the

hyperfine interaction is mainly accountable for internal magnetic interaction due to the absence of spin-orbital coupling based on low atomic numbers. However, in the triplet semiconducting materials the spin-orbital coupling can dominate the internal magnetic interaction. Recently, it has been found that by adjusting the intermolecular SOC strength the triplet semiconductor could show considerable magnetic response on electrical current without magnetic response on electroluminescence.(Chapter 5)<sup>116</sup> And by using the insulating layer, a positive interface induced magnetic response on electroluminescence has been found.<sup>117</sup> In this work, we also apply an insulating layer but with a different triplet semiconductor. While a negative magnetic response in electroluminescence has been observed. It indicates a different magnetic dependent process was involved. And we further change the triplet material into a copolymer with both singlet and triplet emission to perform the experimental studies of insulating layer effect on magnetic field effect on both electrofluorescence and electrophosphorescence. We found the MFE of both the fluorescence and phosphorescence move towards negative sign direction. It indicates the same process would involve in both singlet and triplet materials.

### 6.3 Experiment

The iridium heavy-metal complex molecules: bis(2-(9,9-dibutylfluorenyl)-1-isoquinoline (acetylacetonate) (Ir77), Iridium (III) bis(2-(2'-benzo-thienyl)pyridinatoN,C3')(acetylacetonate) (Ir67) were purchased from America Dye Source Inc, and used as triplet



organic semiconducting material. The copolymer polyfluorene-co-bis(4-phenylbenzothiazole) monomeric acetylacetonate (P2) with both singlet and triplet emission was obtained from Prof. Hsu's Group<sup>118</sup>. The chemical structures of Ir67, Ir77 and P2 are shown in Figure 6.1. The poly(methyl methacrylate) (PMMA) was used as polymer matrix. The poly(vinyl alcohol) (PVA) was used as the insulating layer by spin-cast from the aqueous solution. The Ir77 molecules with PMMA composite and polymer P2 films were spin-cast from chloroform solutions in organic light-emitting devices. The organic light-emitting devices were fabricated with indium tin oxide (ITO) and aluminum (Al) electrodes. The Al electrode was thermally evaporated under the vacuum of  $2 \times 10^{-6}$  Torr. MFE was measured at constant current density  $20 \text{ mA/cm}^2$ . The magnetic response amplitude was given by the relative change in signal intensity caused by applied magnetic field. It can be expressed by  $\frac{I_B - I_0}{I_0}$ , where  $I_B$  and  $I_0$  are the signal intensity with and without an applied magnetic field.

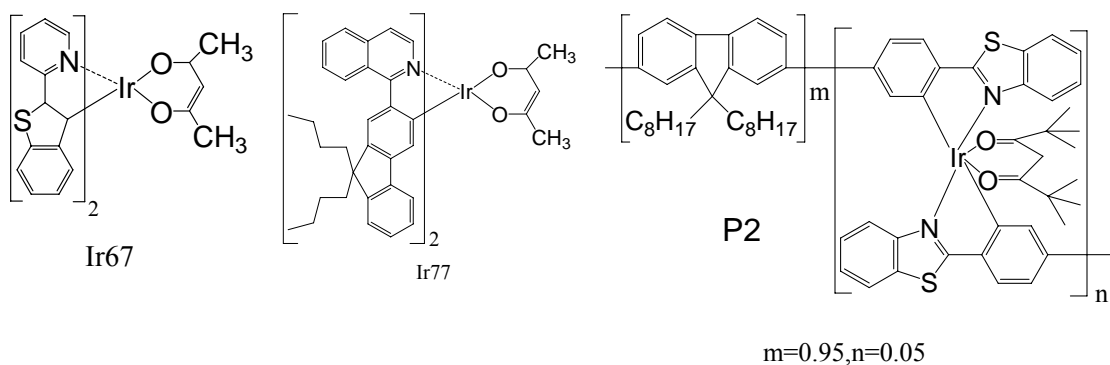


**Figure 6.1 Chemical structures of Ir67, Ir77 and P2.**

## 6.4 Result and Discussion

Figure 6.2 presents the MFE of device with and without PVA layer for different Ir complex Ir67 and Ir77. It is clear that the PVA layer will lead to a negative MFE for Ir77. In the former study from our group, another red Ir complex Ir67 blended in PMMA with PVA insulating layer, a clear positive MFE has been observed.<sup>117</sup> The possible mechanism was due to the carrier accumulated at the Ir composite/PVA interface and the short distance spin-spin interaction of charge carriers. No matter the spin-spin interaction is between electron-hole pairs or same polarity charge carriers, the result of the interrupt from external magnetic field is to increase the triplet ratio and decrease the singlet ratio. In this way the triplet emission should show a positive MFE as we observed in Ir67 and PMMA composite/PVA double layer device. But in Ir77 and PMMA composite/PVA double layer device, the MFE is the opposite sign, which indicates the different magnetic dependent process involved in the Ir77 based device. It should also be noticed that without PVA insulating layer both Ir67 and Ir77 based single layer devices did not present any MFE. This indicates the MFE come from the interface effect.

To determine which process is the dominate process; we make three major change to study this issue. First, we change the PVA layer position to change the charge accumulation. Second, we change the Ir77 concentration to adjust the intermolecular SOC strength.<sup>116</sup> Third, we change the triplet material Ir77 to a polymer P2 with both

singlet and triplet emission to study if singlet signal will also be affected by the PVA insulating layer.

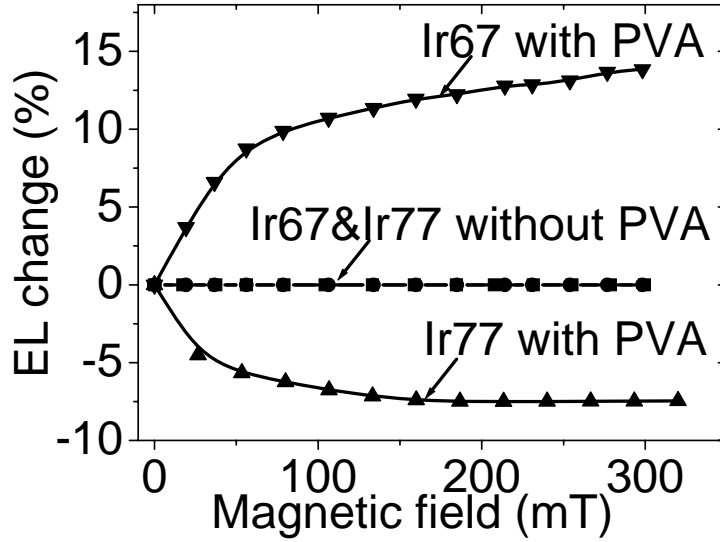


**Figure 6.2 MFE of ITO/ Ir77+PMMA/PVA (5nm)/Al, Ir77:PMMA=4:2.5 and ITO/Ir67+PMMA/PVA (5nm)/Al, Ir67:PMMA=4:2.5.**

As shown in Figure 6.3a, after changing the position of PVA layer from cathode Al side to anode ITO side, the MFE from Ir77 did not change the sign but the amplitude was reduced. And From Figure 6.3b the C-V measurement also indicates there is significant charge accumulation in the device with PVA insulating layer. In the single layer Ir77+PMMA composite device, the capacitance of device almost remains constant at low voltage, followed by a sharp drop at relative high voltage. The sharp drop of the capacitance is due to the recombination of injected electrons and holes, which

consequently reduces the amount of charge carriers stored in the device. On the other hand, the capacitance of the device with PVA insulating layer also remains constant at low voltage range, but increases with the applied voltage and show a peak at median voltage range, and decreases dramatically at high voltage range. The increase and the peak of the capacitance provide a clear evidence for the presence of interfacial charge at the Ir77+PMMA/PVA interface. When PVA layer is at the Al side the MFE amplitude is larger than the MFE when PVA layer is at ITO side. Because the hole mobility in Ir77 is about  $2 \times 10^{-2} \text{ cm}^2 \text{ V}^{-1} \text{ s}^{-1}$  and the electron mobility in Ir77 is about  $3 \times 10^{-7} \text{ cm}^2 \text{ V}^{-1} \text{ s}^{-1}$  [119], the hole will accumulate a lot at PVA/composite interface when PVA layer is at Al side. If the PVA layer is at ITO side the accumulation of holes is less. Therefore, the amplitude might be related to hole accumulation.

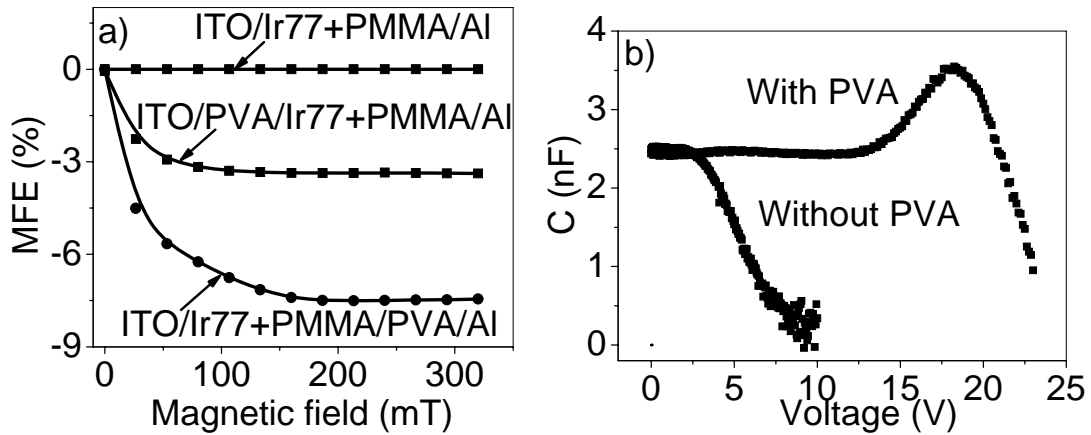


**Figure 6.3 a) MFE of ITO/Ir77+PMMA/Al, ITO/PVA/Ir77+PMMA/Al and ITO/Ir77+PMMA/PVA/Al, Ir77:PMMA=4:2.5, b) C-V measurement for ITO/Ir77+PMMA/PVA/Al and ITO/Ir77+PMMA/Al, Ir77:PMMA=4:2.5.**

We also change the concentration of Ir77 to adjust the intermolecular SOC in the Ir77 composite layer. In general, the MFE is a spin-dependent process. The competition of internal magnetic interaction, such as hyperfine interaction and spin-orbital coupling, and external magnetic field always exists. If the internal magnetic interaction is strong the external magnetic field could not change the spin-dependent process much. Therefore, no clear MFE could be observed in pure heavy metal complex film. But after dispersion into inert polymer matrix whose SOC strength is weak, the intermolecular SOC strength is weakened. As shown in Figure 6.4, no matter the PVA layer is at cathode side (Al) or at anode side (ITO), when the intermolecular SOC is weakened by reduce the concentration of Ir77, the amplitude of MFE becomes larger. It implies the intermolecular SOC is also associated to the MFE mechanism, which means the dominated process should be a spin-dependent process. It should be noted that even for pure Ir77/PVA device the negative MFE could be observed. This indicates the insulating layer PVA could also weaken the intermolecular SOC at the interface of Ir77/PVA. At the interface the surrounding molecules is less than in the bulk, therefore, the intermolecular SOC is weakened.

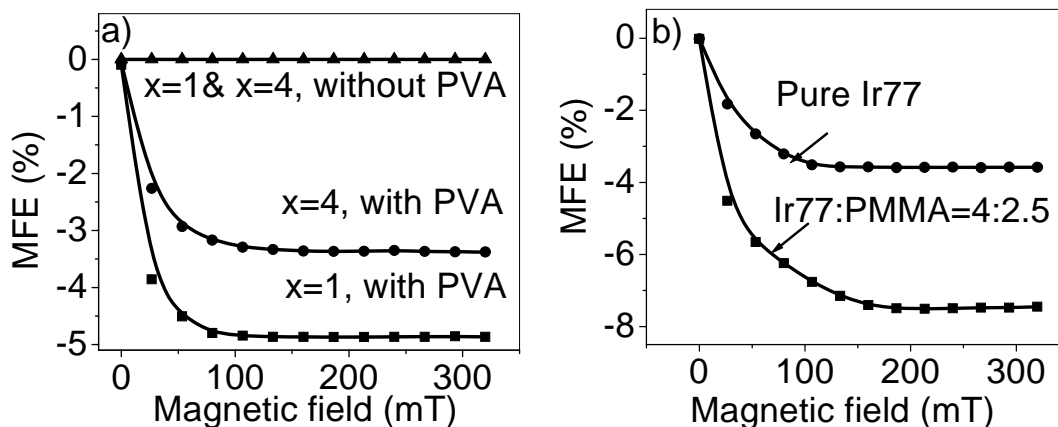


**Figure 6.4 a) MFE of ITO/PVA (5nm)/Ir77+PMMA/Al, Ir77:PMMA=x:2.5, b) MFE of ITO/Ir77+PMMA/PVA(5nm)/Al with different Ir77 concentration.**

To find out which spin-dependent process is dominated in the abnormal negative MFE, we change the triplet phosphorescent into a copolymer P2 with both fluorescence and phosphorescence emission. The copolymer shows the fluorescence at 422 nm and phosphorescence at 593 nm, shown in Figure 6.5a. Figure 6.5b and Figure 6.5c present the MFE change without PVA layer and with PVA layer at cathode side (Al). The MFE of phosphorescence (Figure 6.5b)) is similar to Ir77 composite situation. Without PVA layer it presents negligible MFE, but with PVA layer negative MFE was observed. The fluorescence did show positive MFE without PVA layer, which has been widely observed in organic light emitting devices. While after adding the PVA insulating layer, the fluorescence and phosphorescence follow the same trend, coming towards the negative sign region. Therefore, it is reasonable to account the interface induced negative MFE from fluorescence and phosphorescence to the same mechanism.

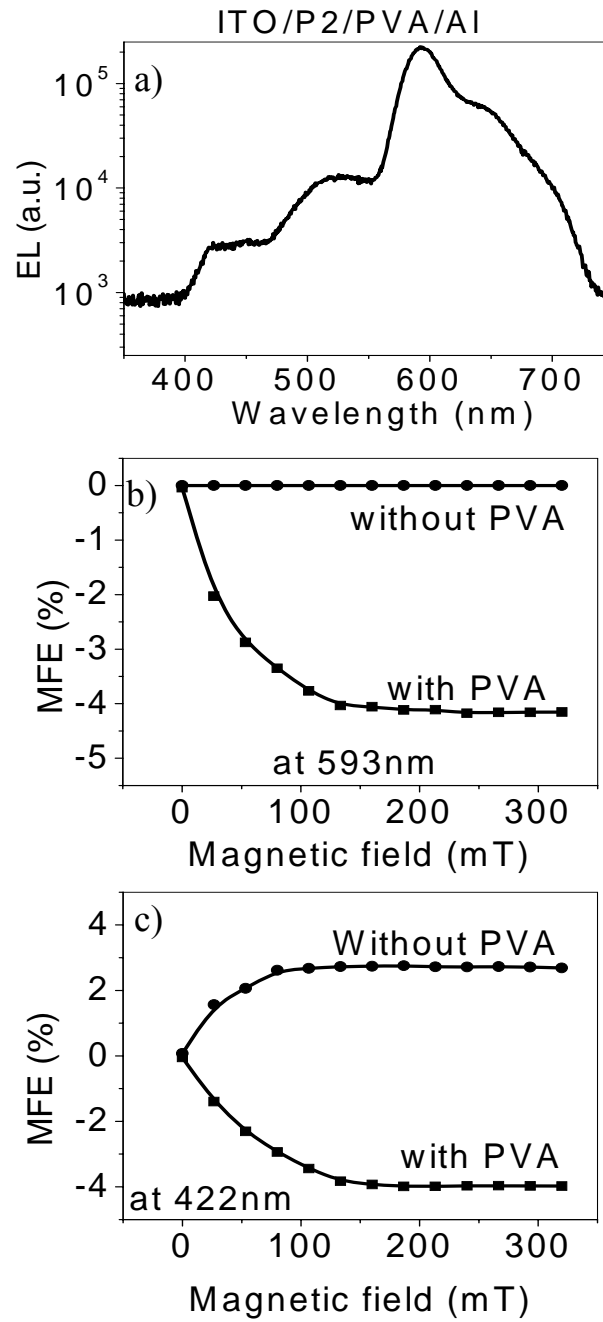


**Figure 6.5** MFE of ITO/P2/PVA (5nm)/Al and ITO/P2/Al.

At last we discuss the possible mechanism for the interface induced negative MFE of phosphorescence based on above experiment results. We already know the dominated process for this negative MFE is a spin-dependent and charge accumulation related process. And it also can be affect both singlet and triplet emission. In general, the MFE has three types of mechanisms.

First, the intersystem crossing based mechanism, the ratio singlet and triplet intermolecular electron-hole pairs would be affected by external magnetic field through Zeeman splitting and they would further affect the singlet and triplet ratio in excitonic states. But this kind of mechanism will usually lead to opposite change to singlet and triplet ratio unless the energy transfer from singlet to triplet exists. If the singlet ratio increases, the triplet ratio would decrease. And in the P2 copolymer the energy transfer effect could be ignored. Because P2 single layer device the phosphorescence shows ignorable MFE and fluorescence did show clear trace of MFE, the energy transfer from singlet state did not transfer MFE from singlet to triplet. The possibility is that most of electrophosphorescence is from the trapping charge in the Iridium unit but not from the energy transfer from fluorescent unit. Therefore, the energy transfer did not affect MFE in double layer device because the inert PVA layer should not affect the energy transfer in P2 layer. As a result, the intersystem crossing based mechanism should lead to opposite change in singlet and triplet emission. We could rule it out according to our P2/PVA double layer device result.



Second, the exciton-charge reaction mechanism, especially the triplet exciton could reaction with charge carriers due to its long life time compare with singlet exciton. The triplet-charge reaction rate constant will decrease with increasing the magnetic field. This will lead to more triplet exciton left from the reaction, which would directly cause positive phosphorescence MFE and secondarily cause negative fluorescence MFE through exciton generation process. But our phosphorescence result for both Ir77 and P2 are negative. Therefore, this mechanism could also be ruled out.

Third, the spin-spin interaction mechanism (bipolaron mechanism), the spin-spin interaction between polarons was interrupted by external magnetic field causing the ratio of singlet configuration decreasing and the triplet configuration increasing. If the polarons are the opposite polarity, it is the short distance intermolecular excited states. Because the singlet and triplet will follow the opposite trend, it would be ruled out. If the polarons are the same polarity, it is the bipolaron, whose singlet bipolaron mobility is higher than triplet bipolarons. In this way the positive MC could be observed. In our devices the charge accumulation at the PVA interface is significant; the bipolarons is highly possible generated at the PVA interface. But our MFE is measured at constant current model. Therefore, the mobility decreasing would lead to the carrier density increasing, which would cause the positive MFE for both fluorescence and phosphorescence<sup>120</sup>. As a result, the spin-spin interaction mechanism also fails to explain the negative MFE on both fluorescence and phosphorescence.

From the above discussion, the three main mechanisms for magnetic field response in organic semiconductors could not be applied. Here we suppose the possible mechanism based on the formation of trion, charged exciton or excited polaron. Recently, the trion, three-polaron complex with two polarons for same polarity and one other polarity polaron, has been observed in PPV-based conjugated polymer.<sup>121</sup> And the trion could be formed by exciton-charge collision and bipolaron-charge collision. The trion can also generate phonons and contribute to the electroluminescence.<sup>122</sup> The trion also has singlet and triplet spin configuration, which are defined from the two polaron with same polarity. If they have anti-parallel spin, the trion is singlet, if they have parallel spin, the trion is triplet. In our devices, due to the insulating layer lots of positive polarons (holes) are accumulated at the insulating interface. They are very likely to form bipolarons and the negative polarons are tunneled from the other side of the insulating layer. As a result, they are pretty possible to collision and form the trions, which can also contribute to electroluminescence. The formation of trions might be spin-dependent process. The singlet and triplet trions have different formation rate. The singlet trions formation rate might be larger than triplet trions, due to the lack of spin-spin interaction between singlet bipolaron and the other opposite polarity polaron. After applying magnetic field, the formation of singlet trions was suppressed, this has been observed in quantum well.<sup>123</sup> The triplet trion formation, which is like the triplet exciton charge reaction will also be reduced by magnetic field. As a result, the total number of trion was reduced. This would leads to the decease in all electroluminescence.

## 6.5 Conclusion

We have observed the interface induced negative MFE in electrophosphorescence only and electrofluorescence and electrophosphorescence coexisting system with the insulating layer. The mechanisms based on intersystem crossing, triplet-charge reaction and the spin-spin interaction failed to explain the phenomena in our device. The possible bipolaron based trion formation mechanism was proposed. It shows that new mechanism for the magnetic field effect on electroluminescence might get involved.

**CHAPTER 7**

**MAGNETO-CAPACITANCE EFFECT IN ORGANIC RADICAL-  
BASED MATERIALS**

## 7.1 Abstract

Organic radical ion pairs can show both singlet and triplet spin configuration. The external magnetic field can change the singlet/triplet ratio and generate magnetic field effects on photoluminescence, electroluminescence, photocurrent and electric current. The singlet and triplet spin configuration of radical ion pair have different electrical dipole moment. The magnetic field effect on capacitance (magneto-capacitance) would also be expected. We studied the magneto-capacitance on radical ion pair system. And by adjusting the spin-orbital coupling strength and separation distance of radical ion pairs, the aptitude and sign of magneto-capacitance can be tuned.

## 7.2 Introduction

It has been found that in organic semiconductors there are several magnetic field effects on electroluminescence<sup>17-23</sup>, electrical current<sup>18,24-43,65</sup>, photocurrent<sup>44-50</sup> and photoluminescence<sup>46,51-56</sup>. These phenomena were related to the electron-hole pairs (excited states)<sup>65</sup> formed in organic materials, which could also be thought as the radical ion pairs. The radical ion pairs have both singlet and triplet states with different spin precessions for the two radicals. When applying magnetic field, it needs to compete with the internal magnetic interaction, such as spin-orbital coupling and hyperfine interaction, to affect the spin dependent processes in radical ion pairs. It is noted that spin-dependent processes must require spin momentum conservation. The spin-momentum conservation can be satisfied by internal magnetic interaction. When an external magnetic field is

comparable to internal magnetic interaction, the spin-momentum conservation can be affected by magnetic field through Zeeman splitting and spin flip by magnetic scattering. As a result, the magnetic field can essentially affect the spin-dependent processes of radical ion pairs and change the singlet/triplet ratio of radical ion pairs. Because the singlet and triplet states have different contribution to emission and transport properties through excited state dissociation<sup>80,81</sup> and excited state charge reaction processes,<sup>75,76</sup> different magnetic responses could be found. The singlet and triplet radical ion pairs would also have different electric dipole moment<sup>124</sup>. Therefore the change in device capacitance would also be expected. Here we present the magnetic generated capacitance change for some radical ion pair systems.

It has been found that the separation distance of radical ion pairs played an important role in determining the magnetic field effects. The distance between radical ion pairs can affect the magnetic field effect by disturbing spin precession and changing exchange energy. The distance effect leads to the difference in MFEs of intermolecular radical ion pairs (relative long distance) and intramolecular radical ion pairs (relative short distance). At relative long distance, the dominated process is the change of exchange energy. While at relative short distance, the dominated process is the relative strong spin-spin interaction, which could change the sign of exchange energy. In this work, we study the magneto-capacitance effect on both intermolecular radical ion pair system and intramolecular radical ion pair system.

### 7.3 Experiment

N,N'-Bis(3-methylphenyl)-N,N'-diphenylbenzidine (TPD), 2,5-Bis(5-tert-butyl-benzoxazol-2-yl) thiophene (BBOT), poly(methyl methacrylate) (PMMA), emeraldine base polyaniline (PANi), 7,7,8,8-Tetracyanoquinodimethane (TCNQ) and 1,2,4,5-Tetrachloro-3-nitrobenzene (TCNB) were purchased from Aldrich, Iridium (III) bis(2-(4,6-difluorophenyl)pyridinato-N,C<sup>2</sup>) (Ir65) was purchased from American Dye Source, Inc. Tetracyanoquinodimethane grafted polyaniline (PANiCNQ) was synthesized as in reference<sup>125</sup> and freshly used. The PMMA composite film was spin-casted from chloroform solution of PMMA and corresponded materials. The PANiCNQ film was casted by dropping the N-Methyl-2-pyrrolidone (NMP) solution of PANiCNQ on pre-cleaned substrate, followed by solvent evaporation at 70°C in vacuum oven. The capacitance was measured by Agilent E4980A LCR meter at 0V DC bias and 50mV AC voltage. The magneto-capacitance was defined as  $\frac{\Delta C}{C} = \frac{C_B - C_0}{C_0}$ , the  $C_B$  and  $C_0$  is the capacitance with and without magnetic field, correspondingly. The light source was white light with standard sun light spectrum.

### 7.4 Results and Discussion

PANiCNQ is a polymer with intramolecular charge transfer state. We choose the PANiCNQ as intramolecular radical ion pair system to study magnetocurrent, whose structure is shown in Figure 7.1. And the absorption spectrum (Figure 7.1a) is similar to

reported result<sup>125</sup>, the peak at about 492 nm indicates the chemical reaction between PANi and TCNQ, the double peaks at about 620-650nm indicates the intramolecular charge transfer.<sup>125</sup>

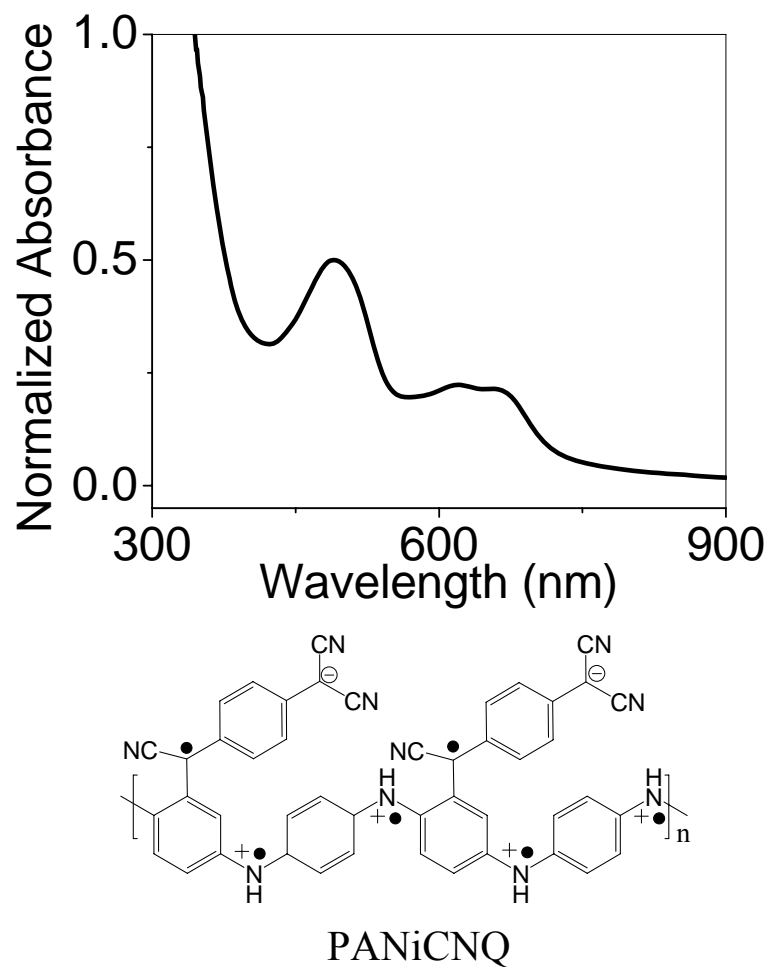


**Figure 7.1 Normalized absorption spectrum of PANiCNQ in NMP and the chemical structure of PANiCNQ.**

The magneto-capacitance of PANiCNQ was shown in Figure 7.2. It should be noted that the fresh synthesized PANiCNQ is diamagnetic material<sup>125</sup> and no clear magnetocurrent



was observed. Therefore, the magneto-capacitance should come from the change of singlet/triplet ratio in radical pair within the repeating unit under magnetic field. The magneto-capacitance is negative, and the absolute value of the magneto-capacitance decreases with increasing the operation frequency. It should also be noted that with increasing the frequency the amplitude of MC is getting smaller. This is due to that the relaxation of electric dipoles from photo-generated radical ion pairs gradually delayed to response the AC electric field under high operation frequency.

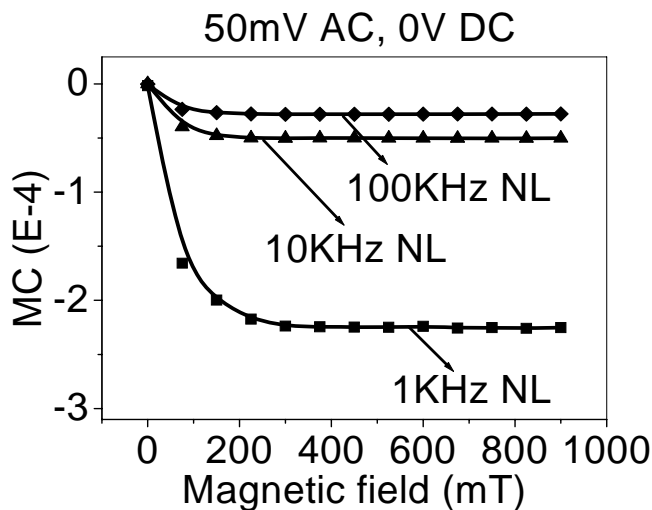


**Figure 7.2 Magneto-capacitance on ITO/PANiCNQ/Al at different frequency.**

The negative sign of the MC might be caused by the exchange energy change. From the chemical structure the separation distance of the radical pairs is roughly about 3~4 C-C bonds. We can assume the length of C-C bond is 0.15 nm, and then the separation distance is about 0.45~0.6 nm. If we consider the bond angle, then the separation distance between radicals can be assumed to be around 0.5 nm. But the separation distance for

exciplex, which are contact intermolecular ion pair, usually is about 0.65~0.75 nm.<sup>126</sup> The small separation distance would have a large influence on exchange energy. With large separation distance, the exchange energy is very small, almost zero. While with small separation distance the sign of exchange energy might be negative, as shown in Figure 7.3. The negative exchange energy has been established in the system of small thickness quantum wall<sup>127</sup> and the theoretical calculation indicates the small distance radical ion pair in organic materials would have negative exchange energy.<sup>128</sup> The negative exchange energy would lead to the magnetic dependent intersystem crossing process is opposite to the intersystem crossing in the intermolecular radical ion pairs with positive or zero exchange energy. As shown in Figure 7.3, in the intramolecular radical ion pairs, the triplet state splitting would lead to increase the triplet ratio and decrease the singlet ratio. Singlet radical ion pair would have larger electric dipole moment than triplet radical ion pair due to that the singlet has more ionic nature in wave function and triplet is more localized.<sup>124</sup> Therefore, the MC becomes negative. This is well supported by our magneto-capacitance results in Figure 7.2.

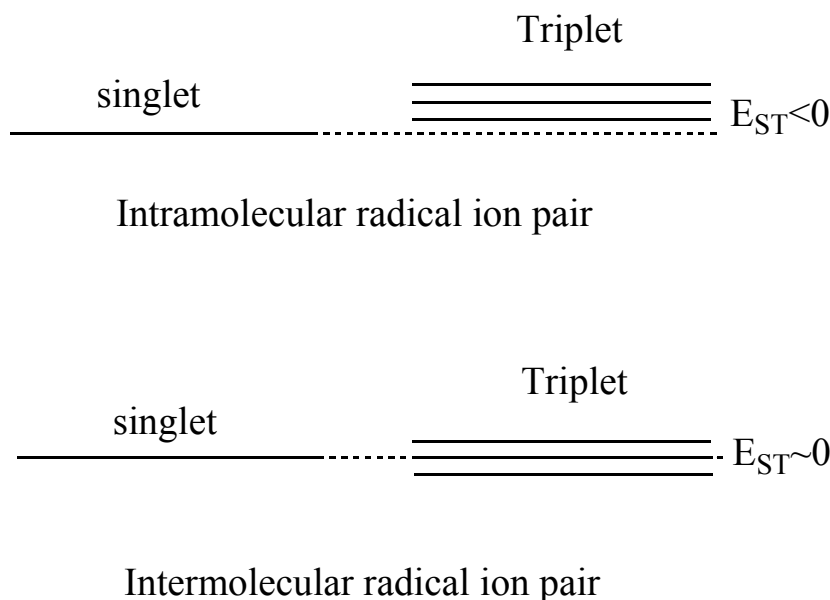


**Figure 7.3 Energy levels of singlet and triplet radical ion pair under magnetic field.**

**a) for intramolecular radical ion pair, b) for intermolecular radical ion pair.**

Exciplex systems were considered as intermolecular contact radical ion pairs under light illumination. We choose two exciplex systems as the intermolecular radical ion pair system. We look at both singlet and triplet dominated systems. The singlet system is BBOT:TPD, whose chemical structure is shown in Figure 7.4. It has been found that BBOT:TPD can show singlet exciplex emission<sup>129</sup>. As shown in Figure 7.5a, only under photo-excitation the device could present positive magneto-capacitance, consist with the exchange energy in large distance radical pair (intermolecular) shown in Figure 7.3. Under photo-excitation the radical ion pair was formed. And the magnetic field would increase the singlet ratio and decrease the triplet ratio through affecting the intersystem crossing. Singlet radical ion pair would have larger electric dipole moment than triplet radical ion pair due to that the singlet has more ionic nature in wave function and triplet

is more localized.<sup>124</sup> Therefore, the magnetic field will cause the positive magneto-capacitance. However, it should be noted that the magneto-capacitance under light illumination has another possible mechanism, magnetic field effect on photocurrent (MFP). The magnetic field change the singlet/triplet ratio at radical ion pair state, the singlet radical ion pair is easier to dissociate than triplet radical ion pair. Therefore, the number of photo-generated charge carriers will increase under magnetic field. It will cause the increase in capacitance. Anyway, the change in capacitance is caused by the intersystem crossing process.

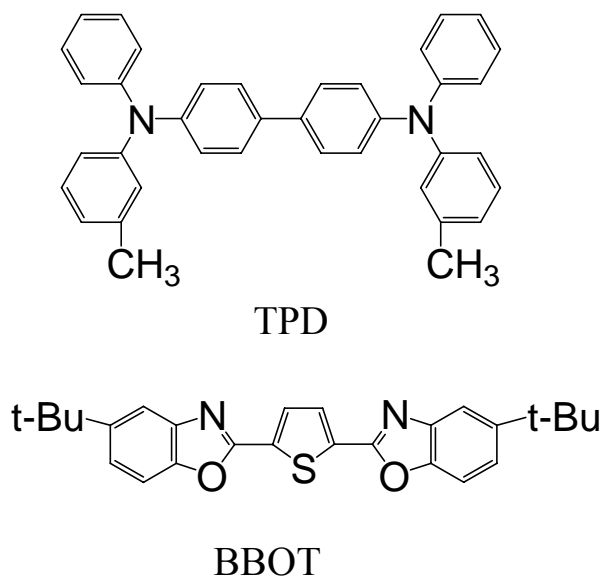


**Figure 7.4 Chemical structures of BBOT and TPD.**

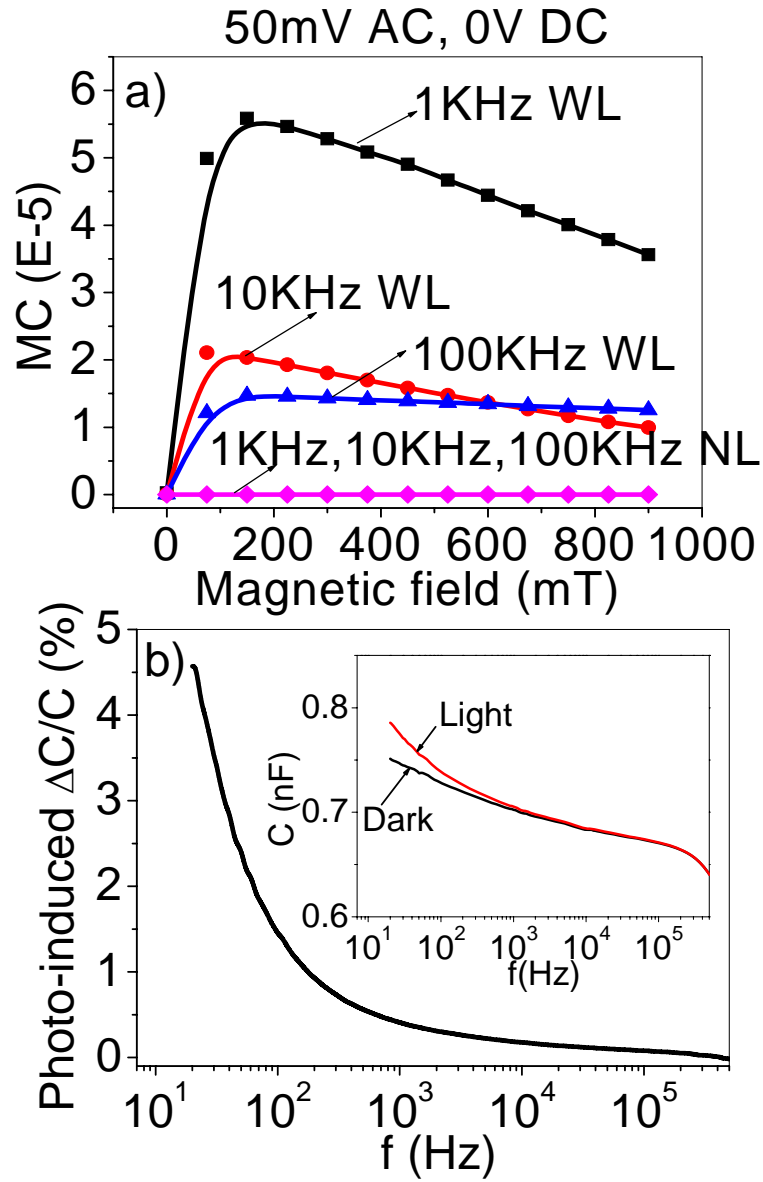


**Figure 7.5 a) Magneto-capacitance of ITO/TPD:BBOT:PMMA=4:4:10/Al, b) Photo-induce capacitance change at different frequency of ITO/TPD:BBOT:PMMA=4:4:10/Al.**

It should also be noted that with increasing the frequency the amplitude of MC is getting smaller. This is due to that the relaxation of electric dipoles from photo-generated radical ion pairs gradually delayed to response the AC electric field under high operation frequency. As shown in the Figure 7.5b, the capacitance under photo-excitation becomes close to the dark capacitance with increasing the operation frequency and the photo-induced capacitance change from photo-generated radical ion pairs becomes smaller. Therefore, the MC, which comes from singlet/triplet dipole change of the photo-generated radical ion pairs, is also getting smaller at high frequency. As a result, adjusting the radical separation can change the spin exchange energy and further tune the sign of magneto-capacitance.

The triplet system is Ir65:TCNB, whose chemical structure is shown in Figure 7.6. They can give triplet exciplex emission (PL spectrum is shown in Chapter 3, Figure 3.9), indicating strong spin-orbital coupling. The lifetime is about 0.4us. Our photo-induced EPR measurement (as shown in Figure 7.7b) also confirmed the intermolecular electron transfer states (radical ion pairs) under photo-excitation. But no clear MC was observed at all operation frequencies as shown in Figure 7.7a, which is different from the BBOT:TPD system. If we compare the singlet and triplet system, the SOC plays important role in MC response.

The singlet/triplet ratio change with magnetic field which should compete with the internal magnetic interactions, such as hyperfine interaction and SOC. In organic

materials the hyperfine interaction is not very strong, only several mT of external magnetic field could compete with it. But if the organic materials contain heavy metal, the SOC strength would be strong. The external magnetic field is difficult to compete with the SOC. As a result, the magneto-capacitance disappears. This indicates the trace of magneto-capacitance is originated from the intersystem crossing process at radical ion pair.

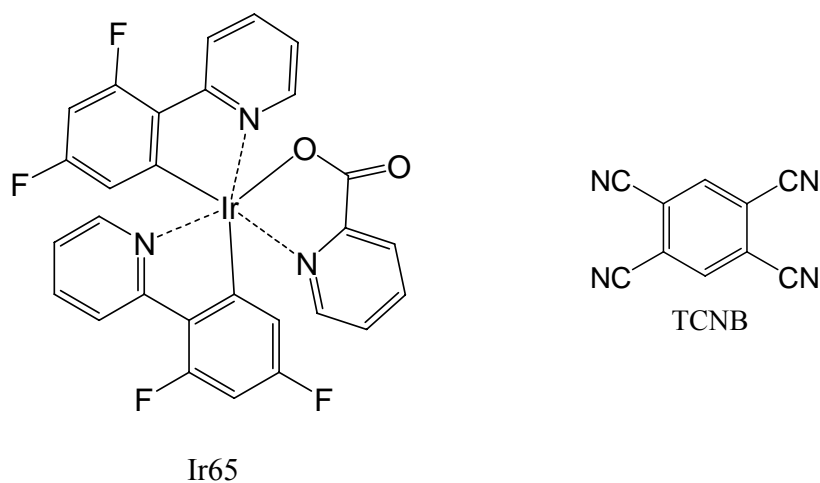


**Figure 7.6 Chemical structure of Ir65 and TCNB.**

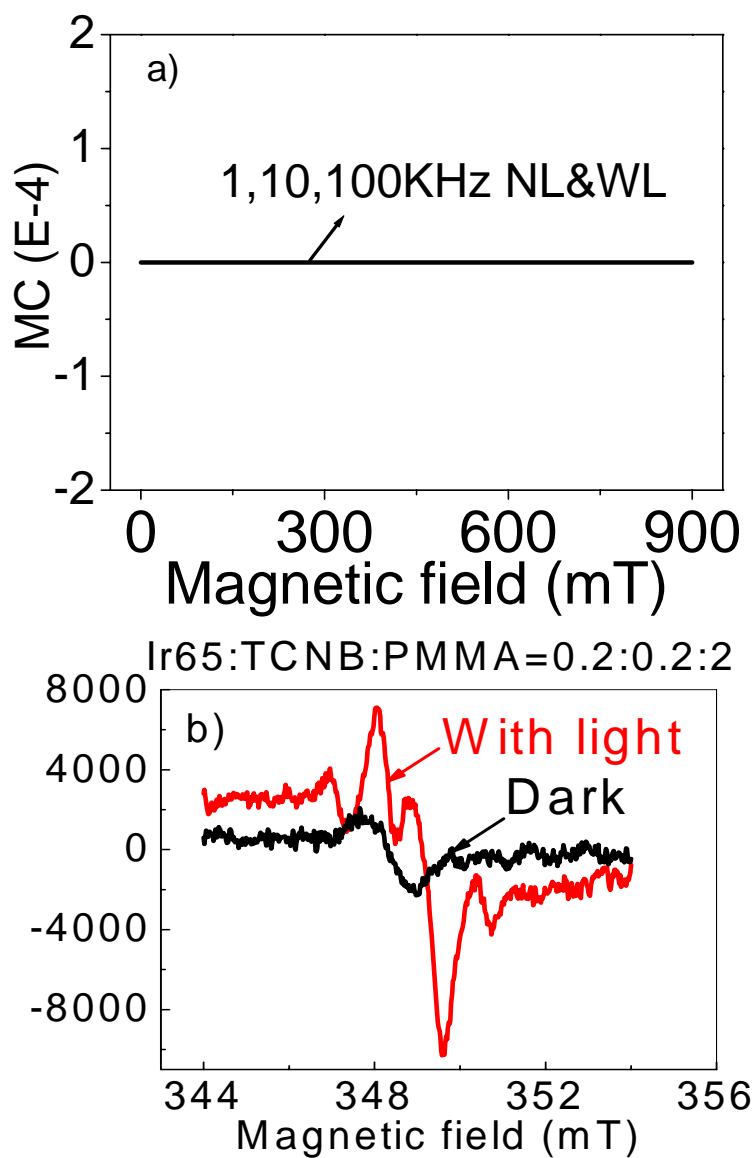


**Figure 7.7 a) Magneto-capacitance of ITO/TPD:BBOT:PMMA=4:4:10/Al, b) Photo-induce capacitance change at different frequency of ITO/TPD:BBOT:PMMA=4:4:10/Al.**



## 7.5 Conclusion

We studied magneto-capacitance on both intermolecular and intramolecular radical ion pair based system. The magneto-capacitance is generated by the magnetic induced change of ratio of singlet/triplet radical ion pairs. The separation distance of the radical ion pair would change the sign of magneto-capacitance. These results indicate a new magnetic response in the organic semiconductors.

## **CHAPTER 8**

### **THE COMPARATION OF MAGNETOCURRENT BETWEEN MAGNETIC AND NONMAGNETIC MODIFIED C<sub>60</sub>**

## 8.1 Abstract

Organic semiconductors exhibit magnetic responses on electrical current (magnetocurrent) under low magnetic field. This response can be found in both nonmagnetic and magnetic organic semiconductors. In non-magnetic organic semiconductors, it is due to the spin dependent intersystem crossing processes of intermolecular electron-hole pairs or bipolarons in organic semiconductors. Then the magnetocurrent would be generated by different dissociation or transport properties of the singlet and triplet states in electron-hole pairs or bipolarons. In magnetic organic semiconductors, it is caused by the alignment of magnetic dipole. Then magnetocurrent would be generated from the changing of charge scattering in transport. We compared magnetocurrent in magnetic and non-magnetic mechanism in modified  $C_{60}$  molecules. Modified  $Fe_xO$  containing donor-acceptor type  $C_{60}$  molecules can show larger magnetocurrent than Fe free  $C_{60}$  molecules with different magnetocurrent vs. magnetic field curves.

## 8.2 Introduction

The phenomena of magnetocurrent have been observed in lots of organic semiconductors. The organic semiconductors can be magnetic<sup>130-133</sup> or nonmagnetic<sup>18,24-43</sup> with different mechanisms. There are several mechanisms for magnetocurrent in nonmagnetic organic

semiconductors based on electron-hole pairs<sup>18,19,28,38,39,63,65</sup> or bipolarons<sup>26,29,34,37,40,42,43</sup>. The external magnetic field can change the spin dependent intersystem crossing processes of intermolecular electron-hole pairs or bipolarons in organic semiconductors. Then the magnetocurrent would be generated by different dissociation and transport properties of the singlet and triplet states in electron-hole pairs or bipolarons. The internal magnetic interactions, such as hyperfine interaction and spin-orbital coupling, are required for spin momentum conservation in nonmagnetic organic semiconductors. In magnetic organic semiconductors, there is another internal magnetic interaction mechanism, the alignment of local magnetic dipole. The local magnetic dipoles from d orbit of the magnetic center, such as Fe, Co atoms, will interact with the conducting  $\pi$  electron through magnetic dipole-dipole interaction.<sup>134</sup> After applying external magnetic field, the local magnetic dipole moment will be aligned. Then magnetocurrent would be generated from the change in magnetic dipole-dipole interaction to affect the conducting charge scattering in transport. The different mechanisms in non-magnetic and magnetic organic semiconductors will lead to different magnetocurrent shape. In this paper, we studied magnetocurrent in modified C<sub>60</sub> containing FeO<sub>x</sub> as magnetic organic semiconductor and Fe-free modified C<sub>60</sub> as nonmagnetic organic semiconductor. We found the different magnetocurrent vs. magnetic field curve based on these two materials, which indicates the different mechanisms.

### 8.3 Experiment

The modified C<sub>60</sub> was provided by Prof. Long Chiang's Group from University of Massachusetts. The poly(methyl methacrylate) (PMMA) was purchased from Sigma-Aldrich and used as received. The modified C<sub>60</sub> was mixed with PMMA with certain weight ratio, and then dissolved in chloroform. The thin film of the composite of modified C<sub>60</sub> and PMMA was spin cast by the above solution on pre-cleaned ITO glass. Then the metal Aluminum was thermally evaporated on top of the thin film under the vacuum of 2x10<sup>-6</sup> torr. The final device was put in the gap between the electromagnet to measure the magnetocurrent under constant forward bias. The magnetocurrent (MC) was defined as  $MC = \frac{I_B - I_0}{I_0} \times 100\%$ , where  $I_B$  and  $I_0$  are the electric current with and without magnetic field. The magnetic hysteresis measurement and temperature dependent magnetization measurement are taken by Prof. Arthur Epstein's Group at The Ohio State University.

### 8.4 Result and Discussion

The chemical structures of magnetic Fe-containing and non-magnetic Fe-free modified C<sub>60</sub> are shown in Figure 8.1. The magnetic FeOx-containing modified C<sub>60</sub>, C<sub>60</sub>(>DPAF-C<sub>9</sub>)-FeOx(1/1,w/w), has additional FeOx unit based on Fe-free nonmagnetic C<sub>60</sub>, C<sub>60</sub>(>DPAF-C<sub>9</sub>). The hysteresis loop curves for C<sub>60</sub>(>DPAF-C<sub>9</sub>)-FeOx(1/1,w/w) at 90K and

300K are shown in Figure 8.2. They clearly indicate the  $C_{60}( > \text{DPAF-C}_9 )\text{-FeOx}(1/1, \text{w/w})$  is magnetic at 90K and 300K. Magnetization saturates with a value of 5.1  $\mu\text{B}$  per formula unit. Theoretically expected saturation value for Fe(III) with spin  $S = 5/2$  is 5.0  $\mu\text{B}$ . For Fe(II) with spin  $S = 3$  is 6.0  $\mu\text{B}$ . Experimental value is close to the average value of these two Fe ions. Coercive field measured at 300 K is less than 10 Oe, which is most likely due to the remnant field of superconducting magnet used for the measurement.

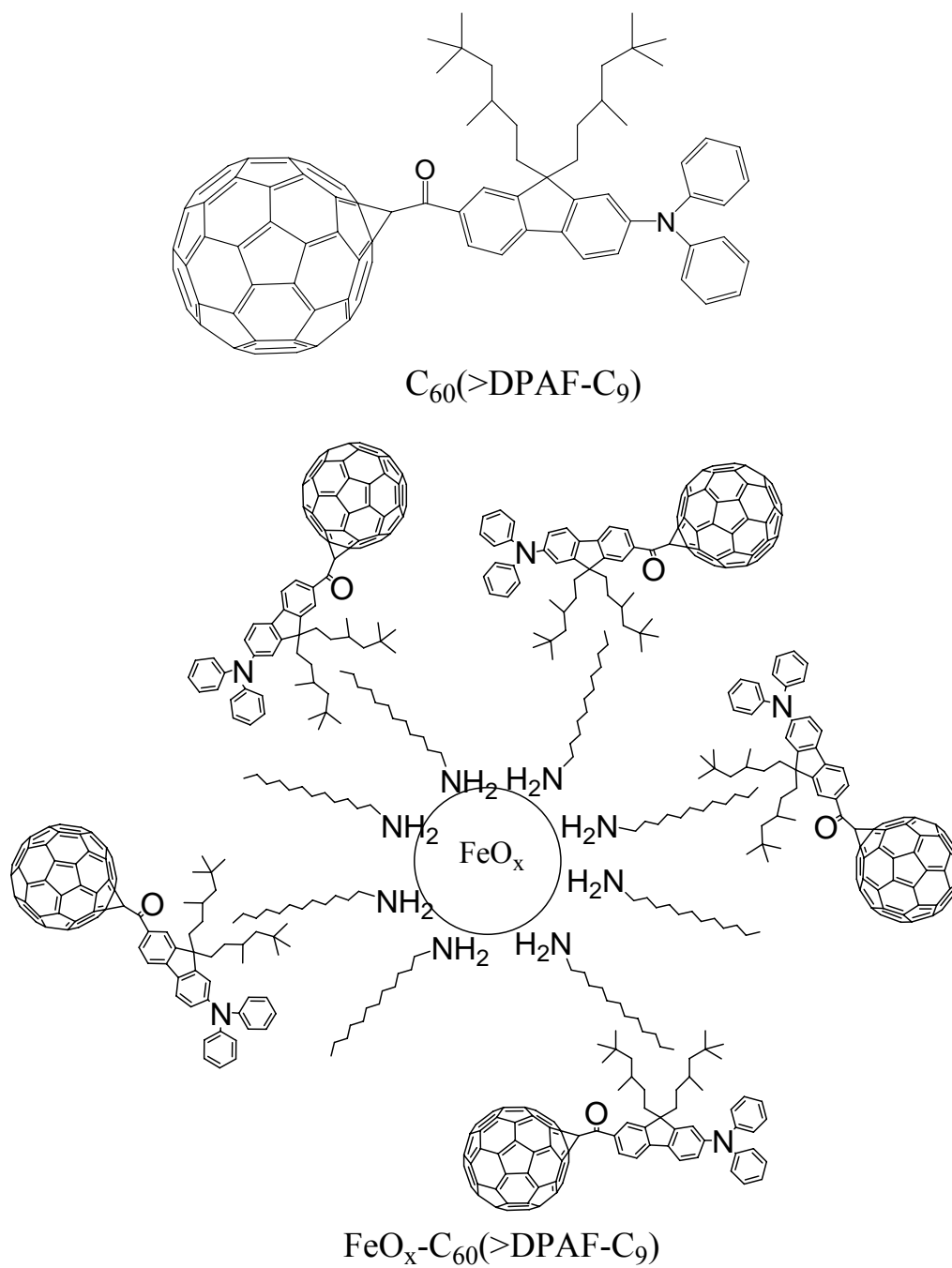


**Figure 8.1 Chemical structure of magnetic and nonmagnetic modified C<sub>60</sub>.**

Figure 8.3 shows the magnetocurrent of the Fe-free and Fe-containing modified  $C_{60}$  in PMMA matrix at 77K. The magnetocurrent is in the common shape as the non-magnetic organic semiconductors. It should be noted that no clear magnetocurrent was observed in the unmodified  $C_{60}$  due to the lack of hyperfine interaction from hydrogen atom in previous report.<sup>57</sup> After the modification the donor group adds the hydrogen atom to provide significant hyperfine interaction. Therefore, considerable magnetocurrent would be expected.

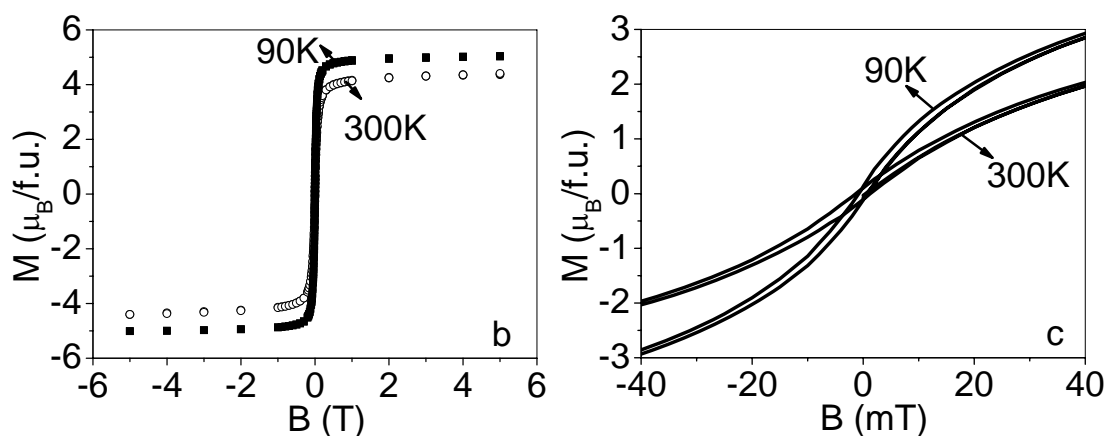


**Figure 8.2 a) M vs H hysteresis loop recorded at 90K and 300K, b) Enlarged M vs H hysteresis loop recorded at 90K and 300K.**

The interesting phenomenon in Figure 8.3 is that the magnetocurrent of Fe-containing modified  $C_{60}$  in PMMA matrix shows much larger amplitude. At 77K as Figure 8.3, the MC curve is obviously different from the MC of Fe-free modified  $C_{60}$ , an inflection point exhibiting at low field range. It is due to combination of the alignment of magnetic dipole and spin-dependent intersystem crossing. At low field the local magnetic dipole from d



orbital of Fe atom will not be completely aligned, thus it shows the curve shape similar to intersystem crossing mechanism and the d- $\pi$  magnetic dipole-dipole interaction is not dominated. After lots of local magnetic dipole aligned by external magnetic field, the conducting charge  $\pi$  electron will scatter differently in transport due to different magnetic dipole-dipole interaction compared to the situation without external magnetic field. In our case the scattering might be reduced in order to increase the mobility of the charges, which will generate a positive MC and also cause the inflection point.

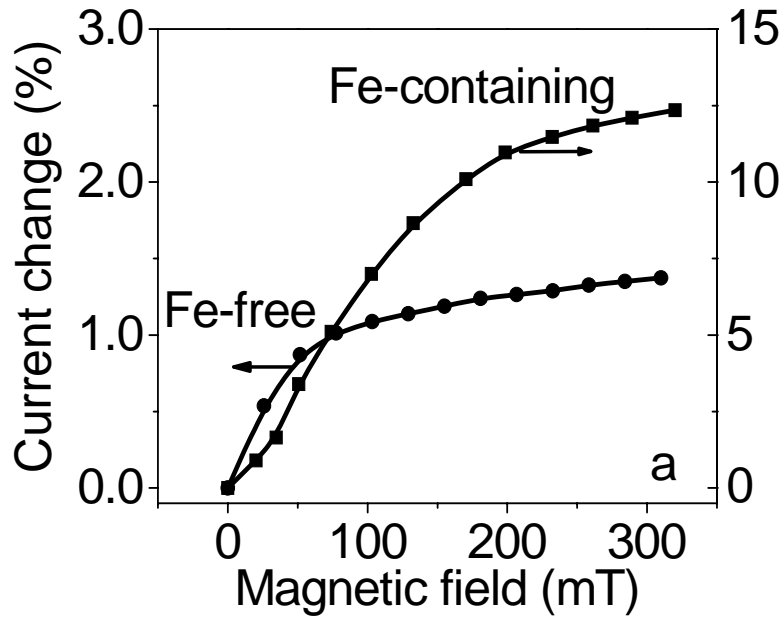


**Figure 8.3 Magentocurrent of Fe-free and Fe-containing modified C<sub>60</sub> device at 77K.**

But at room temperature as Figure 8.4, the magnetocurrent is much smaller than the MC at 77K. And it should be noted that the shape of the magnetocurrent at 300K is different from the magnetocurrent at 77K, but very similar to the MC of Fe-free modified C<sub>60</sub>. If

we compare the MC curves of magnetic modified  $C_{60}$  at 77K and 300K, at first the MC curves are very close to each other due to the intersystem crossing mechanism. Then the different alignment effect at different temperature leads to the difference in curve shape.

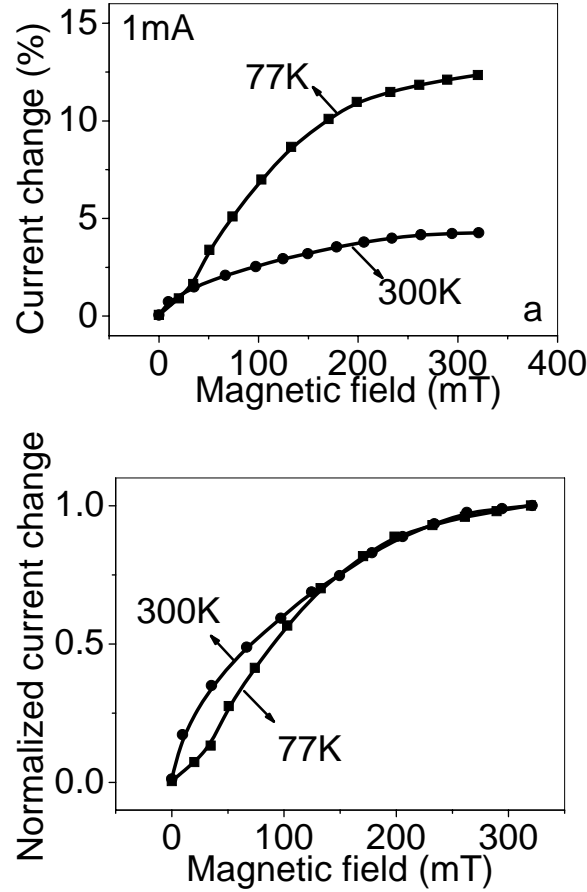


**Figure 8.4 Magnetocurrent of device ITO/ $C_{60}$ (>DPAF- $C_9$ )- $FeO_x$ (1/1,w/w):PMMA (2:4) /Al at different temperature.**

It can be supported by the magnetization with temperature as shown in Figure 8.5. The magnetization is decreasing with temperature, indicating the exchange interaction between magnetic dipole moment disturbed by the thermal energy. At low temperature

the exchange interaction between magnetic dipole is relative strong, we can clearly see the alignment effect magnetocurrent. While at room temperature the exchange interaction is relative weak compared with thermal energy, the magnetocurrent is showing the curve similar to non-mangetic Fe-free modified  $C_{60}$  device.

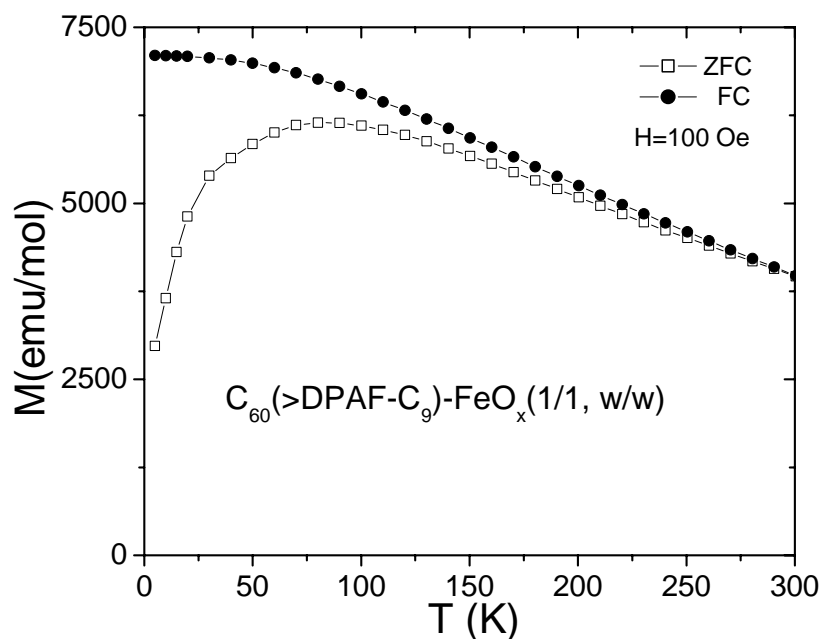


**Figure 8.5 Variation of zero field cooled (ZFC) and field cooled (FC) magnetization with temperature measured at an applied magnetic field of 100 Oe.**

Figure 8.6 shows the normalized curve for both hysteresis and magnetocurrent. It should be also noted that the shape of normalized hysteresis curve at low temperature and the magnetocurrent curve at low temperature are quite different, which suggest the

mechanism in magnetocurrent is still the combination of the magnetic dipole scattering and intersystem crossing in polaron pair.

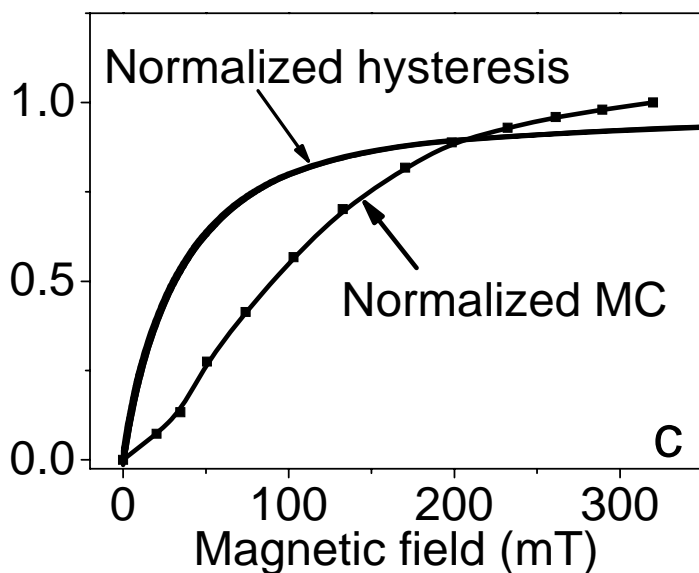


**Figure 8.6 Normalized curve for both hysteresis and magnetocurrent.**

## 8.5 Conclusion

Both magnetic and non-magnetic modified  $C_{60}$  showed clear MC. But the shape of MC curves is different due to different mechanisms. The non-magnetic modified  $C_{60}$  shows similar MC curve to common non-magnetic organic semiconductors based on intersystem crossing mechanism. On the other hand, the MC curve of the magnetic modified  $C_{60}$  shows an additional inflection point and larger magnitude compared with non-magnetic modified  $C_{60}$ . The difference is caused by the combination of the intersystem crossing

mechanism and the magnetic dipole-dipole interaction mechanism. Then the temperature will change the combination of the two mechanisms leading to different MC curve shape.

## CHAPTER 9

### CONCLUSION

Our experiment shows the magnetic field effects in organic semiconductors are originated from intermolecular excited states. The result suggests the external magnetic field not only shows Zeeman splitting effect but also can affect the spin momentum conservation when the external magnetic field is comparable to internal magnetic field.

The separation distance at intermolecular excited states and spin-orbital coupling strength are found to be important for generating magnetic field effects in organic semiconductors. The long or short separation distance at intermolecular excited states can cause relative small or large exchange energy between singlet and triplet intermolecular excited states. When the exchange energy is larger, the splitting energy of magnetic field was too small to affect intersystem crossing process at intermolecular excited states and magnetic field effects could not be observed. Only when the exchange energy is small, the splitting energy of external magnetic field will lead to the change of the intersystem crossing process in intermolecular excited states and generate magnetic field effects.

Spin orbital coupling is another internal magnetic interaction in addition to hyperfine interaction, which has been found important for weak spin orbital coupling materials. Usually strong spin orbital coupling materials will not show magnetic field effects. It suggests the hyperfine interaction would not dominate the spin-dependent process in

magnetic field effects in strong spin orbital coupling materials. However, we found three ways to obtain magnetic field effects in strong spin orbital coupling materials.

First, by using Forster energy transfer effect, we could transfer magnetic field effects from weak spin orbital coupling host to strong spin orbital coupling guest. But the backwards Dexter energy transfer effect from strong spin orbital coupling guest to weak spin orbital coupling guest will suppress magnetic field effects in weak spin orbital coupling host. Therefore, the energy transfer effect can adjust the magnetic field effect in both directions.

Second, by tuning the spin-orbital coupling strength through changing the separation distance, the magnetic field effects could be adjusted. Increasing the spin orbital coupling strength in weak spin orbital coupling strength materials can quench the magnetic field effects. Decreasing the spin orbital coupling strength in strong spin orbital coupling materials could obtain considerable magnetic field effects. But the sensitivity of the different magnetic field effects to strong spin orbital coupling strength is different according to the different processes to form the final product signals. Recombination process will be affected by spin orbital coupling for the second time at the excitonic or intramolecular excited states. While the dissociation process would not be affected by spin orbital coupling again. Therefore, the magnetic field effects on emission are more sensitive to spin orbital coupling strength.

Third, by using semiconducting/insulating interface, where the spin orbital coupling strength is weaker than the bulk in strong spin orbital coupling materials, the spin orbital coupling strength could also be tuned. As a result the magnetic field effect could also be obtained. In addition to weak spin orbital coupling strength at the interface, the charge carriers are also accumulated at the interface. This leads to unexpected negative magnetic field effect on electrophosphorescence. By combining result from both singlet and triplet emission and intersystem crossing model, bipolaron model and triplet charge reaction model, a new mechanism based on trion, which can also contribute to electroluminescence, was proposed. The magnetic field will decrease both singlet and triplet trion formation rate, which will cause the emission from singlet and triplet reduced by magnetic field.

A new magnetic response, magneto-capacitance (MCP), has been observed. Its mechanism is also supposed to follow the intersystem crossing model on radical ion pairs. The magneto-capacitance is generated by the magnetic induced change of ratio of singlet/triplet radical ion pairs and the different electric dipole moment between singlet and triplet radical ion pairs. The separation distance of the radical ion pair would change the sign of magneto-capacitance. The spin orbital coupling will also reduce the MCP.

The internal magnetic interaction can be hyperfine interaction, spin orbital coupling and spin-spin interaction between electrons. The hyperfine interaction and spin orbital coupling are important in nonmagnetic organic semiconductors. But the electron spin-



spin interaction is important in magnetic organic semiconductors. The magnetocurrent for magnetic and nonmagnetic organic semiconductors at different temperature has been compared. The thermal energy will play an important role to determine the dominated internal magnetic interaction. At low temperature the thermal energy is small; it could not disturb the electron spin-spin interaction. The dominated internal magnetic interaction is the electron spin-spin interaction. When the thermal energy is large enough but the temperature is still lower than the Curie temperature, the magnetocurrent will be dominated by the sum of the three internal magnetic interactions.

## REFERENCES

- 1 Su, W. P.; Schrieffer, J. R.; Heeger, A. J., Soliton excitations in polyacetylene. *Phys. Rev. B* **1980**, 22 (4), 2099-2111.
- 2 Tang, C. W.; VanSlyke, S. A., Organic electroluminescent diodes. *Appl. Phys. Lett.* **1987**, 51 (12), 913-915.
- 3 Burroughes, J. H.; Bradley, D. D. C.; Brown, A. R.; Marks, R. N.; Mackay, K.; Friend, R. H.; Burns, P. L.; Holmes, A. B., Light-emitting diodes based on conjugated polymers. *Nature* **1990**, 347 (6293), 539-541.
- 4 Braun, D.; Heeger, A. J., Visible light emission from semiconducting polymer diodes. *Appl. Phys. Lett.* **1991**, 58 (18), 1982-1984.
- 5 Friend, R. H.; Gymer, R. W.; Holmes, A. B.; Burroughes, J. H.; Marks, R. N.; Taliani, C.; Bradley, D. D. C.; Santos, D. A. D.; Bredas, J. L.; Logdlund, M.; Salaneck, W. R., Electroluminescence in conjugated polymers. *Nature* **1999**, 397 (6715), 121-128.
- 6 Tang, C. W., Two-layer organic photovoltaic cell. *Appl. Phys. Lett.* **1986**, 48 (2), 183-185.
- 7 Yu, G.; Gao, J.; Hummelen, J. C.; Wudl, F.; Heeger, A. J., Polymer Photovoltaic Cells: Enhanced Efficiencies via a Network of Internal Donor-Acceptor Heterojunctions. *Science* **1995**, 270 (5243), 1789-1791.
- 8 Konarka website (last accessed June 29, 2011)  
<http://www.konarka.com/index.php/newsroom/konarka-in-the-news/>
- 9 Doubleday, C.; Turro, N. J.; Wang, J. F., Dynamics of flexible triplet biradicals. *Acc.*

- Chem. Res.* **1989**, 22 (6), 199-205.
- 10 Kohler, A.; Beljonne, D., The Singlet-Triplet Exchange Energy in Conjugated Polymers. *Adv. Funct. Mater.* **2004**, 14 (1), 11-18.
  - 11 Yü, L. *Solitons & polarons in conducting polymers*. World Scientific Pub Co Inc, **1988**.
  - 12 Griffiths, D. J. *Introduction to Quantum Mechanics*, Pearson Prentice Hall, **2005**.
  - 13 Kittel, C., *Introduction to Solid State Physics*, Wiley, **1995**.
  - 14 Khudyakov, I. V.; Serebrennikov, Y. A.; Turro, N. J., Spin-orbit coupling in free-radical reactions: on the way to heavy elements. *Chem. Rev.* **1993**, 93 (1), 537-570.
  - 15 Turro, N. J. *Molecular photochemistry*, W. A. Benjamin, Inc, **1965**.
  - 16 Turro, N. J. *Modern molecular photochemistry*, Benjamin/Cummings, **1978**.
  - 17 Schwob, H. P.; Williams, D. F., Charge transfer exciton fission in anthracene crystals. *J. Chem. Phys.* **1973**, 58 (4), 1542-1547.
  - 18 Kalinowski, J.; Cocchi, M.; Virgili, D.; Di Marco, P.; Fattori, V., Magnetic field effects on emission and current in Alq<sub>3</sub>-based electroluminescent diodes. *Chem. Phys. Lett.* **2003**, 380 (5-6), 710-715.
  - 19 Salis, G.; Alvarado, S. F.; Tschudy, M.; Brunschweiler, T.; Allenspach, R., Hysteretic electroluminescence in organic light-emitting diodes for spin injection. *Phys. Rev. B* **2004**, 70 (8), 085203.
  - 20 Davis, A. H.; Bussmann, K., Large magnetic field effects in organic light emitting diodes based on tris(8-hydroxyquinoline aluminum) (Alq<sub>3</sub>)/N,N'-Di(naphthalene-1-

- yl)-N, N' diphenyl-benzidine (NPB) bilayers. *J. Vac. Sci. Technol. A* **2004**, *22*, 1885-1891.
- 21 Wilkinson, J.; Davis, A. H.; Bussmann, K.; Long, J. P., Evidence for charge-carrier mediated magnetic-field modulation of electroluminescence in organic light-emitting diodes. *Appl. Phys. Lett.* **2005**, *86*, 111109.
  - 22 Iwasaki, Y.; Osasa, T.; Asahi, M.; Matsumura, M.; Sakaguchi, Y.; Suzuki, T., Fractions of singlet and triplet excitons generated in organic light-emitting devices based on a polyphenylenevinylene derivative. *Phys. Rev. B* **2006**, *74* (19), 195209.
  - 23 Odaka, H.; Okimoto, Y.; Yamada, T.; Okamoto, H.; Kawasaki, M.; Tokura, Y., Control of magnetic-field effect on electroluminescence in Alq<sub>3</sub>-based organic light emitting diodes. *Appl. Phys. Lett.* **2006**, *88* (12), 123501.
  - 24 Francis, T. L.; Mermer, O.; Veeraraghavan, G.; Wohlgenannt, M., Large magnetoresistance at room temperature in semiconducting polymer sandwich devices. *New J. Phys.* **2004**, *6*, 185-192.
  - 25 Wohlgenannt, M.; Vardeny, Z. V.; Shi, J.; Francis, T. L.; Jiang, X. M.; Mermer, O.; Veeraraghavan, G.; Wu, D.; Xiong, Z. H., Spin and magnetic field effects in organic semiconductor devices. *IEE Proc.-Circuit Device Syst.* **2005**, *152* (4), 385-392.
  - 26 Prigodin, V. N.; Bergeson, J. D.; Lincoln, D. M.; Epstein, A. J., Anomalous room temperature magnetoresistance in organic semiconductors. *Synth. Met.* **2006**, *156*, 757-761.
  - 27 Bobbert, P. A.; Nguyen, T. D.; van Oost, F. W. A.; Koopmans, B.; Wohlgenannt, M.,

- Bipolaron mechanism for organic magnetoresistance. *Phys. Rev. Lett.* **2007**, *99* (21), 216801.
- 28 Hu, B.; Wu, Y., Tuning magnetoresistance between positive and negative values in organic semiconductors. *Nat. Mater.* **2007**, *6* (12), 985-991.
  - 29 Desai, P.; Shakya, P.; Kreouzis, T.; Gillin, W. P., The role of magnetic fields on the transport and efficiency of aluminum tris(8-hydroxyquinoline) based organic light emitting diodes. *J. Appl. Phys.* **2007**, *102* (7), 073710.
  - 30 Bloom, F. L.; Wagemans, W.; Kemerink, M.; Koopmans, B., Separating Positive and Negative Magnetoresistance in Organic Semiconductor Devices. *Physical Review Letters* **2007**, *99* (25), 257201.
  - 31 Desai, P.; Shakya, P.; Kreouzis, T.; Gillin, W. P.; Morley, N. A.; Gibbs, M. R. J., Magnetoresistance and efficiency measurements of Alq<sub>3</sub>-based OLEDs. *Phys. Rev. B* **2007**, *75* (9), 094423.
  - 32 Desai, P.; Shakya, P.; Kreouzis, T.; Gillin, W. P., Magnetoresistance in organic light-emitting diode structures under illumination. *Phys. Rev. B* **2007**, *76* (23), 235202.
  - 33 Bergeson, J. D.; Prigodin, V. N.; Lincoln, D. M.; Epstein, A. J., Inversion of Magnetoresistance in Organic Semiconductors. *Phys. Rev. Lett.* **2008**, *100* (6), 067201.
  - 34 Shakya, P.; Desai, P.; Somerton, M.; Gannaway, G.; Kreouzis, T.; Gillin, W. P., The magnetic field effect on the transport and efficiency of group III tris(8-hydroxyquinoline) organic light emitting diodes. *J. Appl. Phys.* **2008**, *103* (10),

103715.

- 35 Rolfe, N.; Desai, P.; Shakya, P.; Kreouzis, T.; Gillin, W. P., Separating the roles of electrons and holes in the organic magnetoresistance of aluminum tris(8-hydroxyquinoline) organic light emitting diodes. *J. Appl. Phys.* **2008**, *104* (8), 083703.
- 36 Rybicki, J.; Wohlgenannt, M., Spin-orbit coupling in singly charged pi-conjugated polymers. *Phys. Rev. B* **2009**, *79* (15), 153202.
- 37 Bloom, F. L.; Kemerink, M.; Wagemans, W.; Koopmans, B., Sign Inversion of Magnetoresistance in Space-Charge Limited Organic Devices. *Phys. Rev. Lett.* **2009**, *103* (6), 066601.
- 38 Martin, J. L.; Bergeson, J. D.; Prigodin, V. N.; Epstein, A. J., Magnetoresistance for organic semiconductors: Small molecule, oligomer, conjugated polymer, and non-conjugated polymer. *Synth. Met.* **2010**, *160* (3-4), 291-296.
- 39 Prigodin, V. N.; Epstein, A. J., Spin dynamics control of recombination current in organic semiconductors. *Synth. Met.* **2010**, *160* (3-4), 244-250.
- 40 Gillin, W. P.; Zhang, S.; Rolfe, N. J.; Desai, P.; Shakya, P.; Drew, A. J.; Kreouzis, T., Determining the influence of excited states on current transport in organic light emitting diodes using magnetic field perturbation. *Phys. Rev. B* **2010**, *82* (19), 195208.
- 41 Kersten, S. P.; Schellekens, A. J.; Koopmans, B.; Bobbert, P. A., Magnetic-field dependence of the electroluminescence of organic light-emitting diodes: A

- competition between exciton formation and spin mixing. *Phys. Rev. Lett.* **2011**, *106* (19), 197402.
- 42 Wagemans, W.; Koopmans, B., Spin transport and magnetoresistance in organic semiconductors. *Physica Status Solidi (b)* **2011**, *248* (5), 1029-1041.
- 43 Wagemans, W.; Schellekens, A. J.; Kemper, M.; Bloom, F. L.; Bobbert, P. A.; Koopmans, B., Spin-Spin Interactions in Organic Magnetoresistance Probed by Angle-Dependent Measurements. *Phys. Rev. Lett.* **2011**, *106* (19), 196802.
- 44 Frankevich, E. L.; Balabano, E. I., New effect of increasing photoconductivity of organic semiconductors in a weak magnetic field. *Jetp Letters* **1965**, *1* (6), 169-171.
- 45 Frankevich, E. L.; Sokolik, I. A., On the mechanism of the magnetic field effect on anthracene photoconductivity. *Solid State Commun.* **1970**, *8* (4), 251-253.
- 46 Ito, F.; Ikoma, T.; Akiyama, K.; Watanabe, A.; Tero-Kubota, S., Carrier generation process on photoconductive polymer films as studied by magnetic field effects on the charge-transfer fluorescence and photocurrent. *J. Phys. Chem. B* **2005**, *109* (18), 8707-8717.
- 47 Frankevich, E. L.; Lymarev, A. A.; Sokolik, I.; Karasz, F. E.; Blumstengel, S.; Baughman, R. H.; Horhold, H. H., Polaron-pair generation in poly(phenylene vinylenes). *Phys. Rev. B* **1992**, *46* (15), 9320-9324.
- 48 Frankevich, E.; Zakhidov, A.; Yoshino, K.; Maruyama, Y.; Yakushi, K., Photoconductivity of poly(2,5-diheptyloxy-p-phenylene vinylene) in the air atmosphere: Magnetic-field effect and mechanism of generation and recombination



- of charge carriers. *Phys. Rev. B* **1996**, 53 (8), 4498-4508.
- 49 Tajima, H.; Miyakawa, M.; Yasui, M.; Suzuki, N.; Matsuda, M., Photovoltaic effect of organic devices at low temperature and under high magnetic field. *Thin Solid Films* **2009**, 518 (2), 781-785.
- 50 Tajima, H.; Miyakawa, M.; Isozaki, H.; Yasui, M.; Suzuki, N.; Matsuda, M., Magnetophotocurrent effect in organic photovoltaic cells at low temperatures. *Synth. Met.* **2010**, 160 (3-4), 256-261.
- 51 Ito, F.; Ikoma, T.; Akiyama, K.; Kobori, Y.; Tero-Kubota, S., Long-Range Jump versus Stepwise Hops: Magnetic Field Effects on the Charge-Transfer Fluorescence from Photoconductive Polymer Films. *J. Am. Chem. Soc.* **2003**, 125 (16), 4722-4723.
- 52 Schulten, K.; Staerk, H.; Weller, A.; Werner, H. J.; Nickel, B. Magnetic field dependence of the geminate recombination of radical ion pairs in polar solvents. *Z. Phys. Chem.* **1976**, 101(1-6), 371-390.
- 53 Werner, H. J.; Staerk, H.; Weller, A., Solvent, isotope, and magnetic-field effects in geminate recombination of radical ion-pairs. *J. Chem. Phys.* **1978**, 68 (5), 2419-2426.
- 54 Yoshizawa, T.; Mizoguchi, M.; Iimori, T.; Nakabayashi, T.; Ohta, N., Effects of electric and magnetic fields on fluorescence in electron donor and acceptor pairs of pyrene and N-methylphthalimide doped in a polymer film. *Chem. Phys.* **2006**, 324 (1), 26-39.

- 55 Schulten, K.; Epstein, I. R., Recombination of radical pairs in high magnetic fields: A path integral--Monte Carlo treatment. *J. Chem. Phys.* **1979**, *71* (1), 309-316.
- 56 Groff, R. P.; Merrifield, R. E.; Suna, A.; Avakian, P., Magnetic hyperfine modulation of dye-sensitized delayed fluorescence in an organic crystal. *Phys. Rev. Lett.* **1972**, *29* (7), 429-431.
- 57 Sheng, Y.; Nguyen, T. D.; Veeraraghavan, G.; Mermer; Ouml; Wohlgenannt, M.; Qiu, S.; Scherf, U., Hyperfine interaction and magnetoresistance in organic semiconductors. *Phys. Rev. B* **2006**, *74* (4), 045213.
- 58 Nguyen, T. D.; Hukic-Markosian, G.; Wang, F. J.; Wojcik, L.; Li, X. G.; Ehrenfreund, E.; Vardeny, Z. V., Isotope effect in spin response of pi-conjugated polymer films and devices. *Nat. Mater.* **2010**, *9* (4), 345-352.
- 59 Yu, Z. G., Spin-orbit coupling, spin relaxation, and spin diffusion in organic solids. *Phys. Rev. Lett.* **2011**, *106* (10), 106602.
- 60 Rolfe, N. J.; Heeney, M.; Wyatt, P. B.; Drew, A. J.; Kreouzis, T.; Gillin, W. P., Elucidating the role of hyperfine interactions on organic magnetoresistance using deuterated aluminium tris(8-hydroxyquinoline). *Phys. Rev. B* **2009**, *80* (24), 241201.
- 61 Kalinowski, J.; Cocchi, M.; Virgili, D.; Fattori, V.; Di Marco, P., Magnetic field effects on organic electrophosphorescence. *Phys. Rev. B* **2004**, *70*, 205303.
- 62 Nguyen, T. D.; Sheng, Y.; Rybicki, J.; Veeraraghavan, G.; Wohlgenannt, M., Magnetoresistance in  $\pi$ -conjugated organic sandwich devices with varying hyperfine and spin-orbit coupling strengths, and varying dopant concentrations. *J.*

*Mat. Chem.* **2007**, *17* (19), 1995-2001.

- 63 Wu, Y.; Xu, Z.; Hu, B.; Howe, J., Tuning magnetoresistance and magnetic field-dependent electroluminescence through mixing strong-spin-orbital-coupling molecule and weak-spin-orbital-coupling polymer. *Phys. Rev. B* **2007**, *75*, 035214.
- 64 Weil, J. A.; Bolton, J. R., *Electron Paramagnetic Resonance*, Wiley, **2007**.
- 65 Hu, B.; Yan, L.; Shao, M., Magnetic-Field Effects in Organic Semiconducting Materials and Devices. *Adv. Mater.* **21**, 1500 (2009).
- 66 Wagemans, W.; Bloom, F. L.; Bobbert, P. A.; Wohlgenannt, M.; Koopmans, B., A two-site bipolaron model for organic magnetoresistance. *J. Appl. Phys.* **2008**, *103* (7), 07F303.
- 67 Bredas, J. L.; Street, G. B., Polarons, bipolarons, and solitons in conducting polymers. *Acc. Chem. Res.* **1985**, *18* (10), 309-315.
- 68 Zhang, Y.; Liu, R.; Lei, Y. L.; Xiong, Z. H., Low temperature magnetic field effects in Alq<sub>3</sub>-based organic light emitting diodes. *Appl. Phys. Lett.* **2009**, *94* (8), 083307.
- 69 Liu, R.; Zhang, Y.; Lei, Y. L.; Chen, P.; Xiong, Z. H., Magnetic field dependent triplet-triplet annihilation in Alq<sub>3</sub>-based organic light emitting diodes at different temperatures. *J. Appl. Phys.* **2009**, *105* (9), 093719.
- 70 Tolstov, I. V., On the role of magnetic field spin effect in photoconductivity of composite films of MEH-PPV and nanosized particles of PbS. *J. Lumin.* **2005**, *112*, 368-371.
- 71 Kalinowski, J., Coexistence of dissociation and annihilation of excitons on charge

- carriers in organic phosphorescent emitters. *Phys. Rev. B* **2006**, *74*, 085316.
- 72 Levinson, J.; Weisz, S. Z.; Cobas, A.; Rolon, A., Determination of the triplet exciton-trapped electron reaction rate constant in Anthracene crystals. *J. Chem. Phys.* **1970**, *52*, 2794-2795.
- 73 Wittmer, M.; Zschokke-Granacher, I., Exciton-charge carrier interactions in the electroluminescence of crystalline anthracene. *J. Chem. Phys.* **1975**, *63*, 4187-4194.
- 74 Helfrich, W., Destruction of triplet excitons in Anthracene by injected electrons. *Phys. Rev. Lett.* **1966**, *16*, 401-403.
- 75 Ern, V.; Merrifield, R. E., Magnetic field effect on triplet exciton quenching in organic crystals. *Phys. Rev. Lett.* **1968**, *21*, 609-611.
- 76 Steiner, U. E.; Ulrich, T., Magnetic field effects in chemical kinetics and related phenomena. *Chem. Phys.* **1999**, *89*, 51-147.
- 77 Pope, M. & Swenberg, C. E. *Electronic Processes in Organic Crystals*. Oxford Univ. Press, Oxford, **1999**.
- 78 Merrifield, R. E., Theory of magnetic field effects on the mutual annihilation of triplet excitons. *J. Chem. Phys.* **1968**, *48* (9), 4318-4319.
- 79 Johnson, R. C.; Merrifield, R. E., Effects of Magnetic Fields on the Mutual Annihilation of Triplet Excitons in Anthracene Crystals. *Phys. Rev. B* **1970**, *1* (2), 896-902.
- 80 Kalinowski, J.; Szmytkowski, J.; Stampor, W., Magnetic hyperfine modulation of

- charge photogeneration in solid films of Alq<sub>3</sub>. *Chem. Phys. Lett.* **2003**, 378 (3-4), 380-387.
- 81 Wohlgenannt, M.; Vardeny, Z. V., Spin-dependent exciton formation rates in  $\pi$ -conjugated materials. *J. Phys. Condens. Matter* **2003**, 15, R83-R107.
  - 82 Smallwood, I. M., *Handbook of Organic Solvent Properties*. Elsevier: **1996**.
  - 83 Maryott, A. A.; Smith, E. R., *Table of dielectric constants of pure liquids*. U.S. Govt. Print. Off.: Washington, **1951**.
  - 84 Cao, H.; Fujiwara, Y.; Haino, T.; Fukazawa, Y.; Tung, C.-H.; Tanimoto, Y., Magnetic Field Effects on Intramolecular Exciplex Fluorescence of Chain-Linked Phenanthrene and N,N-Dimethylaniline: Influence of Chain Length, Solvent, and Temperature. *Bull. Chem. Soc. Jpn.* **1996**, 69 (10), 2801-2813.
  - 85 Brandrup, J.; Immergut, E. H.; Grulke, E. A.; Abe, A.; Bloch, D. R., *Polymer Handbook* (4th Edition). John Wiley & Sons., **1999**.
  - 86 Fanggao, C.; Saunders, G. A.; Lambson, E. F.; Hampton, R. N.; Carini, G.; Di Marco, G.; Lanza, M., Temperature and frequency dependencies of the complex dielectric constant of poly(ethylene oxide) under hydrostatic pressure. *J. Polymer Science Part B: Polymer Physics* **1996**, 34 (3), 425-433.
  - 87 Kliem, H.; Wagner, A. In *High dielectric permittivity by ionic space charge polarization in polyethylene oxide*, Electrical Insulation and Dielectric Phenomena, 2001 Annual Report. Conference on, 2001; 2001; pp 648-651.
  - 88 Kanno, H.; Sun, Y.; Forrest, S. R., High-efficiency top-emissive white-light-

- emitting organic electrophosphorescent devices. *Appl. Phys. Lett.* **2005**, *86* (26), 263502.
- 89 Tokito, S.; Iijima, T.; Tsuzuki, T.; Sato, F., High-efficiency white phosphorescent organic light-emitting devices with greenish-blue and red-emitting layers. *Appl. Phys. Lett.* **2003**, *83* (12), 2459-2461.
- 90 Al Attar, H. A.; Monkman, A. P.; Tavasli, M.; Bettington, S.; Bryce, M. R., White polymeric light-emitting diode based on a fluorene polymer/Ir complex blend system. *Appl. Phys. Lett.* **2005**, *86* (12), 121101.
- 91 Hu, B.; Karasz, F. E., Blue, green, red, and white electroluminescence from multichromophore polymer blends. *J. Appl. Phys.* **2003**, *93* (4), 1995-2001.
- 92 Reufer, M.; Walter, M. J.; Lagoudakis, P. G.; Hummel, B.; Kolb, J. S.; Roskos, H. G.; Scherf, U.; Lupton, J. M., Spin-conserving carrier recombination in conjugated polymers. *Nat. Mater.* **2005**, *4* (4), 340-346.
- 93 Birks, J. B., *Organic Molecular Photophysics*. Nature Publishing Group: **1975**.
- 94 Burrows, H. D.; Seixas de Melo, J.; Serpa, C.; Arnaut, L. G.; Miguel, M. d. G.; Monkman, A. P.; Hamblett, I.; Navaratnam, S., Triplet state dynamics on isolated conjugated polymer chains. *Chem. Phys.* **2002**, *285* (1), 3-11.
- 95 Chen, F.-C.; He, G.; Yang, Y., Triplet exciton confinement in phosphorescent polymer light-emitting diodes. *Appl. Phys. Lett.* **2003**, *82* (7), 1006-1008.
- 96 Huang, S.-P.; Jen, T.-H.; Chen, Y.-C.; Hsiao, A.-E.; Yin, S.-H.; Chen, H.-Y.; Chen, S.-A., Effective shielding of triplet energy transfer to conjugated polymer by its

- dense side chains from phosphor dopant for highly efficient electrophosphorescence. *J. Am. Chem. Soc.* **2008**, *130* (14), 4699-4707.
- 97 Dediu, V.; Murgia, M.; Maticcotta, F. C.; Taliani, C.; Barbanera, S., Room temperature spin polarized injection in organic semiconductor. *Solid State Commun.* **2002**, *122* (3-4), 181-184.
  - 98 Xiong, Z. H.; Wu, D.; Vally Vardeny, Z.; Shi, J., Giant magnetoresistance in organic spin-valves. *Nature* **2004**, *427* (6977), 821-824.
  - 99 Garditz, C.; Muckl, A. G.; Colle, M., Influence of an external magnetic field on the singlet and triplet emissions of tris-(8-hydroxyquinoline)aluminum(III) ( $\text{Alq}_3$ ). *J. Appl. Phys.* **2005**, *98* (10), 104507.
  - 100 Yusoff, A. R. B. M.; da Silva, W. J.; Serbena, J. P. M.; Meruvia, M. S.; Hummelgen, I. A., Very high magnetocurrent in tris-(8-hydroxyquinoline) aluminum-based bipolar charge injection devices. *Appl. Phys. Lett.* **2009**, *94* (25), 253305.
  - 101 Song, J. Y.; Stingelin, N.; Drew, A. J.; Kreouzis, T.; Gillin, W. P., Effect of excited states and applied magnetic fields on the measured hole mobility in an organic semiconductor. *Phys. Rev. B* **2010**, *82* (8), 085205.
  - 102 Li, F.; Xin, L.; Liu, S.; Hu, B., Direct measurement of the magnetic field effects on carrier mobilities and recombination in tri-(8-hydroxyquinoline)-aluminum based light-emitting diodes. *Appl. Phys. Lett.* **2010**, *97* (7), 073301.
  - 103 Baldo, M. A.; Thompson, M. E.; Forrest, S. R., High-efficiency fluorescent organic light-emitting devices using a phosphorescent sensitizer. *Nature* **2000**, *403* (6771),

750-753.

- 104 Baldo, M. A.; O'Brien, D. F.; You, Y.; Shoustikov, A.; Sibley, S.; Thompson, M. E.; Forrest, S. R., Highly efficient phosphorescent emission from organic electroluminescent devices. *Nature* **1998**, 395 (6698), 151-154.
- 105 Shao, Y.; Yang, Y., Efficient Organic Heterojunction Photovoltaic Cells Based on Triplet Materials. *Adv. Mater.* **2005**, 17 (23), 2841-2844.
- 106 Zheng, W.; Strouse, G. F., Involvement of Carriers in the Size-Dependent Magnetic Exchange for Mn: CdSe Quantum Dots. *J. Am. Chem. Soc.* **2011**, 133 (19), 7482-7489.
- 107 Brouwer, P. W.; Waintal, X.; Halperin, B. I., Fluctuating Spin g-Tensor in Small Metal Grains. *Phys. Rev. Lett.* **2000**, 85 (2), 369-372.
- 108 Rachdi, F.; Bernier, P., Role of the spin-orbit coupling on the ESR of alkali-doped polyacetylene. *Synth. Met.* **1987**, 17 (1-3), 401-404.
- 109 Endo, A.; Suzuki, K.; Yoshihara, T.; Tobita, S.; Yahiro, M.; Adachi, C., Measurement of photoluminescence efficiency of Ir(III) phenylpyridine derivatives in solution and solid-state films. *Chem. Phys. Lett.* **2008**, 460 (1-3), 155-157.
- 110 Onsager, L., Deviations from Ohm's Law in Weak Electrolytes. *J. Chem. Phys.* **1934**, 2 (9), 599-615.
- 111 Baldo, M. A.; Thompson, M. E.; Forrest, S. R., Phosphorescent materials for application to organic light emitting devices. *Pure and Applied Chemistry* **1999**, 71 (11), 2095-2106.



- 112 Hay, P. J., Theoretical Studies of the Ground and Excited Electronic States in Cyclometalated Phenylpyridine Ir(III) Complexes Using Density Functional Theory *J. Phys. Chem. A* **2002**, *106* (8), 1634-1641.
- 113 Stampor, W.; Mezyk, J.; Kalinowski, J., Electroabsorption study of metal-to-ligand charge transfer in an organic complex of iridium(III). *Chem. Phys.* **2004**, *300* (1-3), 189-195.
- 114 Kawamura, Y.; Goushi, K.; Brooks, J.; Brown, J. J.; Sasabe, H.; Adachi, C., 100% phosphorescence quantum efficiency of Ir(III) complexes in organic semiconductor films. *Appl. Phys. Lett.* **2005**, *86* (7), 071104.
- 115 Holzer, W.; Penzkofer, A.; Tsuboi, T., Absorption and emission spectroscopic characterization of Ir(ppy)<sub>3</sub>. *Chem. Phys.* **2005**, *308* (1-2), 93-102.
- 116 Yan, L.; Shao, M.; Graeff, C. F. O.; Hummelgen, I.; Hu, B. to be published (Chapter 5 in this dissertation).
- 117 Shao, M.; Yan, L.; Hu, B., to be published (Chapter 7 in Ph. D. dissertation of Ming Shao).
- 118 Lee, P.-I.; Hsu, S. L.-C.; Lee, J.-F., Pure white-light-emitting diodes from phosphorescent single polymer systems. *J. Polymer Science Part A: Polymer Chemistry* **2008**, *46* (2), 464-472.
- 119 Namdas, E. B.; Hsu, B. B. Y.; Liu, Z.; Lo, S.-C.; Burn, P. L.; Samuel, I. D. W., Phosphorescent light-emitting transistors: harvesting triplet excitons. *Adv. Mater.* **2009**, *21* (48), 4957-4961.

- 120 Nguyen, T. D.; Sheng, Y.; Rybicki, J.; Veeraraghavan, G.; Wohlgenannt, M., Device-spectroscopy of magnetic field effects in several different polymer organic light-emitting diodes. *Synth. Met.* **2010**, *160* (3-4), 320-324.
- 121 Kadashchuk, A.; Arkhipov, V. I.; Kim, C.-H.; Shinar, J.; Lee, D. W.; Hong, Y. R.; Jin, J.-I.; Heremans, P.; aumli; ssler, H., Localized trions in conjugated polymers. *Phys. Rev. B* **2007**, *76* (23), 235205.
- 122 Sun, Z.; Li, Y.; Gao, K.; Liu, D. S.; An, Z.; Xie, S. J., Dynamical study of polaron-bipolaron scattering in conjugated polymers. *Org. Electron.* **2010**, *11* (2), 279-284.
- 123 Andronikov, D.; Kochereshko, V.; Platonov, A.; Crooker, S.; Barrick, T.; Karczewski, G., Temperature dependence of exciton and trion states in CdTe quantum well at high magnetic fields. *Acta Phys. Pol. A* **2005**, *108* (4), 653-660.
- 124 Yin, S.; Chen, L.; Xuan, P.; Chen, K.-Q.; Shuai, Z., Field Effect on the Singlet and Triplet Exciton Formation in Organic/Polymeric Light-Emitting Diodes. *J. Phys. Chem. B* **2004**, *108* (28), 9608-9613.
- 125 Zaidi, N. A.; Giblin, S. R.; Terry, I.; Monkman, A. P., Room temperature magnetic order in an organic magnet derived from polyaniline. *Polymer* **2004**, *45* (16), 5683-5689.
- 126 Kavarnos, G., Fundamental concepts of photoinduced electron transfer. In *Photoinduced Electron Transfer I*, Mattay, J., Ed. Springer Berlin / Heidelberg: **1990**; Vol. 156, pp 21-58.
- 127 Totsuji, H.; Tachibana, H.; Totsuji, C.; Nara, S., Exchange energy for electrons in

- two dimensions: Effects of finite temperature and finite thickness. *Phys. Rev. B* **1995**, *51* (16), 11148.
- 128 Difley, S.; Beljonne, D.; Van Voorhis, T., On the Singlet–Triplet Splitting of Geminate Electron–Hole Pairs in Organic Semiconductors. *J. Am. Chem. Soc.* **2008**, *130* (11), 3420-3427.
- 129 Yang, J.; Gordon, K. C., Organic light emitting devices based on exciplex interaction from blends of charge transport molecules. *Chem. Phys. Lett.* **2003**, *375* (5-6), 649-654.
- 130 Hanasaki, N.; Tajima, H.; Matsuda, M.; Naito, T.; Inabe, T., Giant negative magnetoresistance in quasi-one-dimensional conductor  $\text{TPP}[\text{Fe}(\text{Pc})(\text{CN})_2]_2$ : Interplay between local moments and one-dimensional conduction electrons. *Phys. Rev. B* **2000**, *62* (9), 5839-5842.
- 131 Hanasaki, N.; Matsuda, M.; Tajima, H.; Naito, T.; Inabe, T., Contribution of Degenerate Molecular Orbitals to Molecular Orbital Angular Momentum in Molecular Magnet  $\text{Fe}(\text{Pc})(\text{CN})_2$ . *J. Phys. Soc. Jpn.* **2003** *72*, 3226-3230.
- 132 Hanasaki, N.; Matsuda, M.; Tajima, H.; Ohmichi, E.; Osada, T.; Naito, T.; Inabe, T., Giant Negative Magnetoresistance Reflecting Molecular Symmetry in Dicyano(phthalocyaninato)iron Compounds. *J. Phys. Soc. Jpn* **2006**, *75*, 033703.
- 133 Ishikawa, M.; Asari, T.; Matsuda, M.; Tajima, H.; Hanasaki, N.; Naito, T.; Inabe, T., Giant magnetoresistance response by the  $\pi$ -d interaction in an axially ligated phthalocyanine conductor with two-dimensional  $\pi$ - $\pi$  stacking structure. *J. Mater.*

*Chem.* **2010**, *20* (21), 4432-4438.

- 134 Inabe, T.; Tajima, H., Phthalocyanines Versatile Components of Molecular Conductors. *Chem. Rev.* **2004**, *104* (11), 5503-5534.

## **VITA**

Liang Yan was born in Nanchang, Jiangxi, China, August 1982. He went to Tsinghua University at 1999 to study in Polymer Science and Engineering and obtained the Bachelor's degree in July, 2003. He continued to study in Material Science at Tsinghua University and obtained his Mater's degree in July, 2006. Then he went to University of Tennessee to continue his study in Material Science and Engineering for pursuing his Ph.D. degree under the supervision of Prof. Bin Hu from August, 2006.